FACULTY OF SCIENCE AND TECHNOLOGY

MASTER'S THESIS

Study programme / specialisation: Environmental Engineering/ Offshore Environmental Technology	Spring 2023 Open / Confidential

Author: Bryan Han Xin Chou
ID : 267995

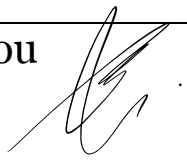

Supervisor at UiS: Prof. Gopalakrishnan Kumar

Co-supervisor: -

External supervisor(s): -

Thesis title:

Influence of Nanoparticles and Media composition on Microalgal growth towards Environmental Remediation

Credits (ECTS): 30

Keywords: Microalgae, nitrogen, phosphorus, wastewater, Produced water, Iron Oxide, N:P, Nanoparticles, biogas Methane , Anaerobic	Number of front pages : 13 Number of thesis pages : 81 Total pages : 94 Stavanger, *June 2023*

Influence of Nanoparticles and Media composition on Microalgal growth towards Environmental Remediation

Master Thesis

by

Bryan Han Xin Chou

University of Stavanger
Faculty of Science and Technology
Department of Chemistry, Bioscience and Environmental Engineering
June 15, 2023

University of Stavanger

This page has intentionally been left blank

Preface

Dear reader,

The journey throughout this thesis has been both challenging and deeply rewarding. I cannot express enough gratitude for the incredible individuals who have surrounded me, patiently supporting and guiding me towards the success of this thesis. Their persistent presence has meant the world to me.

First and foremost, I want to extend my heartfelt thanks and sincere gratitude to my classmates **Emre Can Emer**, **Si Vo**, and **Natalia G Øvestad**. From the very beginning of my master's program, they have been there to offer great expertise, guidance and technical knowledge which were extremely valuable and indispensable throughout the entire thesis program. Furthermore, during the demanding examination periods, especially on the last exam this June, they shared invaluable feedback, despite being busy with their tight schedule. They provided unwavering support, helping me to understand better and improve.

Secondly, I am also immensely grateful to **Prof. Gopalakrishnan Kumar**, who had granted me this incredible opportunity to pursue this master's thesis, challenge myself and expand my horizons. His passion for knowledge, innovative ideas, and creative thinking have influenced my approach to academic research greatly. He helped me realise my potential in a way I never thought possible. Moreover, his guidance has made me a better person and will continue to impact my life's journey positively.

My profound appreciation extends to **Abdul Rahman** for his selfless dedication and mentorship in teaching and guiding me through synthesising nanoparticles. His commitment and enthusiasm for his work have motivated me to strive for excellence in my work with NP.

Fourthly, I would like to express my deepest gratitude to **Kyle Lambert**, **Renée**, **Anton Birkedal**, and especially **Anne Lammertsma**, whom I forged a special connection with during my studies in Svalbard. Despite the great distance between us, they have been a strong pillar of support and were the driving force behind my passion for Arctic studies. I truly miss the times we spent studying together, and the reunion in March left an ineffable mark on my memory. I want to acknowledge **Anne Lammertsma** in particular for her technical digital support and guidance in Latex. Her selfless dedication in offering this assistance, even during her own free time, is something I hold dear and will forever cherish.

Moreover, to **Darya** who had been there encouraging me, being by my side to cheer me on at every step. Thank you for providing me with the strength and motivation I needed to persevere, which gave me the confidence to face every challenge throughout this journey.

Lastly, I must express my deep gratitude towards my *family*, who hold an indescribable significance in my life. Despite the challenges of different time zones, their unwavering support has always remained strong. Whenever I felt overwhelmed on this journey, our comforting presence and conversations reignited my motivation and propelled me towards success. I want to give special thanks to my brother, **Terence Han Ru Chou**, who has been a tremendous inspiration to me academically since our childhood. Despite his busy schedule, his unwavering love and care have been invaluable in advising me along the way.

To every person who has contributed to my thesis and supported me along this unique path, I am eternally grateful for your genuine encouragement, steadfast guidance, and heartfelt support. With your assistance, I was able to accomplish what I had achieved. From the depths of my being, thank you.

Stavanger, 14 June 2023

Bryan Han Xin Chou

Abstract

Scenedesmus sp. is one type of freshwater microalgae widely studied due to its robustness and versatility in growth, high nutrient removal and lipid production, making it a potential candidate as a renewable energy source and wastewater remediation. This helps with the increasing world population and energy demand.

Scenedesmus sp was used in a ten-day bioremediation study on various wastewater (WW): Dissolved air flotation (DAF) and Sequencing Batch Reactors (SBR) effluent, and offshore Produced water (PW), mixed with Bold's base medium (BBM) into five dilutions: Control (BBM only), 25 50, 75 and 100% of WW. *Scenedesmus* sp. grew in all WW with some variation in biomass production and nutrient removal efficiency (RE). Growing in SBR WW resulted in optimal conditions with the highest biomass produced and highest Total Nitrogen (TN) RE of more than 76% despite competitive results from DAF WW. Diluting 75% of SBR WW with BBM showed the most optimal dilution condition, attaining a decent TN and the highest Total Phosphorous (TP) RE of 76.3% and 82.4%. Using only 25% or 100% of SBR is not recommended due to being less cost-effective and being subjected to nitrogen limitation conditions at high WW volume.

Adding metal nanoparticles (NP) in low dosage demonstrated positive outcomes but inhibition at high concentrations. 75% SBR dilution was chosen for the addition of eight Fe_3O_4 NP concentrations: Control (without NP), 1, 2.5, 5, 10, 25, 50 and 100 mg/l of NP. Results showed improved biomass production and nutrient RE and extreme tolerance toward Fe_3O_4. The addition of 2.5mg/l NP resulted in the highest biomass of 3129.6mg/l and the highest TN and TP RE of 89% and 94%, respectively, meeting the nutrient RE requirement from the European Union (EU) regulations. Observation can also conclude that increasing NP concentration decreases growth and biomass production but increases nutrient RE.

The synergy in biofuel production with WW remediation achieved waste and pollutant reduction with energy recovery, promoting sustainable economics. Furthermore, NP-induced stress contributes to biogas production improvement. This was examined with the four biomass produced: Control (without NP), 2.5, 25 and 100mg/l of NP. The addition of 2.5 and 25mg/l of NP resulted in an improvement of 25% more biogas production but a 13% reduction in the presence of 100mg/l of NP. Overall, all samples produced more than 74 % methane content.

In conclusion, adding 2.5 mg/l of Fe_3O_4 NP to *Scenedesmus* sp. cultivation in SBR WW resulted in optimal biomass production, nutrient removal, and improvement in biogas production.

List of Figures

List of Tables

Nomenclature

Commonly Used Terms

BMM ..... Bold's Basal medium

BMP ..... Biochemical methane potential

COD ..... Chemical Oxygen demand

EU ..... Europe Union

NP ..... Nanoparticles

RE ..... Removal Efficiency

ROS ..... Reactive oxygen species

RR ..... Removal Rate

TN ..... Total Nitrogen

TP ..... Total Phosphorous

WW ..... Wastewater

Chemical Formula

CH_4 ..... Methane

Fe_2O_3 ..... Iron (II) oxide

Fe_3O_4 ..... Iron (III) oxide

H_2O_2 ..... Hydrogen Peroxide

NH_4^+ ..... Ammonium

NO_2^- ..... Nitrogen Oxide

NO_3^- ..... Nitrate

ZnO ..... Zinc Oxide

CNTs ..... carbon nanotubes

Fe ..... Iron

Dissolved Air Flotation Cultivation

"x"$_{DAF}$ ..... "x"% of DAF dilution in BBM, DAF WW experiment

C_{DAF} ..... DAF Control which only cultivating in BBM

Greek symbol and Units of measurement

μ ..... Specific Growth Rate

P_x ..... Specific Biomass Productivity

$P_{x,avg}$ ..... Average Biomass Productivity

$Y_{gX/gTN}$ ..... Specific Biomass Yield (TN)

$Y_{gX/gTP}$ ..... Specific Biomass Yield (TP)

ABS ..... Absorbance

N:P ..... Nitrogen : Phosphorous Ratio

S/I ..... Substrate to Inoculum Ratio

TDS ..... Total Dissolved Solids

TN:TP ..... Total Nitrogen : Total Phosphorous Ratio

TS ..... Total Solid

TSS ..... Total SuspendedSolids

Biochemical Methane Potential Experiment

"x"$_{BMP}$ ..... "x" NP concentration of 75% dilution of SBR biomass for BMP test

$Blank_{BMP}$ ..... Inoculum with no substrate

C_{BMP} ..... 75% dilution of SBR WW without NP addition in BMP test

G_{BMP} ..... Inoculum with Glucose as substrate

Addition of Nanoparticles Experiment

"x"$_{SBRNP}$ ..... "x" NP concentration addition in 75% dilution of SBR

C_{SBRNP} ..... 75% dilution of SBR WW without the addition of NP

Produced Water Cultivation

"x"$_{PW}$ ..... "x"% of PW dilution in BBM, PW WW experiment

C_{PW} ..... PW Control which only cultivating in BBM

Sequencing Batch Reactor cultivation

"x"$_{SBR}$ ..... "x"% of SBR dilution in BBM, SBR WW experiment

C_{SBR} ..... SBR Control which only cultivating in BBM

Type of Wastewater

DAF_{WW} ..... DAF in WW Comparison analysis sand experiment

PW_{WW} ..... PW in WW Comparison analysis and experiment

SBR_{WW} ..... SBR in WW Comparison analysis and experiment

DAF ..... Dissolved air flotation

PW ..... Produced water

SBR ..... Sequencing batch reactor

Table of Contents

Introduction

The increase in food and energy consumption increases with the growing world population demand where these sources are limited, which expect to deplete over the years to come. Therefore alternative solutions must be sustainable and essential to fight off this issue. Concurrently, waste production and carbon dioxide emission rise exponentially with these demands, which impose threats to the environment, amplifying the effects of global warming. In treatment of waste comes with a cost, and it may not be accessible to everyone. Therefore it is essential to develop affordable and energy-effective methods for waste remediation (Chandrasekhar et al. 2022). Microalgae have been commonly used for human and animal consumption, cosmetics, and fertilisers due to their high protein contents and rich nutritional values, which have been industrialised over the years. Additionally, microalgae contain bioactive compounds that have been shown to have health-promoting properties (Spolaore et al. 2006). Interest has also spiked and attracted global attention for their potential as a source of renewable energy and remediating pollutants at the same time. This encourages continuous research and development in microalgae, which will eventually change the way food is produced, energy and other valuable product are harvested in an effort to reach carbon neutrality and mitigate greenhouse gas emissions in part of fighting global warming while meeting demand with population growth (Cheregi et al. 2019).

Microalgae are microscopic, single-celled organisms that have a size of a few μ meters. They can form colonies or many-celled macroalgae, which can grow up to 60m long. Apart from producing a significant amount of oxygen we breathe, they form the base of the aquatic food chain, being the primary biomass producer, which is vital to produce the fishes that we eat today. Just like all types of plants, they are capable of photosynthesis and are able to grow in photoautotrophic, heterotrophic and mixotrophic conditions. They are incredibly diverse, with estimated thousands of species identified to date and can be found in almost every aquatic and terrestrial environment on Earth. Microalgae play a critical role in the planet's ecosystem as they are responsible for producing a significant portion of the oxygen we breathe and are the primary food source in the aquatic environments (Posten & Walter, 2012).

Biofuel and biodiesel can be synthesised from feedstock such as plants, trees, several fruits and seeds. A potential feedstock is selected based on both the lipid content and quality as it determines the number of carbon atoms per molecule and its bond structure which then define the fuel properties. In comparison to these biomass sources, the advantages of microalgae are its shorter carbon and growth period with respect to biomass yield at 10 to 100 times more and the versatility of lipid storage

efficiency when culture condition alteration, making them a strong prospect for oil production. For example, its photosynthetic efficiency could range between 3-8 % whereas 0.5% to terrestrial plants (B. Singh et al. 2014). Syncing the biorefinery concept with WW treatment, a compelling solution emerges to fully utilise algae biomass, recover valuable energy resources, and simultaneously reduce waste, pollutants, and CO2 emissions, thereby promoting sustainable economics (Cheregi et al. 2019).

As a feedstock with immense potential for biofuel production, microalgae harness solar energy and employ carbon sequestration mechanisms to generate high amounts of compounds within their biomass, which combination can convert into various biofuel products such as biodiesel, bioethanol, and biomethane (Calicioglu & Demirer, 2022). Moreover, microalgae also demonstrated the ability to produce biohydrogen through photo fermentation, further expanding microalgae applications as a renewable energy source (J. Singh & Gu, 2010). By integrating the biorefinery concept with wastewater treatment, a compelling solution emerges to fully utilise algae biomass, recover valuable energy resources, and simultaneously reduce waste, pollutants, and CO2 emissions, promoting sustainable economics. (Calicioglu & Demirer, 2022)

1.1. Scope of work

In this study, the project is conducted by the University of Stavanger (UiS) and wastewater effluent samples are provided by IVAR WWTP at Grødaland and Akersolution. Dissolved air flotation (DAF) and Sequencing Batch Reactors (SBR) wastewater are collected from IVAR WWTP, and Produced water is collected from an offshore rig by Akersolution. *Scenedesmus* sp. was collected from a local lake and isolated in the laboratory for experimental usage. The microalgae were used for cultivating in these wastewaters with different dilution ratios to analyse the nutrient depletion, total nitrogen and total phosphorous. Fe_3O_4 is produced in UiS and given for the analysis of the nutrient uptake effect with the addition of nanoparticles (NP) at different concentrations. A few of the optimal NP concentrations with the selected wastewater were accumulated and used to conduct an analysis of biogas production.

1.2. Objectives

The aim of this project was to understand how well *Scenedesmus* sp. was able to adapt and grow in different wastewater and at which dilution ratio the microalgae would thrive and remove the most nutrients simultaneously. The wastewater and dilution ratio with the most efficient nutrient depletion rate would be chosen to be cultivated with different concentrations of NP, which would be prepared and sonicated before addition. The concentration of total nitrogen, phosphorous and total suspended solid (TSS) of biomass would be analysed throughout the cultivation period and decision-making. BMP test would be to study the produced biogas, based on the resulting wastewater with the selected dilution ratio and NP concentration, to

understand the viability of potential biofuel production.

Theoretical Background

2.1. Microalgae

Microalgae are photosynthetic organisms commonly found in various aquatic habitats such as lakes and rivers. They exhibit high adaptability and can thrive in diverse and changing environmental conditions, including pH and light intensities fluctuations. They can be classified into different types of species and exist in various sizes at the microscopic level ((Khan et al. 2018)

Microalgae are utilized extensively in various applications in biofuels, health supplements, and cosmetics because they produce valuable compounds, gaining significant attention in the wastewater treatment and renewable energy industries (Khan et al. 2018). Given their ability to thrive in challenging environmental conditions, such as those found in industrial waste, they also contribute to reducing pollutants and greenhouse gases. Examples of pollutants, such as inorganic carbon, nitrogen, and phosphorous, are in wastewater. Some exceptional microalgae species can even remove heavy metals from industrial wastewater, thereby offering a sustainable solution for addressing environmental concerns (Plöhn et al. 2021).

The decision to utilize alternative sources like microalgae instead of food crops such as soy and sunflower was driven by public concerns and objections. Microalgae offer distinct advantages over vegetables due to their diverse fatty acid compositions with higher polyunsaturated fatty acid levels. The quality of the produced biodiesel depends on the parameters of the fatty acid chains. Under optimal conditions, microalgae can synthesize fatty acids, accounting for up to 20% of the dry cell weight, primarily for esterification into glycerol-based membrane lipids. Under stressed conditions, microalgae can accumulate neutral lipids, which can reach up to 50% of its dry cell weight and contain triacylglycerols, the key components for algal biodiesel production ((Oncel, 2013). Yet, these challenges lie in scaling up to commercialize these applications. Ongoing efforts are focused on improving algal systems to make them a cost-effective choice for energy production (Khan et al. 2018)

Various microalgae species with high carbohydrate content are being considered as potential candidates for bioethanol production. Techno-economic analysis plays a crucial role in assessing the feasibility and profitability of commercial bioethanol production from microalgae (Khan et al. 2018).

2.1.1. Nutrients Requirements

Like all plants, microalgae have the same photosynthetic process and require nutrients, which highly influences their growth. Among these factors, growth is limited by nutrient availability.

Light

Light is an important source of energy that determines the microalgae productivity of photosynthesis and growth. (Chowdury et al. 2020). The intensity of light received by individual microalgae cells depends on their depth within the media, as well as the turbidity of the medium and the concentration of biomass. As these factors increase, the absorption of light by the cells decreases. This phenomenon can be observed through three light zones within the media (Darvehei et al. 2018): 1) The photolimitation zone, where the photosynthetic rate increases with increasing light intensity up to a maximum rate. 2) The photosaturation zone, where excess light leads to saturation of the photosynthetic process. 3) The photoinhibition zone, where excessive light inhibits the photosynthetic process of microalgae.

Photoinhibition can also occur due to the maximum biomass concentration in the medium, causing shading and promoting areas with reduced light availability. This shading effect eventually leads to losses in biomass (Chowdury et al. 2020).

Different types of light sources, variations in light wavelength, and light/dark cycles are parameters that impact microalgal growth and the concentration of cellular components. In cultivation, fluorescent lamps and LEDs are commonly used, with LEDs being more popular due to their ability to adjust wavelength for better control over biomass production. For instance, a study conducted on the cultivation of *Chlorella vulgaris* for 14 days using different light wavelengths found that while red LED light initially resulted in higher cell density compared to white light, it decreased thereafter. As a result, growing them under white LED light yielded the highest final cell density, with a 20% difference in comparison. Other light wavelengths, such as red and blue light, have their own production favorability and limitations (Chowdury et al. 2020).

Typically, the maximal productivity is obtained with a constant irradiance ranging from 50 - 100 $\mu E.m^{-2}.s^{-1}$ and to grow microalgae under the white LED light. This amount and condition could vary with microalgae species and their synthesising mechanisms (Chowdury et al. 2020; Darvehei et al. 2018).

Temperature

Temperature is another critical factor that can significantly influence microalgae, even with small changes in degrees. It affects various aspects of microalgal growth, including growth rate, cell size, biochemical composition, and nutrient requirements. Generally, the optimal temperature range from 20 to 35°C, with some species capable of withstanding up to 40°C (Chowdury et al. 2020). For example, *Scenedesmus* sp. demonstrated successful adaptation and growth between 10 - 30°where the maximum specific growth rate lies at 25°C, maximum carrying capacity (the maximum algal

density reached in the culture) and population growth rate lies at 30°C and the highest lipid productivity at 20°C. Growth started to decline significantly beyond 42°C. This leads to a concluding optimal cultivation temperature for *Scenedesmus* sp. at 20°C (Xin et al. 2011). Furthermore, the study found that *Scenedesmus* sp. exhibited increased Nitrogen and phosphorus uptake as the temperature decreased, with the maximum nitrate uptake rate occurring at 15°C. This can be explained as the optimum temperature for enzyme reaction might differ from the optimum growth is species dependent. This increase in nutrient uptake at lower temperatures could be a stress response induced in microalgae to ensure survival and growth (Rhee & Gotham, 1981). The source of heat can originate from the environment or radiate from light sources. If this is not controlled well or accounted for, It could lead to overheating of microalgae cultivation (Chowdury et al. 2020).

Nutrients

Phosphorus (P) and Nitrogen (N) are essential inorganic elements for microalgae growth and organic composition. Other micronutrients, such as Iron (Fe) and Carbon (C), are also required for optimal growth. The amount of nutrients provided in the growth media has a direct impact on the growth of microalgae and can act as a limiting factor. The optimal molecular formula approximation for microalgae growth is as follows: $CO_{0.48}H_{1.83}N_{0.11}P_{0.01}$. Carbon is a major component and makes up about 50% of total biomass. It plays a vital role in synthesising organic compounds, including lipids. Carbon sources can include organic compounds such as sugar and alcohols, as well as CO_2 and bicarbonates for mixotrophic and autotrophic conditions, respectively (Chowdury et al. 2020).

Nitrogen is essential and critical for microalgae growth and can be found between 1 - 14 % in concentration within a microalgae biomass. It is required for the synthesis of vital components such as proteins, nucleic acid, vitamins and photosynthetic pigments. Nitrogen is available in various inorganic and organic forms, and the choice of nitrogen source is microalgae species-dependent. The selection of nitrogen sources could eventually impact the growth rate of microalgae. Furthermore, nitrogen limitation can adversely affect chlorophyll production, causing a reduction in microalgae productivity. This response to metabolic changes to counter nitrogen deficiency, including the accumulation of organic and nitrogen-containing compounds (Chowdury et al. 2020).

Phosphorus is another nutrient that is essential for microalgae, with concentrations ranging from 0.05 to 3.3 % within a microalgae biomass. It is available in different forms, including polyphosphate, pyrophosphate, orthophosphate, and metaphosphate (Chowdury et al. 2020). Similarly to Nitrogen, phosphorous is assimilated through the active transport system in microalgae to support growth and cellular metabolic activities such as energy transfer and the synthesis of cellular components like nucleic acids and deoxyribonucleic acid (DNA). The availability of phosphorus affects the composition of the produced biomass, including lipids and carbohydrates. Phosphorus is often limited in natural environments and is rapidly

depleted by microorganisms. Therefore, phosphorus limitation can impact biomass productivity and promote the accumulation of phosphorus reserves, making it advantageous for applications like wastewater treatment. Studies have also shown that the Nitrogen to Phosphorus ratio (N:P) in the culture media and microalgae can influence growth (Chowdury et al. 2020). Despite the stress-induced created by decreasing biomass productivity due to limiting Nitrogen and phosphorus, this stress can potentially increase synthesis and accumulation of lipids in microalgae which is applicable in biofuel applications (Wan et al. 2014). In general, the N:P ratio is 16:1, but vary depending on the type of microalgae (Chowdury et al. 2020).

Carbon sources, such as carbon dioxide, are necessary for photosynthesis-related processes in microalgae. Based on its molecular formula, typically, half of the total biomass amount is composed of carbon. Since atmospheric CO_2 is limited, supplying solid forms of carbon, such as bicarbonate, or injecting carbon dioxide-rich air into the culture can improve biomass productivity. While this can be advantageous for growth, increasing the supply of CO_2 could simultaneously decrease pH and inhibit growth. Studies found that the amount of CO_2 to achieve maximum biomass growth is species-dependent, with some species tolerating CO_2 concentration up to 20% (v/v). Typically, the optimal CO_2 concentration is between 6 - 7 % for maximum biomass and lipid productivity (Chowdury et al. 2020).

Apart from these macronutrients, microalgae also rely on a certain amount of micronutrients for their growth. Among the micronutrients, magnesium (Mg), sulfur (S), and iron (Fe) are significantly more essential. In comparison, Fe is the most important micronutrient, as its presence is required in many metabolic functions of microalgae, such as photosynthesis and respiratory processes, nitrogen fixation and detoxification/ degradation of reactive oxygen species (ROS). The uptake of micronutrients and macronutrient can influence each other depending on the amounts provided, subsequently affecting the efficiency of microalgae productivity and metabolism. In one study, it was found that a higher dosage of nitrates at a 20:1 N:P ratio increased the amount of iron adsorbed. This effect was insignificant with variations of phosphates and biomass concentration when cultivating *Nannochloropsis* sp but could be associated with increased production of reducing agents such as ferredoxin protein, which helps provide electrons in the assimilation of NO_3^- (Encarnação et al. 2012). Another study cultivates *Monoraphidium* sp. in different Fe^{3+} concentrations showed that an increase in iron concentration resulted in a 27% increase in biomass but a 13% decrease of lipid production over a period of 50 days (Che et al. 2015). Increases in iron concentration can provoke stress on microalgae, promoting lipid accumulation at the expense of productivity, similar to Nitrogen and phosphorous starvation. Moreover, excessive micronutrients, like iron, can lead to metal toxicity and provoke oxidative stress and inhibit growth (Wan et al. 2014).

pH

Changing pH with the addition of external components intended to improve microalgal culture may instead affect them negatively, causing damage to cellular processes, particularly to the pH-sensitive microalgal cytoplasm and its enzymes. pH variation can be influenced by composition, buffering capacity, CO_2 concentration, temperature and metabolic activity of the cell. The optimal pH generally ranges from 6 to 8, and beyond this range, the biomass yield will be reduced. Some species can tolerate pH levels as low as 3 and as high as 10 (Chowdury et al. 2020). The favourable pH of *Scenedesmus* sp. is found to be between 7-9, obtaining maximum productivity and yield of biomass. pH level beyond the range slows down growth, resulting in lower cell density (Difusa et al. 2015; Tripathi et al. 2015).

During the photosynthesis process, hydroxide ions (OH^-) are produced as microalgae grow, leading to an increase in pH due to CO_2 fixation. This encourages the formation of carbonates. Decreasing pH will shift the chemical equilibrium to form CO_2 instead, which is a preferred carbon source for microalgae. The release of CO_2 could also instead be released into the atmosphere, decreasing the availability of carbon sources for microalgae. pH increases with decreasing concentrations of both Nitrogen and phosphorus available to microalgae. High pH promotes the production of ammonia, which can be released into the atmosphere through aeration, and the precipitation of phosphate (Chowdury et al. 2020). Therefore controlling fluctuating pH in the media will maximise the continuous growth of strain.

Salinity

Salinity stress could cause a high amount of ROS to accumulate in cells and reduce photosynthetic pigments like Chl-a, Chl-b and total carotenoid content. This lowers the photosynthetic efficiency, reduces PS II activity and changes the culture colour from green toward yellow with an increase in salt concentration (Pancha et al. 2015). Monitoring salinity is important as it can increase over the period of evaporation, through aeration, or cultivation in open ponds (Chowdury et al. 2020). *Scenedesmus* sp. is categorised as halotolerant, capable of osmotic adjustment to adapt and grow in saline conditions. This is possible through physiological adaptations to stress, such as shifting cell energy storage towards lipids or accumulating osmoprotectants to protect their bio-compounds (Arora et al. 2019). Therefore, inducing microalgae in controlled salinity stress has been found to be helpful in increasing lipid content, particularly high amounts of saturated fatty acids, which are ideal for fuel properties with the possibility of low/negligible changes in biomass (Gour et al. 2020). In one study, *Scenedesmus* sp. exhibited the highest specific growth rate and doubling per day when grown with 40mM of NaCl, and this rate decreased with an increase in salt concentration, accumulating the highest lipid content with 160mN of NaCl (Gour et al. 2020).

2.2. Type of media for Microalgae cultivation

Different types of media are used in microalgae cultivation, and the nutrient composition varies depending on the source, the type of species cultured, and the intended application. Culturing media can also be prepared in the laboratory, adjusting the type and concentration of nutrients according to experimental requirements. Bold's basal media (BBM) (Bold, 1949) is widely used as an optimal medium for cultivating freshwater microalgae and was used in this master's thesis.

However, the use of optimised nutrient media for large-scale applications has been shown to be expensive and less economical. As a result, waste resources have been found to be a cheaper and more sustainable alternative. There are various types of wastewater with different nutrient compositions used for different remediation purposes and compound production. Some wastewater may not contain the major nutrients required for cultivation but can be utilised for other applications, such as maintaining the cultivation temperature. Industrial flue gas emissions, which contain a mixture of gases and high amounts of CO2, can be used as a carbon source for cultivation. Although these gases may contain particles and metals that could potentially have a positive effect on microalgae, they should be supplied in low concentrations and filtered to remove toxic compounds such as H2S. This concept contributes to a circular economy where water resources are fully utilised, and valuable biomass is produced towards the goal of achieving CO2 neutrality for the factory (Cheregi et al. 2019). In this thesis, wastewater was collected from a municipal wastewater treatment plant and an offshore platform.

2.2.1. Municipal Wastwater

Municipal wastewater, for example, is typically rich in essential nutrients such as nitrogen and phosphorus produced by humanism, like urbanisation and agriculture. If not treated properly, it can cause eutrophication in lakes resulting in devastating effects on the environment and wildlife. Moreover, conventional wastewater treatment may not be sufficient to remove some harmful substances effectively and completely. On the other hand, Microalgae have great potential for bio-treating, producing valuable biomass and reducing greenhouse gas emission, which is a huge advantage (C. Wang et al. 2013).

Municipal wastewater can be categorised into three parts with a different nutrient composition that affects microalgae growth: 1) raw sewage found before primary settling. 2) secondary effluent after activated sludge treatment, and 3) centrate, a byproduct of sludge dewatering that contain a high amount of nutrients (L. Wang et al. 2010).

Table 2.1: Characteristics of primary and secondary effluent from different wastewater treatment plant

Source of Wastewater	TS mg/L	TSS mg/L	COD mg/L	TN mg/L	TP mg/L	Reference
Primary Effluent	1977.9	1334.98	224 - 400	38.9 - 52.6	4.23 - 6.8	(Moondra et al. 2021; Msanne et al. 2020; L. Wang et al. 2010)
Secondary Effluent			42.2	11 - 19.1	0.3 -1.5	(Johnson et al. 2008; Msanne et al. 2020)

Comparing the different categories, L. Wang et al. 2010 have found that cultivating with centrate, both with and without autoclaved, results in a high nutrient removal efficiency of around 90% and an almost threefold increase in algae growth rate compared to primary wastewater. In contrast, primary wastewater yields only $\frac{1}{4}$ biomass productivity compared to optimal nutrient media (L. Wang et al. 2010). Moreover, the presence of microbes poses additional challenges when cultivating in primary wastewater, further affecting biomass productivity.

However, the secondary effluent is loaded with inorganics nitrogen and phosphorus, refractory organics and heavy metal, making it highly suitable for microalgae cultivation. Microalgae can effectively remove ammonium, nitrate, phosphate, heavy metals, organic compound and soluble minerals, which are typically targeted in tertiary and quaternary treatment. This approach eliminates the use of reagents for P removal and re-circulation of wastewater for N removal, reduces cost, improves water quality and produces biomass for further application use. (Abdel-Raouf et al. 2012)

2.2.2. Produced water

Produced water is a waste product generated by the oil and gas industry, and it accounts for the highest percentage of the waste produced in these sectors. It is commonly trapped within the rocks in subsurface formation and can be defined as water used during production or processes. During the extraction process, it is brought up to the surface as a byproduct, resulting in a mixture of oil and chemical from drilling, production and treatment. The volume of produced water extracted increases drastically with the age of the well and depletion of oil and gas, leading to a water-to-oil volume ratio of up to 12:1 (Al-Ghouti et al. 2019).

The characteristic of produced water varies depending on geographical location, age, depth and hydrocarbon-bearing formation, extraction methods, type of hydrocarbon produced and reservoir chemical composition. Produced water composition contains a mixture of complex chemicals, which are organic and inorganic, including different types of hydrocarbons and heavy metals (Al-Ghouti et al. 2019). Additionally, the produced water salinity can range from near fresh water to over 200,000ppm Total Dissolved Solids (TDS). Due to this mixture, along with industrial chemical contamination, produced water is likely to be toxic to microalgae (Graham et al. 2017).

Table 2.2: Characteristic of Produced water in different offshore fields in different parts of the world

Source of Produced water	COD mg/L	TN mg/L	TP mg/L	Reference
Offshore, Shiner Texas	27000 - 35000	-	-	(Gomes et al. 2009)
Offshore NGSPWs, USA	2600 - 120000	-	-	(Johnson et al. 2008)
Denver-Julesburg basin	1121 - 3320	28.1	<1.1	(Nicholas & Cath, 2021)
Yanchang oilfield, China	177.1	-	0.083	(Nie et al. 2020)
Ouargla oilfeld, Algeria	3873	56	4.9	(Nicholas & Cath, 2021)

The nutrient content of Produced water primarily consists of inorganic compounds such as sodium, chloride, calcium and bicarbonate, along with high micronutrient concentrations like iron, zinc and manganese, which are essential to microalgae growth. However, the quality of N sources in produced water is relatively lower. They also contain certain organic compounds, such as carboxylic acid (volatile fatty acid) components, that are beneficial to microalgae in low concentrations. Apart from that, produced water also contains pollutants like nickel which may increase the possibility of metal toxicity or be transferred to the coproducts of algal applications (Graham et al. 2017). Studies have also indicated that variations of BTEX aromatics concentration could induce morphological change, such as alterations in cell shape and chlorophyll content, while the presence of heavy metals could lead to microalgal flocculation, both of which lead to inhibiting growth. (Pessôa et al. 2022)

Given the limitation in analysing every component of Produced water, this study focuses on evaluating the nutrient factor that is useful and contributes to microalgae growth.

2.3. Microaglae based advance treatment

Many studies have highlighted the potential of Microalgae as an alternative approach to biological treatment for wastewater in treatment plants. Microalgae possess the robustness to thrive in extreme conditions and the ability to remove nutrients, as well as the ability to take up other pollutants and convert them into biomass. Wastewater treatment typically consists of two processes, primary and secondary treatment, with some systems incorporating a tertiary treatment. During secondary treatment, microbes present in wastewater utilise organic compounds as food, leading to the release of greenhouse gases. Microalgae offer the potential for phytoremediation and the formation of microalgae-bacteria consortia where microalgae take up CO_2, macro and micronutrients, releasing oxygen during photosynthesis, which is subsequently utilised by aerobic bacteria to degrade organic matter into CO_2, soluble phosphorous and different inorganic nitrogen sources. Nitrogen and phosphorus, the key nutrients required by microalgae, are typically derived from the metabolic interconversion of extra-derived compounds and synthetic detergents, respectively. These nutrient can take different form including NH_4^+ (ammonia), NO_2^- (nitrite), NO_3^3 (nitrate) and PO_4^{3-} (orthophosphate) (Udaiyappan et al. 2017).

2.3.1. Nanoparticles (NP)

Ongoing studies on the addition of nanoparticles (NP) to microalgae cultivation have demonstrated positive outcomes, generating significant interest in their potential for enhancement. The incorporation of small quantities of metal NP into microalgae cells can serve as cellular functionality and nutrient supplements. For example, metals such as Cu and Fe play a critical role in photosynthetic electron transport proteins and promote microalgae growth and lipid production. However, high dosages of NP can be toxic to microalgae, causing alterations in their chemistry, inhibiting essential processes, and potentially impacting their morphology (Miazek et al. 2015) (Vargas-Estrada et al. 2020). The concentration at which toxicity occurs primarily depends on the type of NP and the species of microalgae, apart from the other parameters such as culture media, pH, shape and size of the NP. Another advantage of NP addition is their bactericidal properties which inhibit the growth of microbial and fungi populations. This is extremely beneficial as these organisms compete for nutrition with microalgae. Studies have also found that NP can possibly complement nutrient deficiencies in wastewater or adsorb the available nutrient. TiO_2 is an example that limits nutrient availability and has been shown to decrease biomass when cultivated with *Scenedesmus* sp. (Chen et al. 2018). Conversely, Al_2O_3 enhances the growth of *Chlorella* sp. (Ji et al. 2011).

Reactive oxygen species (ROS) are naturally produced during cellular oxidative metabolism in plants, including microalgae, as part of aerobic processes. While ROS have an important role, such as signal transduction and transcription factor expression, they can also be produced in excess during abiotic stress, which leads to increased toxicity, disruption of metabolic activity and oxidative damage to cell

components, which are referred to as oxidative stress. To counteract the harmful effects of ROS, special proteins such as ascorbate peroxidase (APX) or catalase (CAT), antioxidants like ascorbic acid or glutathione (GSH) and various metabolic adaptations are produced or utilised to neutralise or overcome ROS toxicity (Choudhury et al. 2017). The imbalance of ROS causes the inhibitions effect due to the high concentration of NP exposure. When microalgae are stressed, ROS are produced in excessive amounts, leading to oxidative stress and cellular damage. Moreover, NP can also form agglomerates together with microalgae and settle over time. This attachment can damage the cell structure and surface, causing irreversible damage and contributing to NP toxicity with increased exposure. The addition of low NP concentration allows for the presence of sufficient defensive enzymes to control ROS levels, thereby elevating the biomass. However, recent studies have shown that high concentrations of NP can boost biomass significantly at the early growth stage, as the microalgae's defensive mechanisms are able to cope before the exponential increase in ROS accumulation over time (Vasistha et al. 2021).

Oxidative stress can be advantageous when manipulated to target the enhancement of specific compound production, such as pigments, lipids, and peptides, which are produced when the cell's defensive mechanisms are triggered in response to metal stress. However, this method may have an impact on cell number, growth rate and dry cell weight (Miazek et al. 2015). For instance, studies have observed an increase in lipid content in *Scenedesmus* sp. when grown in the presence of 150mg/l SiC NP, resulting in a 40% increase in lipid production. It was found that the stress condition stimulated the activity of enzyme acetyl-coenzyme A carboxylase, increasing the synthesis efficiency and catalysing the biosynthesis of algal lipids (Ren et al. 2020). Also, *Scenedesmus obliquus* was growth in the presence of carbon nanotubes, Fe_2O_3 NP and MgO NP, resulted in increase lipid productivity by 8.9%, 39.6% and 18.5% at 5mg/l 5mg/l and 40mg/l concentration respectively. Furthermore, it was also observed that higher NP concentration led to inhibition of cell growth and biomass accumulation (He et al. 2017). Exposure to metal has also been found to alter the fatty acid profile of microalgae, improving the quality and properties of biodiesel (Miazek et al. 2015).

2.4. *Scenedesmus* sp.

Scenedesmus sp. is a non-flagellated, unicellular green microalgae that typically exhibits a spiny shape. It is commonly found arranged linearly in colonies of two or more cells and has a size of about 5 - 13 μm (Jena et al. 2014). These freshwater microalgae are commonly found as the dominant species in fresh lakes and rivers. They are widely studied due to their adaptability, tolerance and capability to high nutrient and heavy metal removal as well as high lipid production. They can obtain a nutrient removal efficiency of more than 80%. These studies correlate to many applications within the wastewater treatment sector (Plöhn et al. 2021).

Notably, *Scenedesmus* sp. is recognised for its efficiency in photosynthesis, nutrient

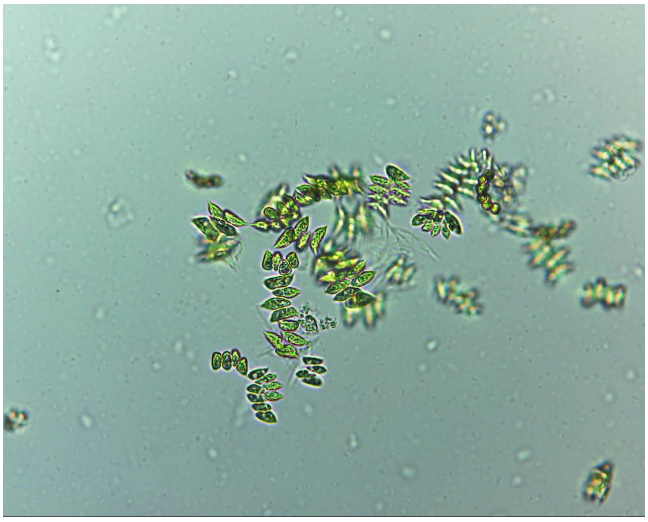

Figure 2.1: *Scenedesmes.*sp arranged in colonies of 4, 8 and more cells, seen under an optical microscope with x40 magnification.

removal, rapid growth, high lipid production rates, and significant amounts of fatty acids. It also possesses resistance to carbon dioxide and ammonium, making it a favourable choice for biofuel production (Soares et al. 2018). In addition to its conventional use as an algae species, *Scenedesmus* sp. is often employed as a bio or pollution indicator to detect physical and chemical changes in the environment (Bauer et al. 2012).

Table 2.3: Nutrient profiles of wastewaters, amount of wastewater dilution used, and the nutrient removal rates by *Scenedesmus* sp.

Source of wastewater	Nutrients composition (mg/l)	Dilution	Removal efficiency %	Reference
Settled Sewage	36.07 TN 9.58 TP	100% WW	46 TN 88 TP	(Tam & Wong, 1989)
Activated Sludge	24.17 TN 10.04 TP	100% WW	32 TN 61 TP	(Xin, Hong-Ying, & Jia, 2010)
Raw WW	79.8 TN 28.69 TP	50% WW	93 TN 61 TP	(Oliveira et al. 2018)
Effluent after AS	11-14 TN 1-1.5 TP	100% WW	>95 TN >95 TP	(Shen et al. 2015)
WW Effluent	30 TN	100% WW	93 TN	(Amini Fard et al. 2019)

Despite the capabilities of *Scenedesmus* sp., the efficiency of nutrient removal can also depend on the availability of different nitrogen sources in the cultivation media. In one study conducted by Xin, Hong-ying, et al. 2010, *Scenedesmus* sp. was grown in BBM and was found to exhibit fast growth when ammonium is used as a nitrogen source. However, inhibition of growth and nutrient removal was observed during the stationary growth phase. On the other hand, when nitrate and urea were used as nitrogen sources, *Scenedesmus* sp. exhibited high Total Nitrogen (TN) removal efficiency of 90% and 87.8% and Total Phosphorus (TP) removal efficiency of over 90%. Furthermore, it did not grow well with ammonium, resulting in a low TN and TP removal efficiency of 31% and 76%, respectively. This could be attributed to the release of H+ due to ammonium uptake during photosynthesis which inhibited growth (Xin, Hong-ying, et al. 2010).

Table 2.4: Nutrient profiles of Produced water, cultivation methods, and the nutrient removal rates by *Scenedesmus* sp.

Type of Microalgae	Nutrient Composition (mg/l)	Methods	Removal Efficiencies %	Reference
Chlorella sp.	32.43 TN 0.17 TP	100% PW	16.4 TN	(Das et al. 2019)
Scenedesmus Sp.	27.6 TN 180 TP	5 different dilution of PW	63.76 TP 58 TM	(Das et al. 2019)
Scenedesmus Sp.	35.8 TN 277.8 TP	4 different dilution of PW	63.7 TN 55 TP	(Hakim et al. 2018)
Chlorella			58.8 TN 73.2 TP	(Hakim et al. 2018)
Neochloris			55.2 TN 57.2 TP	(Hakim et al. 2018)
Dictyosphaerium sp.			61.1TN 88.3 TP	(Hakim et al. 2018)
Monoraphidium sp.			62.9 TN 35.2 TP	(Hakim et al. 2018)

Furthermore, Xin, Hong-Ying, Ke, et al. 2010 found that the removal of phosphorous was not influenced by the concentration ratio between nitrogen and phosphorous (N:P), whereas nitrogen removal was affected by phosphorus limitation. The optimal N:P should be as close as the Microalgae N:P ratio to be at 7.2:1, based on the empirical formula. They found that efficient removal of both nutrients occurred when

the N/P ratio ranged between 5:1 and 8:1. *Scenedesmus* sp. adjusted its nutrient removal preferences when the N:P ratio deviated from its elemental composition. In addition, when *Scenedesmus* sp. was grown in low nutrient concentrations, it resulted in high lipid content accumulation but low biomass production. Therefore it is suggested to accumulate large quality of biomass before inducing lipid accumulation with nutrient limitation conditions for optimal results. (Xin, Hong-Ying, Ke, et al. 2010).

In this thesis, *Scenedesmus* sp. was used to study the bioremediation of wastewater. The microalgae were cultivated in three different types of wastewater: Dissolved Air Flotation effluent (DAF), produced water (PW), and Sequencing Batch Reaction effluent (SBR). Subsequently, Iron nanoparticles (NP) would be added to investigate their influence on the bioremediation and biogas production of *Scenedesmus* sp. Tables 2.3 and 2.4 are data from literature studies on *Scenedesmus* sp. and other microalgae cultivated in similar media of WW and PW.

Methods

3.1. Material and methods

3.1.1. Pre-culture Preparation

Most equipment was covered with aluminium foil. For glassware, the foil was placed on the openings, and the remaining parts were wrapped. A steam tape was applied to each apparatus to indicate steam exposure. Apparatus were transferred into TOMY SX-700E for autoclaving at 120 °C for 100 minutes. Subsequently, the equipment was transferred to a closed cabinet and exposed to UV light for 10 minutes before the start of the experiment. Rubber tubes and rods were cleaned with ethanol instead.

Figure 3.2: Equipment placed in the closed cabinet for UV exposure

3.1.2. Wastewater

Two wastewater (WW) samples were collected from IVAR Grødaland: one from the primary treatment effluent (DAF) and another from the secondary treatment effluent (SBR). Additionally, one WW sample was obtained from an offshore platform by Akersolution, known as produced water. To remove suspended solids, all WW were filtered through 0.7 μm Whatman^{TM} Glass Microfiber filters. Subsequently, the filtered WW were autoclaved to sterilise them and eliminate any bacteria and pathogens. Before and after sterilisation, the filtered WW were extracted and analysed for parameters such as Chemical Oxygen Demand (COD), Total Phosphorus (TP), Total Nitrogen (TN), and Total Suspended Solids (TSS).

3.1.3. Experiment design

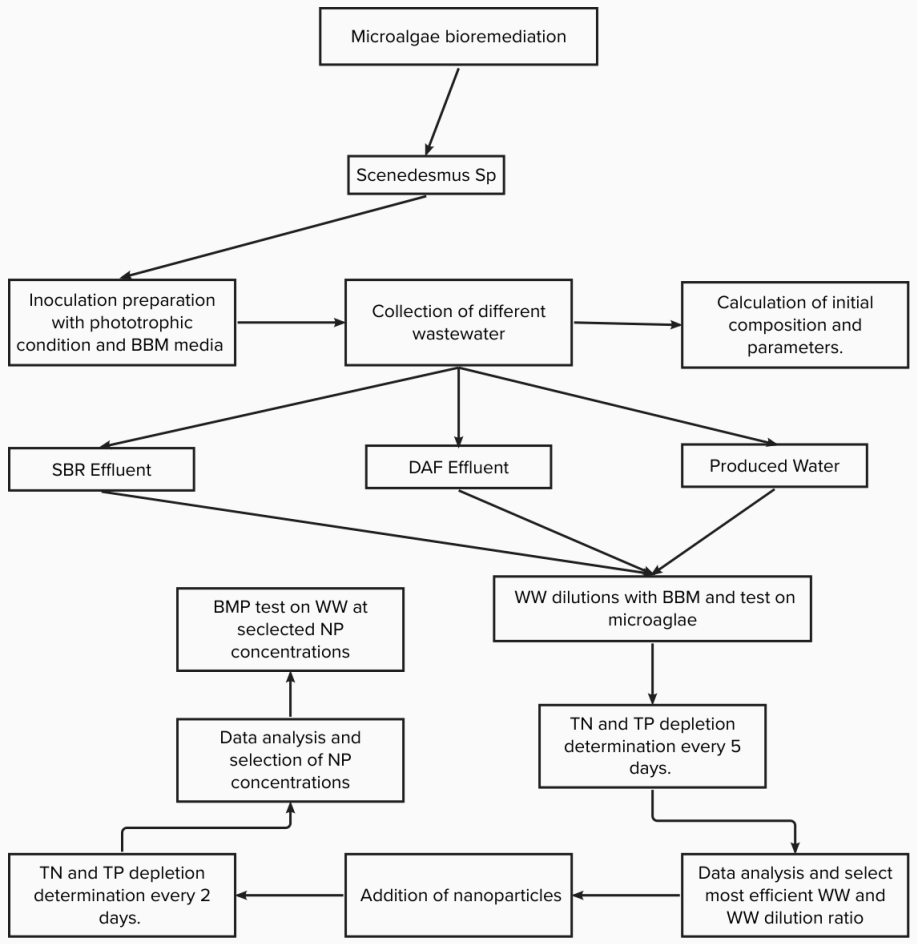

Figure 3.3: Experimental design and workflow of the thesis.

Microalgae cultivation

Scenedesmus sp. was collected from a local lake and isolated in the laboratory for usage in this experiment. The microalgae were cultured in BBM (Bold's Basal Medium) as the growth medium. For each WW experiment, the microalgae were inoculated at a 1:10 fraction of BBM in a 250 ml conical flask, with a total volume of 100 ml. The BBM medium composition was as follows g/l : 25 $NaNO_3$, 7.5 $MgSO_4.7H_2O$, 2.5 $NaCl$, 7.5 K_2HPO_4, 17.5 KH_2PO_4, 2.5 $CaCl_2.2H_2O$, 11.42 H_3BO_3, 50 $EDTA$, 31 KOH, 4.98 $FeSO_4.7H_2O$, 1 H_2SO_4. Additionally, a trace elements solution was added to the medium solution of (gL^{-1}): 8.82 $ZnSO_4.7H_2O$, 1.44 $MnCl_2.4H_2O$, 0.71 MoO_3, 1.57 $CuSO_4.5H_2O$, 0.49 $Co(NO_3)_2.6H_2O$. The mother cultures of *Scenedesmus* sp. were grown photoautotrophically in a closed system. The temperature was controlled at 22°C, and the light density was maintained at 100± 10 W/m^2 with a 12-hour light-dark cycle and intermittent orbital shaking at 120 rpm by using a shaker. The microalgae were allowed to grow until they reached the logarithmic growth phase, typically around 5-6 days. Then, they were transferred to

the different WW samples, using the same fraction, to allow acclimatisation and adaptation to the individual WW conditions (Figure 3.4). The microalgae were further cultured until reaching a specific concentration before the start of the experiment.

Figure 3.4: *Scenedesmus* sp. cultured with WW as growth media in an incubation cabinet with a controlled condition. This was to allow microalgae to adapt to individual WW

Once the microalgae reached a concentration of 2 g/L, they were added to the experiment media of 1:10 ratio (Microalgae: experiment media). The dilution ratios of experiment media were % of WW with BBM, at 25%, 50%, 75% and 100%. 500 ml conical flasks were used for each dilution sample, with a total volume of 200 ml. (Eida et al. 2018). To create mixotrophic conditions, each sample was provided with a continuous air supply at a flow rate of 0.2vvm. This setup allowed the microalgae to utilise both organic and inorganic carbon from the wastewater, air and light energy for growth (Figure 3.5). Each set of experiments was conducted in duplicate and lasted for approximately 10 days. Measurements of Total Suspended Solids, Total Nitrogen (TN), and Total Phosphorus (TP) were initially taken and then repeated every five days throughout the cultivation period. After 10 days, the cultivation was terminated, and data collected, along with corresponding graphs, were analysed to evaluate the performance of microalgae cultivation in different WW samples.

Only for produced water, it was filtered through 0.7 μm Whatman^{TM} Glass Microfiber filters once again after autoclaving to remove any newly generated suspended solids. This additional filtration step ensures the removal of any particulate matter that may have been introduced during the autoclaving process.

Following the completion of the experiment, the remaining microalgae biomass was collected and packed into 50 ml centrifuge bottles. The biomass was then centrifuged to separate the microalgae cells from the liquid medium. This process facilitated the concentration and preservation of the microalgae biomass for future use or analysis.

Figure 3.5: WW experiment setup in the incubator in the incubation cabinet with additional air pump and controlled condition.

3.1.4. Nanoparticles (NP)

Pure Fe_3O_4 NP were synthesised chemically at UiS. The experiment was conducted under supervision and guidance. The synthesis process can be summarised in four steps, as shown in Figure 3.6:

1. $F3_3O_4$ solution was produced after adding and mixing the calculated amount of compounds inside a 3-neck round bottom flask. The required amount of compounds was calculated via $F3_3O_4$ stoichiometry equations equation.
2. The $F3_3O_4$ precipitation was extracted from the liquid by placing the magnet on the bottom of the flask and allowing it to settle. This was done a few times by washing the precipitation with distilled water.
3. Fe_3O_4 NP powder was collected into an airtight glass bottle and purged with nitrogen gas to prevent oxidation for the preservation of Fe_3O_4. The picture also showed the magnetism capability when placed on top of a magnet.
4. Fe_3O_4 NP powder was collected into an airtight glass bottle and purged with nitrogen gas to prevent oxidation for the preservation of Fe_3O_4. The picture also showed the magnetism capability when placed on top of a magnet.

After selecting the desired WW and dilution ratio, the newly set up experiments were supplemented with Fe_3O_4 nanoparticles (NPs) at eight different concentrations: (0, 1, 2.5, 5, 10, 25, 50 and 100 mg/l) Each experiment was conducted in duplicate to ensure reproducibility and accuracy of the results. To initiate this experiment, the microalgae biomass from the previous experiments, which corresponds to the desired dilution ratio, was diluted with distilled water to achieve a similar initial biomass used in the chosen wastewater (WW) experiment. The total working volume for each experiment was maintained at 200 ml to ensure consistency across all samples. By maintaining the same initial biomass and total working volume, any variations in the experimental results could only be attributed to the different concentrations of iron oxide NPs

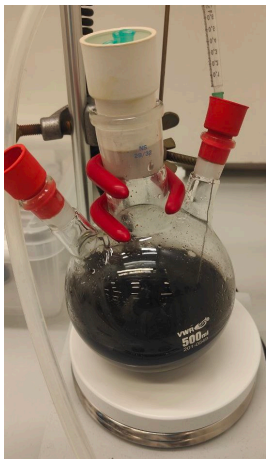

(a) step 1 - Fe_3O_4 solution in 3 neck round bottom flask

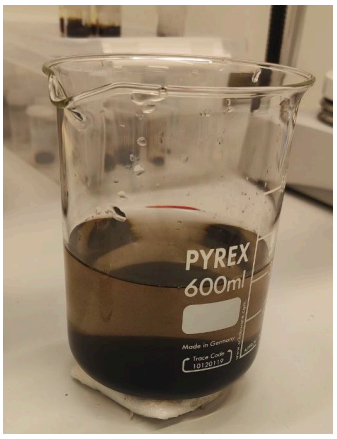

(b) Step 2 - Fe_3O_4 extraction from liquid using a magnet

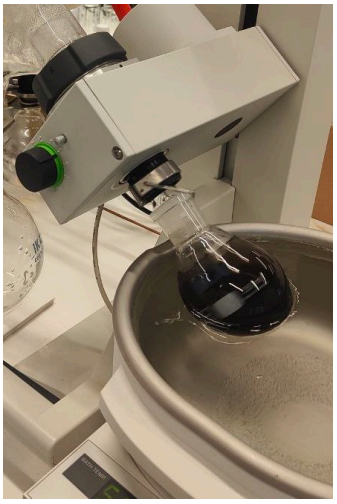

(c) Step 3 - Drying of Fe_3O_4 NP by rotary evaporator

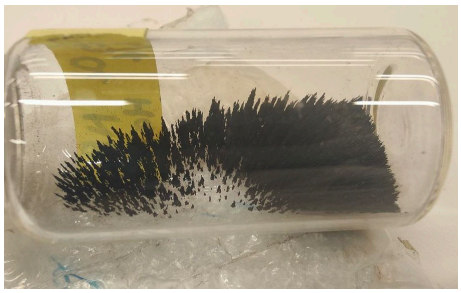

(d) Step 4 - Fe_3O_4 NP collected and tested with magnet

Figure 3.6: A summary of $F3_3O_4$ NP synthesis steps starting from a to d.

added to the samples.

Sonication of nanoparticles

The iron oxide nanoparticles (NP) were carefully weighed according to the desired concentrations and distributed into empty glass tubes. Each test tube was added with 1 ml of deionised water to facilitate the sonication process. The sonication was carried out using a Branson 2510 ultrasonic bath, which generated a sweep frequency of 40 Hz. The test tubes containing the NPs and water were marked for identification and then securely attached to a clamping stand, ensuring they were positioned in the water bath.

The NPs were subjected to sonication for a duration of one hour. This ultrasonic treatment aimed to achieve complete homogenisation of the NPs, ensuring they were uniformly dispersed in the solution. However, if any clumps or agglomerates of NPs were still visible after the initial sonication period, the test tubes were gently shaken and returned to the ultrasonic bath for an additional hour of sonication.

The objective was to obtain a well-dispersed and homogenous suspension of NPs, free

Figure 3.7: NP after sonication lined up in increasing concentration from left to right

from any visible clumps, which was crucial for ensuring consistent and accurate results in the subsequent experiments.

3.1.5. Biochemical methane potential (BMP) manual method

The biochemical methane potential test is an anaerobic digestion test to understand the methane production potential of an organic substrate under anaerobic conditions. The process occurs in an oxygen-free condition with a controlled temperature where the anaerobic organism digests the organic substrate to produce biogas which is primarily composed of methane and carbon dioxide (González-Fernández et al. 2012).

Table 3.5: Nutrient, buffer and trace elements composition used for BMP test

Component	Theoretical Concentration (mg/ 200ml)	Actual Concentration (mg/ 200ml)
KH_2PO_4	100	100.74
NH_4Cl	106	107.33
$Cacl_2 \cdot 2H_2O$	15	15.72
$MgCl_2 \cdot 6H_2O$	20	20.47
$FeCl_2 \cdot 4H_2O$	4	4.67
$NaHCO_3$	800	800.78
$MnSO_4 \cdot 4H_2O$	3	3.22
$CuSO_4 \cdot 5H_2O$	1	107
$CoCl_2 \cdot 6H_2O$	0.025	0.05
$FeSO_4 \cdot 7H_2O$	5	5.62

The dilutions with the selected concentrations were utilised as substrates for testing biogas production. Sludge was collected from IVAR to be used as an inoculum, and a 1:1 ratio of inoculum to substrate (ISR) was applied to determine the appropriate

concentration. To determine the concentration required, the volatile solids (VS) of the inoculum were compared against the Chemical Oxygen Demand (COD) of the substrate, following the method described by (González-Fernández et al. 2012). Glucose was used as the positive control in this experiment.

The empty BMP bottles were autoclaved to ensure cleanliness. Each bottle, with a capacity of approximately 100ml, was divided into two parts: 35ml of headspace and 65ml of working volume. The working volume consisted of 50ml of inoculum and substrate, 10ml of nutrient plus buffer, and 5ml of deionised (DI) water. The nutrient and buffer media were prepared, containing various compounds as specified in Table 3.5. The pH of the sample media was adjusted to approximately 7-8 using HCl and NaOH, and the values were recorded. Subsequently, the bottles were capped and sealed with metal caps using a clamping tool to ensure a tight seal and prevent any openings. To create a closed system, two needles were injected into the bottles as an inlet and outlet for degassing the oxygen using nitrogen (Figure 3.8). The bottles were allowed to degas for 1 minute.

Figure 3.8: 2 needles acted as an inlet and outlet, and nitrogen was used to purge out oxygen to create anaerobic conditions.

The sealed bottles were placed on a shaker inside the Fermaks drying oven incubator, where a constant temperature of 37.5°C was maintained (Figure 3.9). The shaker was set to run at 150 rpm to prevent sedimentation from occurring in the bottles. Gas measurements were recorded twice daily by injecting a glass syringe into the bottles and measuring the volume of gas produced. This measurement procedure was repeated for a few days. If there was a minimal amount of gas produced during the second measurement, the frequency of measurements was reduced to once per day.

Figure 3.9: BMP Bottles placed on the shaker inside the incubator

Figure 3.10: Gas chromatography on BMP bottles was analysed using Agilent Technologies 7890B GC system

The biogas characterisation was conducted using the Agilent Technologies 7890B GC system, as shown in Figure 3.10. Prior to turning on the machine, the valves of the hydrogen, nitrogen, and oxygen cylinders were opened. The machine was then allowed to run and stabilise for an hour before the experiment commenced. To ensure stability, the pressure and temperature readings from all sensors were

Figure 3.11: Insert the gas through a metal inlet tube immediately after extracting gas to prevent gas contamination

double-checked by pressing the corresponding buttons on the machine, such as "oven," "front inlet," and "valve."

After completing the aforementioned procedure, the "prep run" button was selected to initiate the experiment. Gas was extracted from the bottle, and the corresponding value was recorded. To minimise the presence of oxygen in the measurement, the gas was immediately injected into the metal inlet tube, as depicted in Figure 3.11. This process was repeated for all samples.

3.1.6. Analysis and calculation

Total Solids (TS), Total Suspended Solids (TSS) and Volatile Suspended Solids (VSS) measurement

Total Solids (TS) represent the complete amount of solid matter present in a sample and can be further divided into total suspended solids (TSS) and total dissolved solids through the process of filtration. Volatile suspended solids (VSS) represent the portion of suspended solids that can be volatilised through high-temperature ignition.

To begin the analysis, samples were collected and placed in clay plates, and their weights were measured using a Mettler Toledo XP204 balance. Each sample was marked for identification purposes. The samples were then placed in a VWR Dry-line oven at 105°C and allowed to dry for a minimum of 24 hours before being reweighed.

For the determination OF TSS, Whatman^{TM} filter papers were used. The filter papers were individually weighed, and the sample was extracted at the designated volume and filtered through the filter paper with a specific pore size based on the experimental requirements. To expedite the filtration process, a vacuum pump was employed. The filter paper containing the suspended solids from the sample was reweighed and placed in the oven to dry under the aforementioned parameters.

After the dried sample was reweighed, it was transferred to a Nabertherm muffle furnace B170 and ignited at 550°C for a period of 6 hours. Following the ignition process, the sample was allowed to cool in the oven, and the clay plate was reweighed to calculate the VSS.

The TS and VS are calculated as follows:

$$TS(mg/l) = \frac{(Weight_{Dry\ sample\ with\ clay\ plate} - Weight_{clay\ plate})(mg)}{Volume_{sampling}(l)} \tag{3.1}$$

$$TSS(mg/l) = \frac{(Weight_{dry\ sample\ with\ filter} - Weight_{filter})(mg)}{Volume_{filtering}(l)} \tag{3.2}$$

$$VSS(mg/l) = \frac{(Weight_{Inigited\ sample\ with\ clay\ plate} - Weight_{clay\ plate})(mg)}{Volume_{sampling}(l)} \tag{3.3}$$

Chemical oxygen demand (COD) measurement

The oxidation test involved the use of a hot sulfuric acid solution containing potassium dichromate, with silver sulfate serving as the catalyst. This test aimed to measure the concentration of oxidised organic and inorganic compounds in the sample. It produced a concentration of unconsumed yellow $Cr_2O_7^{2-}$ or green Cr^{3+} ions, which could be determined photometrically. For the measurement, the Spectroquant® COD cell test kit (Hg-free) with a serial number 1.09773 was utilised. This test kit has a measurement range of 100-1500 mg/COD. To begin, 2 ml of the sample was added to the reaction cell, and the contents were vigorously mixed within the cell. The reaction cell was then placed in a preheated thermoreactor at 148°C for a

duration of 120 minutes. After digestion, the reaction cell was removed from the thermoreactor and allowed to cool before being measured in the photometer.

Total Nitrogen (TN) measurement
In accordance with Koroleff's method, the oxidation of organic and inorganic compounds into nitrate occurs using a reacting agent in the thermoreactor. In the Spectroquant® Nitrogen (total) cell test kit, this reaction takes place with 2,6-dimethylphenol (DMP), resulting in the formation of 4-nitro-2,6-dimethylphenol, which can be measured photometrically. Alternatively, a benzoic acid derivative can also be used to react with nitrate, forming a red nitro compound. Both methods allow for the determination of nitrate concentration.

Spectroquant® Nitrogen (total) cell test kit is available in different versions, each with a unique serial number: 1.14763.0001, 1.00613.0001, and 1.4537.0001. These kits have different measurement ranges, with the first kit measuring in the range of 10-150 mg/l N and the other two measuring in the ranges of 0.5-15 mg/l N. It is important to consider the maximum COD of the sample before conducting the TN (total nitrogen) test to ensure reliable data. Therefore, sample dilution may be necessary. All tests followed the same procedure except for the sample preparation step. For kits 1.00613.0001 and 1.4537.0001, 10 ml of pretreated sample was required, while for kit 1.14763.0001, only 1 ml of pretreated sample was needed, along with 9 ml of DI water. The prepared sample was pipetted into an empty cell. Then, 1 microspoon of N-1K and 6 drops of N-2K were added to the cell, and the contents were mixed thoroughly. The reaction cell was digested in the preheated thermoreactor at 120°C for 60 minutes.

After digestion, the reaction cell was removed from the thermoreactor and allowed to cool. It was then shaken after 10 minutes. Next, 1 ml of the digested sample supernatant and 1 ml of N-3K were transferred to the reaction cell and mixed. However, for kit 1.4537.0001, an additional step was required. Prior to adding the digested sample supernatant, 1 microspoon of N-3K (in powder form) was added to the reaction cell and vigorously mixed for 1 minute. Afterwards, 1.5 ml of the digested sample supernatant was added to the cell. The reaction mixture was left for 10 minutes before being measured in the photometer.

Total Phosphorous (TP) measurement
Ascorbic acid was used to reduce the molybdophosphoric acid formed when orthophosphate ions reacted with molybdate ions, resulting in the formation of phosphomolybdenum blue (PMb), which could be measured photometrically.

The Spectroquant® Phosphate (total) cell test kit, with serial numbers 1.14729.0001 and 1.4543.0001, was used for the measurement of phosphate concentration. The first kit had a measurement range of 0.5 - 25mg/l $PO_4 - P$, while the second kit had a range of 0.05 - 5mg/l $PO_4 - P$. To ensure reliable data, the maximum COD of the sample was considered before conducting the phosphate test, and sample dilution was performed if necessary. Both tests followed the same procedure except for the sample preparation

step. For kit 1.14729.0001, 1 ml of pretreated sample was added to the reaction cell, while for kit 1.4543.0001, 5 ml of pretreated sample was used. One dose of P-1K was added to the reaction cell, and the contents were mixed before placing the cell in the preheated thermoreactor at 120°C for 30 minutes.

After the digestion step, the reaction cell was removed from the thermoreactor and allowed to cool. Then, 5 drops of P-2K and one dose of P-3K were added to the cell, and the cell was vigorously shaken. The reaction mixture was left for 5 minutes before being measured in the photometer.

Kinetic growth parameters and calculation

The microalgae biomass was extracted at regular intervals during the experiment, and the solutions obtained were filtered and dried to determine their VSS values in mg/L. These VSS values were used for further calculations.

The specific growth rate μ is a measurement of the rate at which the biomass increases over a specific period of time, expressed in units of (h^{-1}). It can be calculated using the equation shown in Equation 3.4. This measurement provides valuable insights into the efficiency and performance of biomass production in a given growth medium (Esteves et al. 2022).

$$Specific\ growth\ rate,\ \mu = \frac{ln((X_{biomass\ at\ t_2})/(X_{biomass\ at\ t_1}))}{t_2 - t_1} \tag{3.4}$$

where: X represents biomass (mg/l) selected on specific time period represented as t_2 and t_1 (d)

Biomass productivity (P) is defined as the rate at which biomass is produced over a specific period of time, expressed in units of mg/l/d. It can be calculated using the equations shown in Equations 3.5 and 3.6. These calculations provide valuable insights into the capability and potential of growth using the given growth medium (Esteves et al. 2022).

$$Specifc\ Biomass\ Producivity,\ P_x = \frac{X_{biomass\ at\ t_2} - X_{biomass\ at\ t_1}}{t_2 - t_1} \tag{3.5}$$

where: X represents biomass (mg/l) selected on specific time period represented as t_2 and t_1 (d)

$$Average\ Biomass\ Producivity,\ P_{x,\,avg} = \frac{X_{final} - X_{inital}}{t_{final}} \tag{3.6}$$

Where: X represents biomass selected on the initial and final period of the experiment and time is represented as the total time (d) to selected biomass produced.

Biomass yield $Y_{x/s}$, expressed by the biomass produced amount per unit of specific nutrient removed. In this experiment, the nutrients TN (total nitrogen) and TP (total

phosphorus) are used to assess the relationship between biomass production and nutrient consumption. Biomass yield can be represented as $Y_{g\,biomass/g\,TN}$ and $Y_{g\,biomass/g\,TP}$ or expressed as a ratio. It can be calculated using Equation 3.7. A higher value indicates a higher efficiency of biomass production by microalgae per unit of nutrient provided (Esteves et al. 2022).

$$Biomass\ Yield, Y_{x/s} = \frac{P_{x,\,avg}}{Nutrient\,removal\,rate} \tag{3.7}$$

Where: $P_{x,avg}$ (mg/l/d) represents average biomass productivity against nutrient removal rate, TN or TP (mg/l/d). Specific biomass yield is calculated using a specific nutrient removal rate instead.

Nutrient removal calculation

Nutrient removal is measured by the amount of nutrients consumed by the microalgae over a specific period of time. This parameter can be expressed in the following forms: average nutrient removal rate, specific nutrient removal rate, and nutrient removal efficiency. The nutrients referred to here are TN (total nitrogen) and TP (total phosphorus), as measured using the test kit.

The average nutrient removal rate, RR (mg/l/d), is defined as the rate of change in nutrient consumption over the entire experiment. It is calculated using Equation 3.8 (Esteves et al. 2022).

$$Average\ Nutrient\ Removal\ Rate, RR = \frac{S_{final} - S_{intial}}{t_{Final}} \tag{3.8}$$

Where: S represents the nutrient measured in the initial and final period of the experiment, and time is represented as the total time (D) of nutrient removed.

Specific nutrient removal rate (SNR) (mg/g/d) is defined as the rate of nutrient removal per unit of biomass. This measurement quantifies the efficiency of nutrient uptake by the microalgae. It is calculated using Equation 3.9 (Esteves et al. 2022).

$$Specific\ Nutrient\ removal\ rate = \frac{S_2 - S_1}{X_2 - X_1} \tag{3.9}$$

Where: S represents the nutrient removed at a selected specific time period represented as S_2 and S_1 (mg/l), and X (g/l) represents the nutrient removed at a selected specific time period represented as t_2 and t_1.

Nutrient removal efficiency, RE (%) determines the percentage of nutrient removal achieved by the microalgae in a given time period. It provides insights into the effectiveness of microalgae in removing nutrients from the growth media. Nutrient removal efficiency is calculated using the equation given. 3.10 (Esteves et al. 2022).

$$Nutrient\ Removal\ Efficiency(\%) = \frac{S_2 - S_1}{S_2} \cdot 100 \tag{3.10}$$

Where: S represents the nutrient removed at a selected specific time period represented as S_2 and S_1 (mg/l).

The calculations of nutrient removal parameters provide valuable insights into the capabilities of microalgae and the effectiveness of the chosen growing media in removing nutrients. These calculations play a crucial role in evaluating, designing, and optimising experiments to achieve better results. By understanding the nutrient removal potential of microalgae and its relationship with the growing media, researchers can make informed decisions to improve the efficiency and effectiveness of nutrient removal processes.

3.1.7. N:P ratio

The N:P ratio is a valuable tool for understanding the availability and limitation of nitrogen and phosphorus nutrients in the environment and various processes. This ratio is particularly useful in evaluating and optimising nutrient concentrations for optimal conditions, taking into account the specific microalgae species and growth media being used.

In the context of nutrient availability in the media, a ratio of less than 1 indicates a higher phosphorus concentration compared to nitrogen. Higher nitrogen concentration produced a ratio greater than 1. A ratio of less than 10 suggests that phosphorus may be limiting, while a ratio greater than 20 suggests that nitrogen may be limiting.

When comparing changes in nutrient availability in the media, a decrease in the N:P ratio indicates a treatment that is effectively removing more nitrogen than phosphorus. Conversely, an increase in the ratio suggests a treatment that is effectively removing more phosphorus than nitrogen. If the change in ratio is the same, it indicates that both nutrients are being reduced equally.

In terms of comparing changes in nutrient removal rates, a ratio greater than 1 suggests a higher rate of nitrogen removal, while a ratio less than 1 indicates a higher rate of phosphorus removal. A ratio of 1 signifies an equal removal rate for both nutrients.

3.1.8. Biogas and methane gas calculations

Biogas measured in ml were collected at each point of time during the experiment and was summed up to obtain the cumulative volume to plot a graph. Using gas chromatography, the methane content % of each sample was recorded and the methane amount in ml contained in each sample was calculated. After that, all the samples are subtracted with the methane volume obtained by blank to remove any background gas production (Mussgnug et al. 2010). Methane gas for each sample is calculated with the equation 3.11

$$Methane\ volume,\ \frac{ml\ CH_4}{g\ COD} = \frac{(Biogas_{Sample} - Blank)(ml)}{(COD(g/l) * Volume(l))_{Sample}} \tag{3.11}$$

Where: $Biogas_{Sample}$ represents the selected sample biogas, and blank represent sample with no substrate. Use the sample COD and volume that was used for the preparation of the BMP

Results and Discussion

4.1. Wastewater characteristics

In this section, the following wastewater will be labelled as the following for identification: Dissolved air flotation effluent DAF_{WW}, Sequencing Batch Reactors SBR_{WW} and Produced water PW_{WW}

The nutrient profiles and characteristics of the wastewater are listed in the table below. In comparison to the range reported by previous studies, the values differ. $DAF_{WW}$and SBR_{WW} exhibited a mix of lightly brownish and orange colors. Additionally, particles were observed floating in the medium, causing some turbidity. The wastewater had total solids (TS) of 1074 and 1622 mg/l and total suspended solids (TSS) of 175 and 86.7 mg/l, respectively. These values are lower than those reported in one study, which recorded TS and TSS of 1977.9 and 1334.98 mg/l for the primary wastewater effluent. Moreover, the TS in $DAF_{WW}$is higher than that in SBR_{WW}, but the suspended solids are lower. This difference could be attributed to an increase in TDS due to chemical additions during the water treatment process.

Table 4.6: Characteristic of wastewater used for experiment cultivation before autoclaved

	DAF_{WW} mg/l	SBR_{WW} mg/l	PW_{WW} mg/l
Total Suspended Solid	175	86.7	3272.3
Total Solid	1074	1622	86658
COD	1245	505	33250
TN	112	108.5	6720
TP	16.4	4.3	10.5

Referring to table 2.1, the primary and secondary effluents have COD levels below 400 mg/l, TN levels below 52.6 mg/l, and TP levels below 6.8 mg/l. These values differ significantly from what was measured in this experiment, as shown in Table 4.6. Several factors could have contributed to this difference, such as the type of waste collected and treated, the location, the processes/filters used before treatment, and the type of biological microorganism present in the water. The value disparity could also be attributed to the wastewater extraction method, where improper homogenisation may have caused a higher concentration of collected sediments. For instance, one study characterised wastewater collected from Saint Paul, Minnesota,

Figure 4.12: PW_{WW} (Left) and SBR_{WW} (Right) after autoclaving. PW_{WW} looked clear while SBR_{WW} showed orange and slightly brown in colour. Particles could be seen suspended in both mediums, with more over in PW_{WW}.

for microalgae cultivation and reported COD, TP, and TN levels of 2344, 211, and 91 mg/l, respectively (Zhou et al. 2012). Upon comparing the measured values, most of the data from SBR_{WW} are lower than those from DAF_{WW}, which aligns with the process flow.

PW_{WW} also varied depending on factors such as geological location and the extraction method. The PW_{WW} used in this experiment appeared white, translucent and contained suspended solids. After filtration, the suspended solids collected by the filter were orange in colour, while the filtered PW_{WW} were clear and transparent.

High TS and TSS were measured at 86658 and 3272.3 mg/l, respectively. This was likely due to the presence of sea salt remaining in the measurements, resulting from the high salinity of the produced water and possible heavy chemical compounds. Referring to Table 2.2, the general COD, TN, and TP levels were found to be up to 120000, 56, and 4.9 mg/l, respectively, exhibiting some variation from the PW_{WW} used in this experiment at 86658, 6720, and 10.5 mg/l. While the COD values were well within the expected range, the higher nitrogen value could be a result of chemical additions mixed into the PW_{WW} during the oil extraction process. Furthermore, the differing values in 2.2 could be attributed to variations in the collection points of the PW_{WW}.

Table 4.7: Chemical concentration of wastewater after autoclave

	DAF_{WW} mg/l	SBR_{WW} mg/l	PW_{WW} mg/l
COD	566	233	20370
TN	134	83	24
TP	9.2	4	6

Solid particles were observed in excessive amounts after autoclaving the wastewater, specifically in PW_{WW}. This precipitation could be produced by chemical reactions or the degradation of certain compounds during pressurisation and the high temperature of the autoclave. Since the solid particles were present in small amounts in SBR_{WW} and DAF_{WW}, only PW_{WW} underwent an additional filtration process. Moreover, the chemical concentrations in these wastewaters were re-analysed before commencing the experiment.

The chemical concentration of the wastewater was found to decrease after autoclaving, suggesting that the precipitation may have caused this change (refer to Table 4.7). Particularly, the TN concentration in PW_{WW} reduced significantly from 6270 to 24 mg/l.

4.2. Growth of *Scenedesmus* sp. in different concentrations of wastewater

In Eida et al. 2018's study, they found that mixing 75% wastewater with 25% BBM or a 50% mixture of each resulted in increased production of lipid-rich microalgae while conserving water and nutrients. Additionally, they observed improved growth of *Scenedesmus* sp. and enhanced nutrient removal when wastewater was mixed with BBM, compared to growing in BBM alone. The nutrient removal efficiency was particularly significant for TP (approximately 90%) and a high amount for TN. This demonstrated the economic benefits of using wastewater mixed with BBM to cultivate *Scenedesmus obliquus* for biodiesel production (Eida et al. 2018). Based on this economic approach, the current experiment aimed to explore the environmental aspects of using different dilutions of wastewater mixed with BBM to investigate the growth efficiency of *Scenedesmus* sp. and its nutrient removal capabilities.

In this experiment, five different dilutions of wastewater with BBM were used to grow *Scenedesmus* sp., and three data points were collected throughout the experiment to determine which type of wastewater would support more efficient growth of the microalgae, correlating with its nutrient removal capabilities. Day 5 and day 10 were selected for analysis as they represented key transitions in the growth phase of *Scenedesmus* sp. By day 4/5, the microalgae reached the end of the lag phase and entered the exponential growth phase, which continued until day 8/9. By day 10, the cells began to enter a stationary growth phase, slowly decline and die (Nayak et al., 2013). The experimental results demonstrate that *Scenedesmus* sp. was able to grow in all of the wastewater samples successfully.

4.2.1. Dissolved air flotation Effluent

The following labels will be used as acronyms for DAF WW dilutions in this discussion: C_{DAF}; contains only BBM, 25_{DAF}, 50_{DAF}, 75_{DAF} and 100_{DAF}. The wastewater itself will be represented as DAF_{WW}. Referring to the growth curves in figure 4.13, the initial biomass concentration started at 121.5 mg/l and exhibited slow growth within the first

5 days. The biomass range on day 5 varied between 252.25 to 411.5 mg/l, with C_{DAF} obtaining the highest biomass concentration and 100_{DAF} at the lowest. After day 5, the growth of all dilutions increased exponentially, reaching a range of 1350 to 2357 mg/l, with 25_{DAF} resulting at the highest biomass concentration and 100_{DAF} at the lowest. This clearly distinguished the lag and exponential phases of *Scenedesmus* sp. growth.

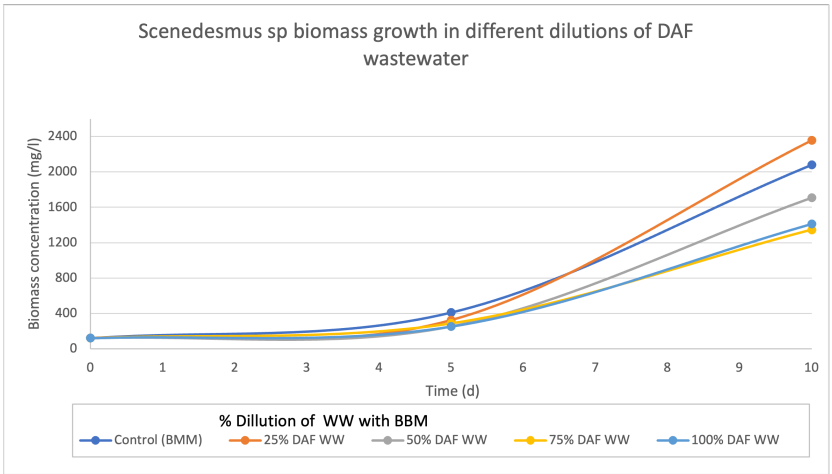

Figure 4.13: Biomass concentration growth of *Scenedesmus* sp. in 5 different dilutions of DAF_{WW}, cultivated in 10 days.

The value gap between all the biomass concentration were closer on day 5, suggesting that the microalgae had just started to adapt to the new environment and grow. As expected, C_{DAF} was at the highest with optimal conditions. The decreased biomass concentration trend with respect to dilution on day 5 could be due to a longer adaptation time. This kind of trend can also be seen in this study by Fazal et al. 2021, where *Chlorella vulgaris* was seen growing more in BMM in autotrophic conditions than in diluted wastewater and undiluted wastewater in mixotrophic conditions on the transition of lag to the exponential growth phase (Fazal et al. 2021). Figure 4.13 also showed that the microalgae were able to adapt better in 25_{DAF} than in C_{DAF}, which could be possible that it had the right amount of nutrients needed for optimal conditions. Referring to table 4.8, 25_{DAF} also showed the highest biomass productivity. Others showed lower biomass productivity than C_{DAF}, which explains the highest final biomass obtained by 25_{DAF}. Most of the dilution has a specific growth rate higher than the C_{DAF} except for 75_{DAF}, therefore also indicates that the microalgae grew well in DAF_{WW} and possible that no harmful contaminants were present to hinder growth. Furthermore, the decreased biomass concentration trend with respect to dilution could also be seen on day 10, which suggested that high nutrient composition could cause microalgae not fully assimilate them. One study that grew *Scenedesmus* sp. with different dilutions had shown that higher biomass was produced in 75% dilution than 100% in domestic wastewater (Silambarasan et al. 2021). As a comparison to the study, this experiment used BBM to dilute, which explains a decreasing trend starting from 25_{DAF} instead.

In terms of specific biomass yield, $Y_{gX/gTP}$ values were higher than $Y_{gX/gTN}$ all dilutions except for the control, indicating that phosphorus was the most limiting factor affecting biomass production when growing in DAF_{WW}. Moreover, 25_{DAF} exhibited significantly higher $Y_{gX/gTN}$ and $Y_{gX/gTP}$ values indicating its efficient utilisation of phosphorus for biomass production compared to the other dilutions. The negative value of $Y_{gX/gTP}$ in C_{DAF} was attributed to an increase in phosphorus concentration observed at the end of the experiment.

Table 4.8: Kinetic growth parameters calculated for the samples with different dilution grown in DAF_{WW}

	Specific growth rate	Final biomass	Productivity P mg/L/d		Specific biomass yield g/g	
DAF_{WW}	μ	mg/l	Avg	Max	$Y_{gX/gTN}$	$Y_{gX/gTP}$
C_{DAF}	0.324	2079.0	195.75	333.50	88.98	-108.75
25_{DAF}	0.397	2357.0	223.6	406.55	77.09	496.78
50_{DAF}	0.381	1707.0	158.6	290.60	27.82	96.09
75_{DAF}	0.308	1350.0	122.9	212.25	16.60	129.32
100_{DAF}	0.344	1411.0	129.0	231.75	14.99	280.33

4.2.2. Produced water

The following labels will be used as the acronym of the wastewater dilution in this discussion: C_{PW}; contains only BBM, 25_{PW}, 50_{PW}, 75_{PW} and 100_{PW} and produced water used is represented as PW_{WW}. Referring to the PW_{WW} growth curve in figure 4.14, it was difficult to identify the different growth phases due to only 3 points given. So assumptions were given based on this analysis.

The initial biomass concentration of *Scenedesmus* sp. in the presence of PW_{WW} was 48.75mg/l, and it exhibited linear growth without a distinct lag phase until day 5. Among the different dilutions, 50_{PW} had the highest biomass concentration at 865 mg/l, while 75_{PW} had the lowest at 333 mg/l. The absence of a lag phase could evidently be the microalgae's acclimatisation prior to salt tolerance during the initial inoculation. Initially, both 50_{PW} and 25_{PW} showed good growth with biomass concentrations of 865 mg/l and 695 mg/l, respectively, surpassing the biomass concentration of C_{PW} at 690mg/l. Cultures with PW_{WW} eventually reached a stationary phase or even experienced a decline in biomass after day 5. C_{PW} and 75_{PW} exhibited continuous growth, with C_{PW} outperforming the other dilutions and achieving the highest biomass concentration of 1120.5 mg/l, representing a 40% increase compared to 75_{PW} at 540mg/l in biomass. 50_{PW} and 100_{PW} reached a stationary phase with only 10% increase, resulting in a final biomass concentrations of of 990mg/l and 415mg/l, respectively. As it happens, 25_{PW} experienced a sharp decline in biomass by approximately 50%, resulting in a final biomass concentration

of 375mg/l.

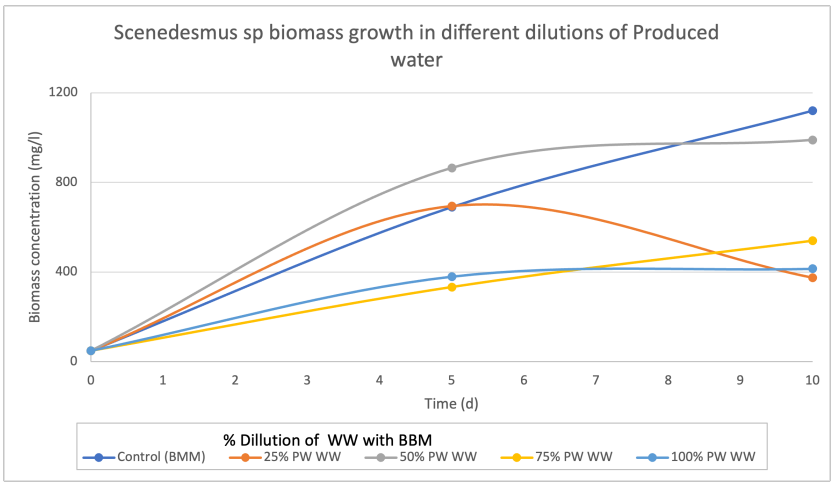

Figure 4.14: Biomass concentration of *Scenedesmus* sp. growing in 5 different dilutions in PW_{WW} in 10 days.

In this experiment, since there was no observed lag phase, the specific growth rates calculated for the exponential growth phase were from day 0 to 5 instead. The table 4.9 provides insight into the relationship between specific growth rate and biomass yield for each dilution. C_{PW} and 25_{PW} demonstrated a close relationship between their biomass yield and specific growth rate, indicating that the microalgae were able to produce a consistent amount of biomass for each gram of the respective nutrient used. 50_{PW} exhibited the highest specific growth rate and productivity, resulting in the highest biomass concentration after day 5. On the other hand, 25_{PW} achieved high maximum productivity but the lowest average productivity due to the decline in biomass after day 5. While C_{PW} had the lowest biomass yield, it achieved the highest final biomass. This can be attributed to a higher nitrogen uptake for biomass production compared to 50_{PW}, which resulted in a higher biomass yield. Both 50_{PW} and 100_{PW} demonstrated greater biomass production with increased phosphorous intake, while 75_{PW} exhibited increased biomass production through nitrogen uptake. A similar trend was observed for 25_{PW}, where biomass production increased significantly, resulting in the second-highest specific growth rate but a substantial decrease in biomass during the stationary phase. C_{PW} maintained a gradual increase in biomass after the exponential growth phase and ultimately achieved the highest final biomass, despite having a lower growth rate.

Scenedesmus sp. are known to be halotolerant microalgae capable of adjusting osmotically and adapting to saline conditions (Arora et al. 2019), which is evident from their growth in this experiment. Figure 4.15 shows the change in colour of the culture with increasing dilution of produced water. In the case of 100_{PW}, the microalgae were observed under a microscope, as shown in Figure 4.16. They appeared to be clustered in groups with some unknown particles. This suggests that *Scenedesmus* sp. may have lost its pigment due to environmental stress, a

Table 4.9: Kinetic growth parameters calculated for the samples grown with the different dilutions of PW_{WW}

PW_{WW}	Specific growth rate μ	Final biomass mg/l	Productivity P mg/L/d		Specific biomass yield g/g	
			Avg	Max	$Y_{gX/gTN}$	$Y_{gX/gTP}$
C_{PW}	0.530	1120.5	107.18	128.25	27.48	22.37
25_{PW}	0.531	375.0	32.63	129.25	65.25	65.25
50_{PW}	0.575	990.0	94.12	163.25	117.66	209.17
75_{PW}	0.384	540.0	49.12	56.92	70.18	28.73
100_{PW}	0.411	415.0	36.63	66.25	24.42	64.25

phenomenon observed in other microalgae under high salinity conditions (Das et al. 2019). A study conducted with multiple microalgae grown in 100% produced water also reported similar findings (Das et al. 2019). In that study, it was observed that *Scenedesmus* sp. and *Chlorella* sp. were able to grow and survive, while other microalgae started losing their pigments. In line with our experiment, *Scenedesmus* sp. exhibited linear growth until day 3 and reached a stationary growth phase before day 6. The biomass then fluctuated and plateaued at around 400 mg/l. It was found that *Scenedesmus* sp. was able to grow in produced water by utilising the residual phosphorus, nitrogen, and other trace metals present in the inoculum. Additionally, studies have shown that *Scenedesmus obliquus* possesses the capability to consume nitrogen and amino substituents from nitrogen-containing aromatic compounds (e.g., aminonaphthalenes and nitrobenzoates) as nitrogen sources (Das et al. 2019).

Figure 4.15: Cultivation in PW_{WW}, done in duplicates after 10 days. They were arranged as followed from left to right: C_{PW}, 100_{PW}, 75_{PW}, 50_{PW} and 25_{PW}. The colour of the media changed with increasing dilution.

A similar trend was observed in a study by Nadersha and Hassan, 2022, where microalgae containing a mixture of dominant *Chlorella* cells and the presence of *Nannochloropsis* sp. exhibited reduced or no lag phase depending on the dilution ratio of the PW. This was achieved by subjecting the microalgae to multiple acclimatisation cycles with PW, which was necessary for their adaptation to the high

salinity and toxicity levels. Furthermore, the stagnant or decreased biomass could be the reaction triggered by various environmental stress factors, including high toxicity, salinity, specific characteristics of the PW, and micronutrient deficiencies. These challenges pose significant obstacles to microalgae as they must maintain ionic balance to cope with osmotic stress and combat the interference of reactive oxygen species (ROS) during photosynthesis (Nadersha & Hassan, 2022).

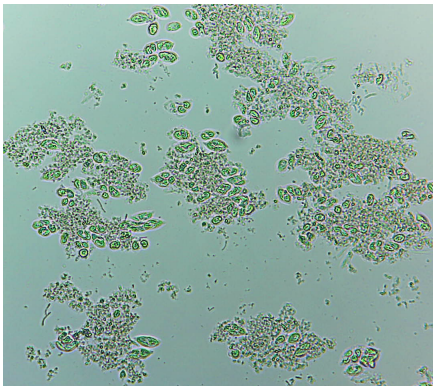

Figure 4.16: *Scenedesmus* sp. in 100_{PW} under the microscope on day 10, showed clustering of cells around unknown particles.

4.2.3. Sequencing Batch Reactors effluent

The following labels will be used as the acronym of the wastewater dilution in this discussion: C_{SBR}; contains only BBM, 25_{SBR}, 50_{SBR}, 75_{SBR} and 100_{SBR} while SBR wastewater will be referred as SBR_{WW}. Referring to the growth curves in Figure 4.17, all of the dilutions showed relatively consistent growth throughout the three data points. However, due to the limited number of data points, it is challenging to determine the exact growth phases. Therefore, assumptions are made based on this analysis. The initial biomass concentration started at 168 mg/l. Most dilutions showed linear biomass growth. The biomass range on day 5 varied from 782 to 378 mg/l, with 75_{SBR} obtaining the highest biomass and 25_{SBR} at the lowest. The growth continued to increase linearly, except for C_{SBR}, where it exhibited exponential growth after day 5. By day 10, the biomass range reached 1600 to 825 mg/l, with 100_{SBR} having the highest biomass and 25_{SBR} at the lowest. As no lag phase was visible, it can be inferred that the microalgae acclimatised to the SBR_{WW} during the growth of the mother culture.

Given the limited number of data points and the difficulty in differentiating the growth phases of the microalgae, it is challenging to determine the exact exponential growth phase of the SBR_{WW} culture. Based on literature studies, the exponential phase for *Scenedesmus* sp. typically starts after 5 days (Nayak et al. 2013). In comparison to DAF_{WW} and PW_{WW} experiments, the growth curve for the SBR_{WW} experiment appears almost linearly. When comparing the growth rates calculated from 0-5 days and 5-10 days, it can be observed that the growth rates during the first 5

days were higher than those during the subsequent 5 days. Therefore, the data after day 5 were used to calculate the specific growth rate. 100_{SBR} exhibited the highest growth rate at 0.229μ followed by 25_{SBR} at 0.156μ, with C_{SBR} and 75_{SBR} having the lowest at 0.071μ. 25_{SBR} showed the second-highest specific growth rate but the lowest final biomass among the dilutions, indicating that the biomass growth was exponential and more pronounced after day 5. On the other hand, 75_{SBR} had the lowest specific growth rate at 0.071μ but the third-highest biomass, suggesting that the biomass growth reached a plateau after 5 days.

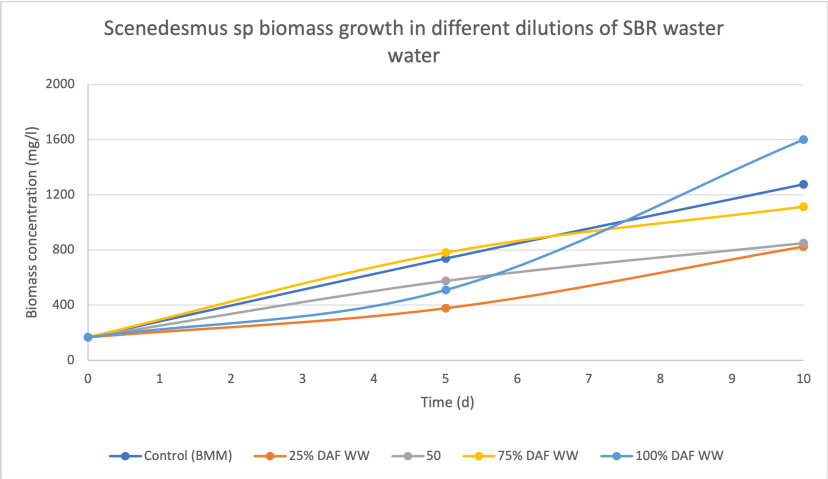

Figure 4.17: Biomass concentration of *Scenedesmus* sp. growing in 5 different dilutions of SBR_{WW} in 10 days.

100_{SBR} surpassed C_{SBR} in biomass comparison by 25%, which pointed out that 100_{SBR} provided optimal conditions for *Scenedesmus* sp. Furthermore, 100_{SBR} achieved the highest productivity at a maximum of 218 mg/l/d and the highest final biomass of 1600 mg/l. 75_{SBR} showed a productivity value close to the optimal condition at 122.9mg/l/d and a final biomass of 1115mg/l. When comparing these two dilutions, the biomass yield in terms of $Y_{gX/gTN}$ was the same, but 100_{SBR} had a $Y_{gX/gTP}$ value that was ten times higher than 75_{SBR}. This is because 100_{SBR} produced a large amount of biomass while using significantly less phosphorous, around 85% phosphorous less compared to 75_{SBR}, showing the efficiency of phosphorous usage. On average, productivity appeared to increase with increasing dilution, except for C_{SBR}. However, 25_{SBR} had a higher maximum productivity but lower final biomass and $Y_{gX/gTP}$ compared to 50_{SBR}. Similar observations were made when comparing 75_{SBR} to C_{SBR}, where the maximum productivity was higher but resulted in lower final biomass and both biomass yield values. As such, the lack of data points for evaluating the growth phases of the microalgae may have influenced the results and their interpretation.

In the context of cultures growing in SBR_{WW}, it is important to understand how $Y_{gX/gTP}$ and $Y_{gX/gTN}$ values contributed to biomass growth during nutrient consumption. The optimal condition was observed at 27.82 $Y_{gX/gTN}$ with 75_{SBR} and

100_{SBR} being close to the values at 21.04 and 20.75 $Y_{gX/gTN}$ respectively. Despite having a lower final biomass, 75_{SBR} exhibited a higher biomass yield than 100_{SBR}, which suggest more biomass could be obtained from nitrogen removal by 75_{SBR}. Furthermore, 75_{SBR} demonstrated good nutrient removal efficiency, which was closest to the optimal condition.

Table 4.10: Kinetic growth parameters calculated for the sample grown with the different dilution of SBR_{WW}

	Specific growth rate	Final biomass	Productivity P mg/L/d		Specific biomass yield mg/L/d	
SBR_{WW}	μ	mg/l	Avg	Max	$Y_{gX/gTN}$	$Y_{gX/gTP}$
C_{SBR}	0.109	1275	110.70	114.00	27.68	22.82
25_{SBR}	0.156	825	65.70	89.40	13.69	34.58
50_{SBR}	0.078	850	68.20	81.60	12.40	86.33
75_{SBR}	0.071	1115	94.70	122.80	21.04	72.29
100_{SBR}	0.229	1600	143.20	218.00	20.75	753.68

4.3. TN and TP removal of *Scenedesmus* sp. in different concentrations of wastewater

In this section, the nutrient removal, Total Nitrogen (TN) and Total Phosphorous (TP) of each experiment were analysed, 3 points were taken similarly on days 0, 5 and 10 and using the formula given in the analyse section to calculate the values produced in the tables below. Experimental results show that *Scenedesmus* sp. could remove a good amount of nutrients from all of the wastewater.

4.3.1. Dissolved Air Flotation Effluent

In the context of the wastewater dilutions used in this discussion, they are labelled in acronym as follows: C_{DAF}; contains only BBM, 25_{DAF}, 50_{DAF}, 75_{DAF} and 100_{DAF} represent different dilutions of DAF wastewater, with DAF wastewater itself denoted as DAF_{WW}. Increasing the dilution of DAF_{WW} resulted in an increase in TN concentration but a decrease in TP initially. All samples showed an efficient reduction in TN, bringing the TN levels close to a range of 31 to 43 mg TN/l. However, there was an increase in TP observed with C_{DAF} showing an increase and a decrease for 25_{DAF} after day 5 during the experiment. Overall, most of the samples demonstrated better removal of both nutrients compared to C_{DAF}. 75_{DAF} exhibited the highest removal rates for TN and TP at 69.81% and 66.67% respectively. On the other hand, sample 25_{DAF} had the lowest removal rates of 40.28% for TN and 14.52% for TP as shown in Figure4.11.

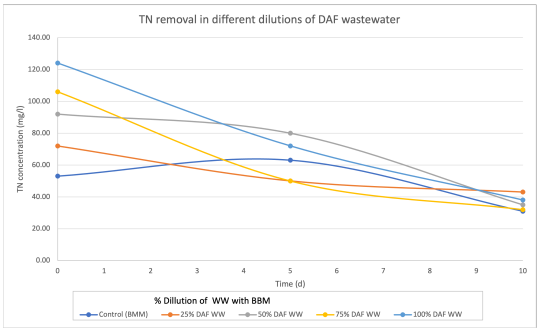

(a) TN removal of samples with different DAF_{WW} dilutions

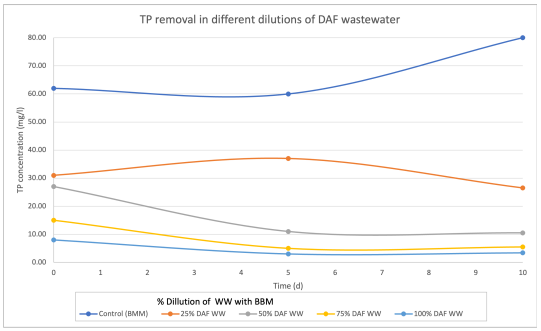

(b) TP removal of samples with different DAF_{WW} dilutions

Figure 4.18: Nutrient removal of sample from different DAF_{WW} dilution in 10-day cultivation

All media had started and ended to be phosphorus limiting except 100_{DAF}, which had a ratio close to 16 (Redfield ratio) before and eventually became both nutrient limiting. The N:P ratio decreased in all media, indicating that nitrogen removal was more efficient than phosphorus removal. This suggests that there was still a relative availability of phosphorus in the media, but the microalgae preferred nitrogen uptake. When comparing the N:P ratio based on the Redfield ratio to the final N:P ratio of the samples, most samples showed an increase, except for 50_{DAF}. The negative value observed for C_{DAF} was due to the increase in TN concentration during the cultivation. As an increasing N:P ratio indicates a higher nitrogen removal rate, the decrease in the ratio in 50_{DAF} suggests that different cellular processes might have influenced higher phosphorus reduction, resulting in a lower ratio. Additionally, the N:P ratio of 50_{DAF} remained relatively stable throughout the experiment, indicating the consistent reduction of both nutrients. Despite having the highest TP removal rate (1.65 mg/l/d) and specific removal rate (0.97 mg/g/d), 50_{DAF} did not exhibit a high TP biomass yield. Similarly, 100_{DAF}, which had the highest TN removal rate and specific removal rate, had the lowest TN biomass yield. On the other hand, 25_{DAF} achieved the highest final biomass and yield, despite showing the lowest nutrient removal rate and efficiency.

Microalgae are known to acquire nitrogen from various sources, including NH_4^+, NO_3^- and NO_2^-, with NH_4^+ being more favourable due to its lower energy requirement to uptake. This preference towards NH_4^+ uptake could potentially lead to higher biomass growth. Additionally, other nutrients such as COD could also play a role which they may serve as easier-to-consume nutrients when present in higher amounts, especially considering the higher proportion of BBM in the media (Silambarasan et al. 2023). In certain cases, high nitrogen concentrations in the media could induce stress in the microalgae, leading to the accumulation of nitrogen for the production of other compounds, such as lipids. This could potentially explain the observed higher biomass growth. Overall 50_{DAF} to 100_{DAF} demonstrated significant removal of TN and TP, with efficiency levels above 60%.

Table 4.11: The N:P ratio, nutrient removal rates, and specific removal rates of TN and TP obtained in DAF_{WW} experiment

	TN:TP ratio			Max Removal efficiency %		AVG Removal Rate (RR) mg/l/d		Specific Removal Rate mg/g	
DAF	Before	After	Based on RR	TN	TP	TN	TP	TN	TP
C_{DAF}	0.85	0.39	-1.22	41.51	3.23	2.20	-1.8	1.06	-0.87
25_{DAF}	2.32	1.62	6.44	40.28	14.52	2.9	0.45	1.23	0.19
50_{DAF}	3.41	3.33	3.45	61.96	61.11	5.70	1.65	3.34	0.97
75_{DAF}	7.07	5.82	7.79	69.81	66.67	7.40	0.95	5.48	0.70
100_{DAF}	15.50	11.18	18.70	69.35	62.50	8.60	0.46	6.09	0.33

4.3.2. Produced Water

The following labels will be used as the acronym of the wastewater dilution in this discussion: C_{PW}; contains only BBM, 25_{PW}, 50_{PW}, 75_{PW} and 100_{PW} and produced water will be represented as PW_{WW} Figure 4.19 depicts the nutrient removal of *Scenedesmus* sp. in the PW_{WW} experiment. Initially, there was a decrease in TN and TP concentrations with increasing dilution. This decrease can be attributed to the low nutrient content in PW_{WW}, as indicated in Table 4.7. Throughout the experiment, there were fluctuations in TN concentration, while TP consumption remained relatively constant. Towards day 5, 50_{PW} and 100_{PW} exhibited an increase in TN concentration before subsequently decreasing, while 25_{PW} and 75_{PW} experienced a decrease in TN concentration before showing an increase again. All samples demonstrated a huge variable TN removal efficiency from 26% to 62.5%, with 100_{PW} achieving the highest TN removal efficiency surpassing C_{PW} at about 0.6% . Furthermore, varying TP removal efficiencies were also observed from 16.67% to 95% with 75_{PW} and 100_{PW} at the highest surpassingC_{PW} by approximately 16%.

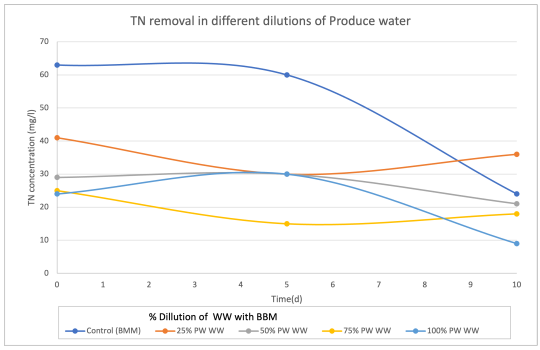

(a) TN removal of sample in different dilutions of PW_{WW}

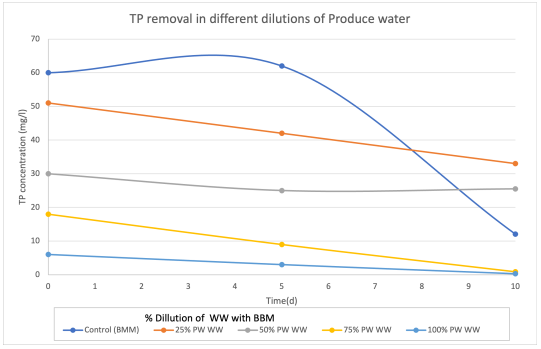

(b) TN removal of sample in different dilutions of PW_{WW}

Figure 4.19: Nutrient removal of different PW_{WW} in 10-day cultivation

Table 4.12: The N:P ratio removal rates and specific removal rates of total nitrogen (TN) and total phosphorus (TP) in PW_{WW} experiement

	TN:TP ratio			Max Removal efficiency %		AVG Removal Rate (RR) mg/l/d		Specific Removal Rate mg/g	
PW	Before	After	Based on RR	TN	TP	TN	TP	TN	TP
C_{PW}	1.05	1.98	0.81	61.90	79.83	3.90	4.79	3.48	4.27
25_{PW}	0.80	1.09	0.28	26.83	35.29	0.50	1.80	1.33	2.56
50_{PW}	0.97	0.82	1.78	27.59	16.67	0.80	0.45	0.81	0.45
75_{PW}	1.39	20.00	0.41	40.00	95.00	0.70	1.71	1.30	3.17
100_{PW}	4.00	30.00	2.63	62.50	95.00	1.50	0.57	3.61	1.37

All samples in the PW_{WW} experiment exhibited phosphorus limitation, as indicated by the TN: TP ratio starting at less than 5 and increasing during the experiment. The highest TN:TP ratio achieved was 30:1 for 100_{PW} followed by 20:1 for 75_{PW}. The lowest was observed at 50_{PW}, where it slightly decreased, obtaining 0.82:1. This suggests that when cultivating with PW_{WW}, microalgae preferentially took up phosphorus over nitrogen. 100_{PW} had the highest TN ratio calculated based on the nutrient removal rate, followed by 50_{PW}, while the rest of the samples had ratios below 1. This indicates a higher likelihood of phosphorus uptake compared to nitrogen when using PW_{WW} as a growth medium. These ratio values also increased with dilution. On day 5, both 25_{PW} and 75_{PW} showed a wide difference in ratio values as TN increased. This was due to 75_{PW} being more efficient in TP removal at 95%, compared to 35.29% for 25_{PW}. A similar comparison can be observed for 100_{PW}, which had a final ratio of 30 and a TP removal efficiency of 95%. In contrast, C_{PW} exhibited a ratio based on RR close to 1, indicating a relatively equal reduction in both nutrients.

Although 100_{PW} showed equivalent reduced efficiency as C_{PW} and both 100_{PW} and 75_{PW} surpassed control in TP removal efficiency, they exhibited low biomass and productivity. PW_{WW} is known to contain high salinity, heavy metals, and hydrocarbons, which induce stresses on microalgae, such as osmotic stress, that inhibit growth, especially at high dilutions. The microalgae may utilise nutrients to accumulate from other sources as a defence mechanism. This defence mechanism could involve the production of exopolysaccharides and osmoregulatory solutes, lipid accumulation, and a reduction in photosynthetic activity, all of which can affect microalgae biomass production (Pessôa et al. 2022). 50_{PW} exhibited the lowest nutrient removal efficiency despite having the second highest biomass compared to 100_{PW} at 415 mg/l. This indicates growth inhibition when microalgae were grown in higher concentrations of PW_{WW}. On the other hand, 25_{PW} showed low nutrient reduction efficiency but had relatively low final biomass despite decent biomass yield,

productivity, and specific growth rate, which can be explained by the decrease in biomass after the 5^{th} day to the 10^{th} day, from 695 to 375 mg/l.

All of the dilutions exhibited lower removal rates compared to C_{PW}. This can be attributed to the stress factors affecting nutrient uptake and creating sub-optimal conditions for microalgae growth. It appears that increasing concentration leads to a shift in nutrient preference by the *Scenedesmus* sp. This observation is further supported when comparing the higher nutrient removal efficiency of each sample or the change in the N:P ratio. The salinity-induced stress effect is evident in 25_{PW}, which demonstrated one of the third highest removal rates but had a low biomass yield. On the other hand, 50_{PW} exhibited a low nutrient removal rate despite having higher biomass.

4.3.3. Sequencing Batch Reactors Effluent

The following labels will be used as the acronym of the wastewater dilution in this discussion: C_{SBR}; contains only BBM, 25_{SBR}, 50_{SBR}, 75_{SBR} and 100_{SBR} and SBR wastewater will be represented as SBR_{WW}. In the SBR experiment, TN concentration increased with dilution, with 100_{SBR} having the highest concentration and C_{SBR} at the lowest, 83mg/l and 51mg/l, respectively. On the other hand, TP concentration decreased with dilution, with C_{SBR} having the highest concentration and 100_{SBR} at the lowest, 54mg/l and 4mg/l, respectively. These trends aligned with the higher TN and lower TP content in the SBR WW medium, as indicated in Table 4.7. In terms of nutrient removal, the microalgae were able to remove over 75% of TN in all samples while TP removal remained below 50% TP except for 75_{SBR}. 50_{SBR} and 100_{SBR} achieved approximately 2-3% higher TN removal compared to C_{SBR} with removal efficiencies of 82.09% and 83.13% respectively. Similarly, 75_{SBR} achieved approximately 2% higher TP removal than the control, with a removal efficiency of 82.39%. TN depletion showed a consistent gradual decrease throughout the experiment, while TP removal displayed some variation. All samples exhibited immediate consumption of TN and TP, except for C_{SBR} and 25_{SBR}, which showed a lag phase before TP was consumed. At the end of the experiment, all samples reduced TN concentration below 15 mg/l, with 100_{SBR} having the highest concentration (14 mg/l) and C_{SBR} at the lowest concentration (11 mg/l). The TP concentration showed a wider range, with 25_{SBR} having the highest concentration (24.8 mg/l) and 100_{SBR} the lowest concentration (2.1 mg/l), as shown in Figure 4.20

In Table 4.13, it can be observed that SBR_{WW} exhibited nitrogen limitation, as indicated by the increase in TN: TP ratio with increasing dilution. For instance, 50_{SBR} and 100_{SBR} observed a decrease in ratio whereas 25_{SBR} and 75_{SBR} observed an increased in ratio. This demonstrates the preference for nutrient uptake with increasing dilution, where a similar trend is observed in the cultivation with PW_{WW} and DAF_{WW}. The ratio based on nutrient removal rate also showed a preference for nutrient uptake. 100_{SBR} had the highest ratio at 36.32, resulting in the highest TN removal efficiency and removal rate at 83.13% and 6.9, respectively. This reduced the TN: TP ratio to 6.67. Similarly, 50_{SBR} achieved the second-highest ratio based on

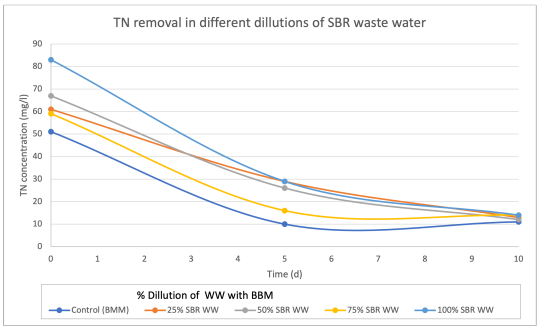

(a) TN removal of samples with different dilutions of SBR_{WW}

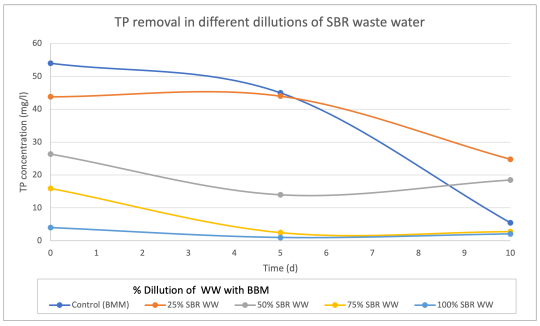

(b) TP removal of samples with different dilutions of SBR_{WW}

Figure 4.20: Nutrient removal of samples with different SBR_{WW} dilution in 10-day cultivation

nutrient removal rate due to its high TN removal rate of 82.09%, which reduced the nitrogen content to a level lower than TP, resulting in a low ratio of 0.65. Comparing the control samples (BMM) cultivated in all media, C_{SBR} and C_{PW} exhibited similar ratios based on nutrient removal rate, ranging between 0.81 and 0.82 However,C_{DAF} showed a different ratio. This indicates the consistency of microalgae growth under the same conditions, despite being grown in different mother cultures and time, except for C_{DAF}, where an increase in nitrogen concentration was observed. This discrepancy could be attributed to experimental errors or excessive evaporation due to aeration during the experimental phase. The ratio also suggests that, under optimal conditions, the nutrients were depleted at a relatively equal rate each day. Furthermore, as the ratio based on RR approached 1, it indicated that both nutrients were being depleted at a similar rate, which is consistent with the observations of removal efficiency and removal rate.

Growing in DAF_{WW} and PW_{WW} seems to have reduced biomass produced as dilution increases, while the productivity in SBR_{WW} increases with increased dilution.

Table 4.13: The N:P ratio removal rates and specific removal rates of total nitrogen (TN) and total phosphorus (TP) on samples with different dilutions of SBR_{WW}

	TN:TP ratio			Max Removal efficiency %		AVG Removal Rate (RR) mg/l/d		Specific Removal Rate mg/g	
SBR	Before	After	Based on RR	TN	TP	TN	TP	TN	TP
C_{SBR}	0.94	2.00	0.82	80.39	80.81	4.00	4.85	3.14	3.80
25_{SBR}	1.39	0.52	2.53	78.69	43.38	4.80	1.90	5.82	2.30
50_{SBR}	2.54	0.65	6.96	82.09	46.97	5.50	0.79	6.47	0.93
75_{SBR}	3.71	5.00	3.44	76.27	82.39	4.50	1.31	4.04	1.17
100_{SBR}	20.75	6.67	36.32	83.13	47.50	6.90	0.19	4.31	0.12

As mentioned, all cultivation demonstrated excellent TN removal efficiency of more than 75% and only C_{SBR} and 75_{SBR} achieved TP removal efficiency of more than 80%, while the others were around 40%. Referring to Table 4.13, 50_{SBR} and 100_{SBR} were able to efficiently remove more TN compared to C_{SBR}. None of the cultures achieved optimal TP removal efficiency, but only 75_{SBR} surpassed C_{SBR} at 82.39%. This indicates that 50_{SBR} and 100_{SBR} were optimal for TN removal, while 75_{SBR} was optimal for TP removal. Moreover, 75_{SBR} had both TN and TP removal efficiencies closest to C_{SBR}, suggesting that this dilution was the most efficient.

Excluding C_{SBR}, 100_{SBR} showed the highest TN removal rate followed by 50_{SBR} at 6.9 and 5.5 mg/l/d while the rest was less than 5, and 25_{SBR} had the highest TP removal rate at 1.9mg/l/d followed by 75_{SBR} at 1.31mg/l/d. Despite the differences, cultivating in SBR_{WW} had very consistence and stable increase in removal rate with around the range of 4.5 to 6.9mg/l/d. 100_{SBR} had the lowest TP removal rate of 0.19mg/l/d, which could be due to less amount of phosphorous at 4mg/l therefore causing nitrogen to be the limiting nutrient.

All samples' specific nutrient removal rate exceeded the specific TN removal rate of C_{SBR} but fell behind when compared to the specific TP removal rate. 50_{SBR} achieved the highest specific TN removal rate of 6.47 mg/g/d, followed by 25_{SBR} at 5.82mg/g/d. Despite 100_{SBR} having the highest average TN removal rate, it only had a specific TN removal rate of 4.31. This is due to the high amount of nutrient uptake compared to the biomass produced. As these rates exceeded the C_{SBR} removal rates, it indicates that cultivating in SBR_{WW} promotes the depletion of nitrogen rather than phosphorus. This conclusion is also supported by comparing the specific TP removal rates, which decrease with increasing dilution. Excluding C_{SBR}, the highest specific TP removal rate was observed in 25_{SBR} at 2.3 mg/g/d, followed by 75_{SBR} at 1.17 mg/g/d, while the rest were below 1 mg/g/d.

4.4. Comparison and analysis of all wastewater experiment

The following labels will be used as the acronym of the wastewater dilution in this discussion: C_{SBR}; contains only BBM, 25_{SBR}, 50_{SBR}, 75_{SBR} and 100_{SBR} and DAF_{WW}, SBR_{WW} and PW_{WW} represent the different wastewater that the sample cultivated.

In this graph comparison 4.21, biomass productivity was used instead of specific growth rate and final biomass, as there were only 3 data points collected for each experiment. It was difficult to identify the appropriate exponential phase to calculate the optimal specific growth rate, and the initial biomass masses varied across the three experiments. Additionally, the specific nutrient removal rate used to plot the graph was derived from the TN: TP ratio calculated from the specific nutrient removal rate. Taking the logarithm of TN: TP helped to reduce the wide range for analysis purposes. The productivity values corresponding to each dilution are obtained from the bar charts, while the specific nutrient removal rate values are represented by

points with different shapes that correspond to different wastewater types.

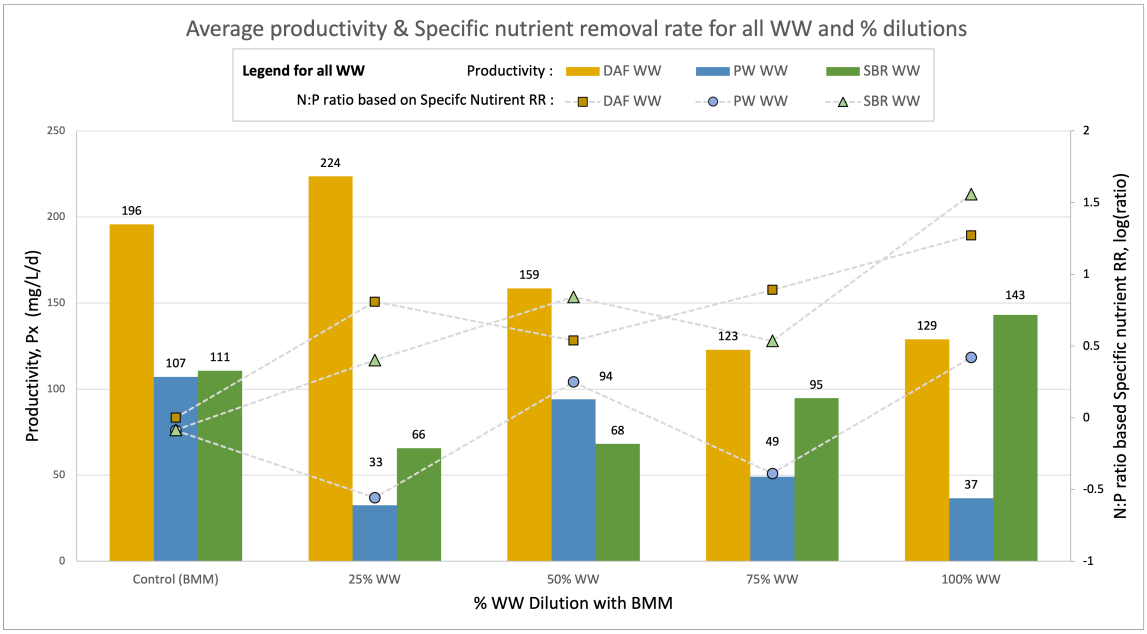

Figure 4.21: Comparison of Specific nutrient removal rate in N:P ratio (as linear graphs) and Avg productivity (bar charts) for all wastewater. The logarithm is applied to TN: TP, helping to reduce the wide range for analysis purposes. Each WW is input with its own unique colour on both graphs for comparison and identification purposes.

In the graph, it is evident that microalgae grown in DAF_{WW} exhibited the highest biomass productivity among all samples, except for 100_{DAF} where it was slightly suppressed by 12% compared to SBR_{WW}. As expected, productivity was lowest in PW_{WW} due to the additional osmotic stress that microalgae had to cope with. The biomass productivity of C_{DAF} appeared to be higher during the DAF_{WW} experiment, while C_{SBR} and C_{PW} showed similar productivity levels. This discrepancy could be attributed to the differences in the composition of the BBM medium used during the experimental period. Due to equipment limitations and long lead times for required tools, the experiments were conducted sequentially, starting with DAF_{WW}, followed by SBR_{WW} and lastly PW_{WW} However, all microalgae were acclimatized to their respective WW before cultivation began. Considering similar specific nutrient removal rates, the higher biomass productivity observed in DAF_{WW} could be due to the excess availability of certain nutrients in the BBM media used. In contrast, growing in DAF_{WW} and PW_{WW} showed a decrease in biomass productivity with increasing dilution, while productivity increased in SBR_{WW} instead. This suggests that higher dilutions in DAF_{WW} and PW_{WW} had inhibitory effects on growth, possibly due to the presence of toxic compounds that were detrimental to microalgae while microalgae thrived better in SBR_{WW} possibly due to the effluent produced during different treatment processes. SBR_{WW} underwent secondary treatment such as biological treatment and filtering, which aided in the removal of contaminants and toxic compounds, despite the lower nutrient content as compared to DAF_{WW}. Some

dilutions were able to surpass the optimal biomass concentration produced by its control(BMM) sample in each experiment, indicating that appropriately diluting wastewater with the right dilution ratio has the potential to enhance the growth efficiency of *Scenedesmus* sp.

Also, all experiments showed an increased trend of specific nutrient removal rates and nutrient favouritism with each increase. The higher the values and the more favouritism toward nitrogen compared within each wastewater and the higher the nitrogen rate in general. Growing in PW_{WW} exhibited the lowest nutrient removal rates, while DAF_{WW} and SBR_{WW} showed varying differences. Comparing 100_{DAF} and 100_{SBR}, 100_{SBR} displayed higher removal rates than 100_{DAF}. This could be due to the high TN concentration in DAF_{WW} at 134mg/l compared to SBR_{WW} at 83mg/l and that SBR_{WW} media had easier consumable nitrogen sources than 100_{DAF}.

Referring to the graphs in4.22, SBR_{WW} shows the highest TN removal and the highest TP removal fluctuation among different WW samples at various dilutions. The control (BMM) in each WW showed different nutrient removal efficiencies, although they had similar specific removal rates. These variations can be explained by the increase in TN values in C_{DAF} as well as the initial nutrient concentrations in C_{SBR} and C_{PW}, which differ with a slight variation in the removal efficiency. TN removal efficiency increased with increasing dilution, and cultivation with 100% wastewater showed better TN removal efficiency than its control (BMM) counterpart. In the case of PW_{WW}, the best TP removal efficiency was achieved at 75_{PW} and 100_{PW} reaching up to 95%. 75_{SBR} has better TP removal efficiency than 75_{DAF}, and the same trend was observed between 100_{SBR} and 100_{DAF} Therefore, the most efficient dilution for TN removal efficiency was found to be 100% WW, while for TP removal efficiency, the optimal dilution was determined to be 75% WW

Scenedesmus sp. has been extensively studied and utilized in WW applications due to its resilience, adaptability, and bioremediation capabilities. Its potential for high lipid and starch accumulation also makes it a promising candidate for biofuel production. Studies have shown that *Scenedesmus* sp. could achieve over 70% nutrient removal efficiency. Tam and Wong, 1989 conducted experiments with *Scenedesmus* sp. and *Chlorella vulgaris* using 100% settled sewage and activated sewage with low and high algal concentrations. Despite the slower growth rate in activated sewage, which may be attributed to lower nutrient content, the WW still provided sufficient nutrients to support algal growth. Although *Chlorella vulgaris* exhibited better results, *Scenedesmus* sp. achieved an average $NH_4^+ - N$ removal efficiency of 87.9% and an average TP removal efficiency of 70-80% for all treatments and removal in settled sewage. The researchers concluded that higher algal concentration and physiological changes could effectively enhance nutrient uptake (Tam & Wong, 1989). Xin, Hong-Ying, and Jia, 2010 investigated the growth of various microalgae species in secondary effluent and found that all microalgae adapted well to the culture conditions. *Scenedesmus* sp. exhibited the highest final biomass and lipid accumulation and achieved over 98% TP removal and TN removal. Moreover, the lipid content sharply increased to 31%, and the maximum population growth rate was

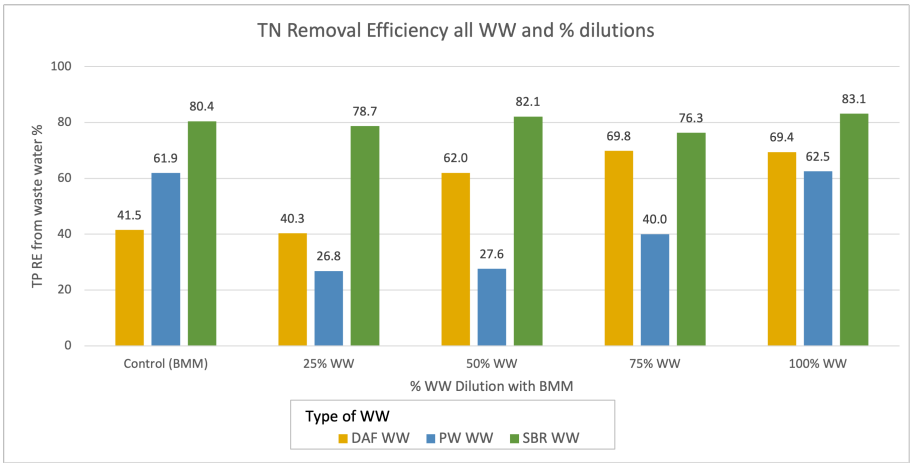

(a) TN removal comparison of all WW at all dilutions experimented.

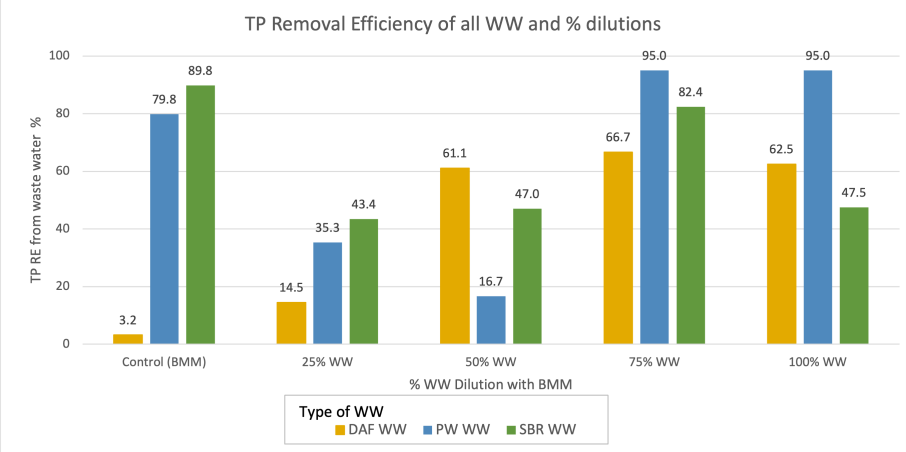

(b) TP removal comparison of all WW at all dilutions experimented.

Figure 4.22: Nutrient removal of all dilution in 10-day cultivation. Each colour represents the different WW; yellow ((DAF_{WW}), blue (PW_{WW}) and green (SBR_{WW}). Each dilution will have all 3 wastewater of the same dilution compared side to side.

observed on day 10. Due to the low nutrients in the medium at 1.41mg/l, they concluded that the enhancement of lipid accumulation and content was due to nitrogen deficiency (Xin, Hong-Ying, & Jia, 2010). Amini Fard et al. 2019 also compared the nutrient removal efficiency between commercial wastewater treatment and *Scenedesmus* sp. cultivation, which they found that it achieved better TN removal efficiency, up to 93% compared to conventional treatment methods. The increase in nitrogen content between the inlet and outlet effluent correlated with increased microalgae growth (Amini Fard et al. 2019). Oliveira et al. 2018 conducted a study on *Scenedesmus* sp. growth in filtered raw wastewater and observed that the N:P ratio influenced microalgae nutrient preference, with optimal growth occurring at around 30. Despite the WW being nitrogen-deficient, it resulted in 93% total nitrogen removal and 61% orthophosphate removal (Oliveira et al. 2018).

The research on microalgae growth in PW is still in its early stages but has gained increasing interest in recent years. The most commonly studied microalgae for PW cultivation were *Scenedesmus* sp. and *Chlorella* sp. Researchers faced several challenges that hindered microalgae growth in PW, including the presence of BTEX (benzene, toluene, ethylbenzene, and xylene) and heavy metals, turbidity, salinity, and low concentrations of nitrogen and phosphorous (Pessôa et al. 2022). Das et al. 2019 studied six microalgae strains, including three freshwater and three marine species, in both PW with and without the addition of nutrients. Only *Chlorella* sp and *Scenedesmus* sp. were able to grow, while the other strains experienced a lost in pigmentation and decreased biomass in both types of produced water. The biomass achieved were higher with the addition of nutrient. It is mentioned that the possibility of growth could be driven by the residual nutrient from the inoculum, given the limited phosphorous in PW. *Scenedesmus obliquus* demonstrated the ability to utilize nitrogen-containing aromatic compounds such as aminonaphthalenes and nitrobenzoates as nitrogen sources, indicating its potential for survival in PW. Additionally, some nitrogen compounds could be made available through the degradation of these organic compounds by bacteria (Das et al. 2019). Hakim et al. 2018 investigated the potential application of various microalgae for PW. *Scenedesmus* sp. was able to grow in the 100% PW_{WW} with the presence of BTEX, heavy metals, and high pH. The high pH conditions caused the necessary trace metals to precipitate, promoting microalgae growth. The highest biomass of *Scenedesmus* sp. was observed in 50% PW dilution, resulting in approximately 60% TN removal and 55% TP removal efficiency. This study also suggested the possibility of toxic pollutant removal, such as BTEX, by *Scenedesmus* sp. (Hakim et al. 2018).

The growth of *Scenedesmus* sp. in different types of wastewater can lead to changes in its morphology, including shape, size, and pigmentation. Figure 4.23 shows the observations made under an optical microscope at 40x magnification. When grown in SBR_{WW} and DAF_{WW}, the number of unicells decreased and produced a rounder shape. Additionally, single-cell *Scenedesmus* sp. could be observed in SBR_{WW}. In PW_{WW}, coenobia with up to 8 cells were predominantly retained, but they appeared lighter in colour compared to other wastewater types. The reduction in pigment with increased dilution could also be visually observed in figure 4.15. These changes in morphology are responses to various environmental conditions, both abiotic and biotic stresses, and are referred to as phenotypic plasticity. The specific changes observed depend on the growth phase, species, and survivability factors. For example, predation can trigger the formation of colonies in *Scenedesmus* sp. through the release of certain chemicals, and individual cells tend to relax back to their individual state when the threat is no longer present (Lürling, 2003). Nitrogen starvation or stress conditions have been found to enlarge cell size and promote the accumulation of lipid droplets (Sulochana & Arumugam, 2020). Figure 4.24, showed the *Scenedesmus* sp. grown in 100% SBR_{WW} for 17 days, where grey coagulation of biomass was observed, along with an increase in cell size and the absence of microalgae coenobia.

Based on the observations and analysis, it can be concluded that DAF_{WW} and

(a) BMM grown *Scendesmus* sp., show colony of up to 10 cells.

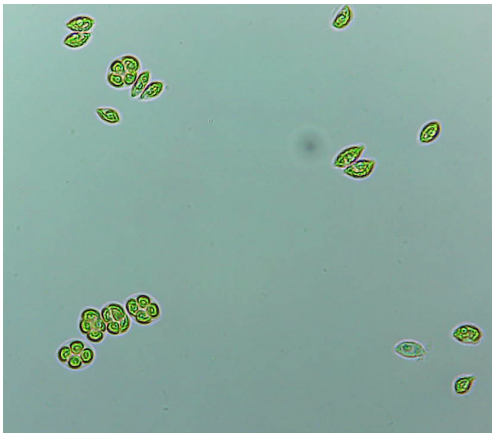

(b) DAF_{WW} grown *Scendesmus* sp., with smaller rounded shapes in the colony up to 4 cells

(c) PW_{WW} grown *Scendesmus* sp., with lighter pigment in the colony up to 8 cells

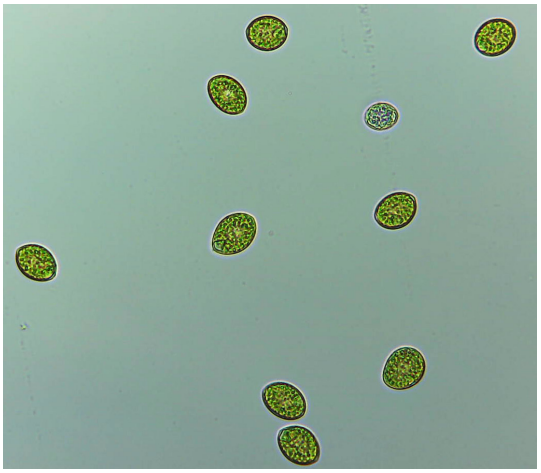

(d) SBR_{WW} grown *Scendesmus* sp., with bigger rounded shaped in single cells

Figure 4.23: These *Scenedesmus* sp. were observed through the optical microscope at 40x magnification. *Scenedesmus* sp. shape and size after 10-day cultivation in different 100% WW had been observed with changes in microalgae morphology. This is possibly due to the different WW compositions.

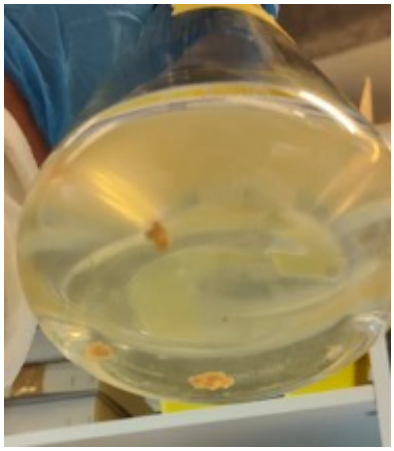

(a) Grey biomass coagulation is observed in the sample growth in 100_{DAF}

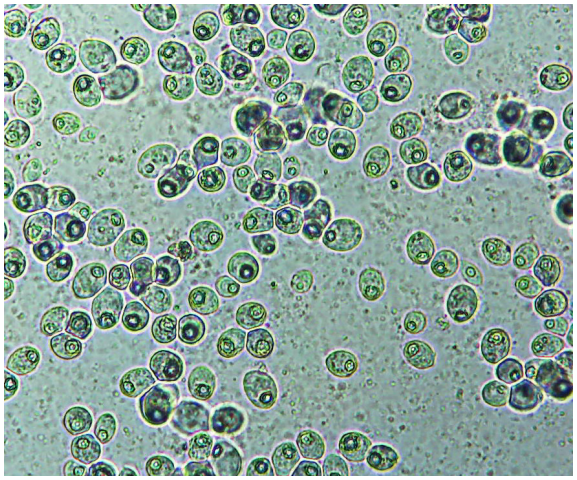

(b) Grey biomass under 40x optical microscope, observed *Scenedesmus* sp. enlarge, oval and clustered together.

Figure 4.24: *Scenedesmus* sp. after 17 days of cultivation in 100% SBR

SBR_{WW} are better choices for cultivating *Scenedesmus* sp. compared to PW_{WW}. PW_{WW} had lower biomass productivity despite achieving high TN and TP removal efficiencies at 95% TN and TP removal at 100_{PW}. The presence of high salinity stress, hydrocarbons, and heavy metals in PW_{WW} can greatly affect the survivability of *Scenedesmus* sp. despite being halotolerant to some extent. As DAF_{WW} and SBR_{WW} were a competitive choice, in comparison to 100% wastewater dilution, the biomass productivity and specific nutrient removal rate is higher in 100_{SBR}. The higher nitrogen concentration in 100_{DAF} could induce stress factors on *Scenedesmus* sp. In practical applications, using SBR_{WW} would be a better choice as it has undergone secondary treatment and filtration, removing possible biological contaminants or other microorganisms that could induce toxicity, growth inhibition, and competition with microalgae cultivation.

Among all the dilutions of SBR_{WW}, 75_{SBR} exhibited optimal growth. Despite having slightly lower biomass productivity and TN removal efficiency compared to 25_{SBR}, 75_{SBR} excelled in TP removal with an efficiency of 82.4%. Although the nutrient removal rates were similar between 25_{SBR} and 75_{SBR}, 75_{SBR} utilized more wastewater and achieved close to optimal conditions, making it a cost-effective choice for practical wastewater applications. The slight addition of BBM created a more favourable environment for *Scenedesmus* sp. in terms of nutrient uptake. In comparison, 100_{SBR} was nitrogen-limiting, as indicated by the N:P ratio of 20.75, resulting in a lower TP removal rate and efficiency. Therefore, 75_{SBR} was chosen for upscaling, along with the addition of nanoparticles (NP).

4.5. Iron Oxide Nanoparticles Addition and its impact

In this section, we discuss the experiment using 75_{SBR} with additional different NP concentrations in mg/l. The labelling in this section for discussion will be written based on each NP concentration value: C_{SBRNP} ;(75% dilution SBR WW without the addition of NP), 1_{SBRNP}, 2.5_{SBRNP}, 5_{SBRNP}, 10_{SBRNP}, 25_{SBRNP}, 50_{SBRNP} and 100_{SBRNP} and 75% dilution of SBR wastewater is represented as 75_{SBR}

Due to time constraints and limited space, the *Scenedesmus* sp. obtained from the previous SBR_{WW} experiments were mixed, centrifuged, and washed with distilled water multiple times before dilution. This was done to achieve a similar initial microalgae biomass used in the SBR_{WW} experiment, which was approximately 160 mg/L. As a result, the morphology and physiochemical composition of *Scenedesmus* sp. may vary and mixed throughout the experiment, as they have acclimated to different dilutions of SBR_{WW}, as shown in figure 4.25.

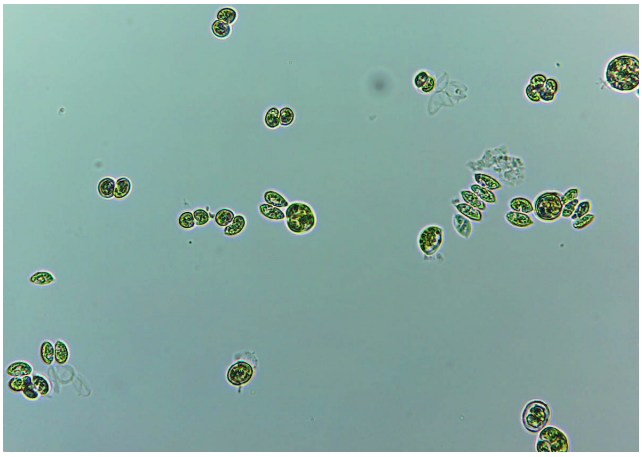

Figure 4.25: Scenedemus sp under optical microscope x40 magnification. A mixed morphology and unicell were observed in the initial biomass, which was used for the start of the experiment with the addition of NP

During the addition of Fe_3O_4 nanoparticles, flocculation and coagulation were observed, visually forming aggregates with the constant gentle shaking of the flask. The number of flocs increased with time and NP concentration, as shown in Figure 4.26a. This type of reaction is commonly utilized in enhanced primary wastewater treatment where dosing Fe^{2+} and Fe^{3+} into wastewater promotes the coagulation and flocculation of suspended and colloidal solids. The microalgae were attracted to the NP due to surface charge neutralization through counter ion adsorption, as depicted in Figure 4.26b. The formation of flocs could also be attributed to the hydrolysis of water molecules by iron, leading to polymerization and the formation of cationic metal polymers that facilitate polymer bridging. The addition of NP also resulted in a darker colouration of the samples, which turned darker with increased NP concentration.

Scenedesmus sp. demonstrated good growth in all samples, as they started to turn

greener every day. Samples were still darker with increased NP concentration.

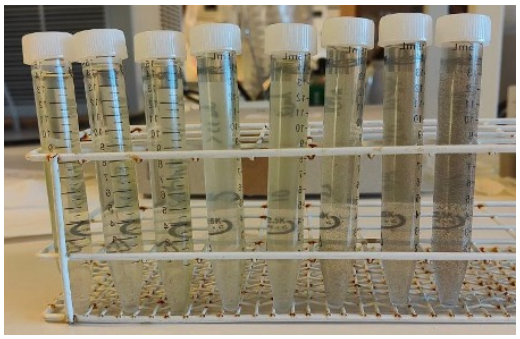

(a) Samples were collected in 20ml centrifuge tubes after inoculation and addition of NP. The samples were arranged in increased NP concentration order starting with C_{SBRNP} to 100_{SBRNP} from left to right. The number of floes could be seen as denser with increasing dilution.

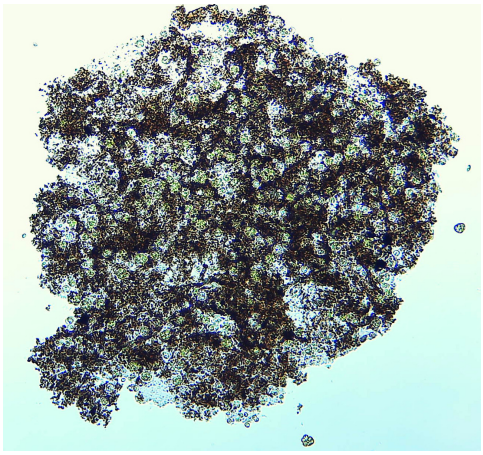

(b) NP Floe viewed under the optical microscope of x25 magnification after inoculation and NP addition. Microalgae could be seen attracted all over the floe, showing signs of flocculation.

Figure 4.26: Flocculation of NP after preparing to start the experiment and analysis physically and under a microscope.

4.5.1. Effect of Iron nanoparticle addition on *Scenedesmus* sp. growth

The C_{SBRNP} sample in this experiment was compared to the 75_{SBR}sample from the SBR_{WW} experiment. Both samples had similar experimental setups and parameters, except for the timeframes and batches of SBR_{WW} used. A new set of SBR WW was used for the addition of the NP experiment due to the depletion of the remaining SBR wastewater. This analysis was aimed at studying the possible differences in nutrient removal and growth between the two samples. After dilution with BMM, both samples contained slightly different TN and TP concentrations, as shown in Table 4.14. In Figure 4.28, both started to increase exponentially from about the same biomass concentration with 10mg/l difference, without a lag phase. However, C_{SBRNP} ended with 23% more biomass concentration than 75_{SBR}, with values of 1457 mg/l and 1115 mg/l, respectively. The maximum biomass achieved in C_{SBRNP} was 1663 mg/l. Regarding nutrient concentrations, C_{SBRNP} ended with a higher TN concentration of 23.2 mg/l compared to 75_{SBR}, but having similar TP concentration with a difference of 0.07 mg/l. However, C_{SBRNP} did manage to remove TN down to 15.3 mg/l, which was close to the TN concentration in 75_{SBR}. The increase in TN values in C_{SBRNP} occurred concurrently with a decrease in biomass, as shown in Figure 4.28 where the N:P ratio increase and the biomass decrease in day 8. Furthermore, it appears that *Scenedesmus* sp. in C_{SBRNP} uptake more nitrogen than phosphorous, whereas, in 75_{SBR}, it consumed more nitrogen than the phosphorous. Both C_{SBRNP} and 75_{SBR} exhibited changes in nutrient preference between days 5-6, as shown by the fluctuation in N:P ratios over time. The initial nutrient preference could be influenced by the availability of easily consumable nitrogen and phosphorus sources, while the changes during

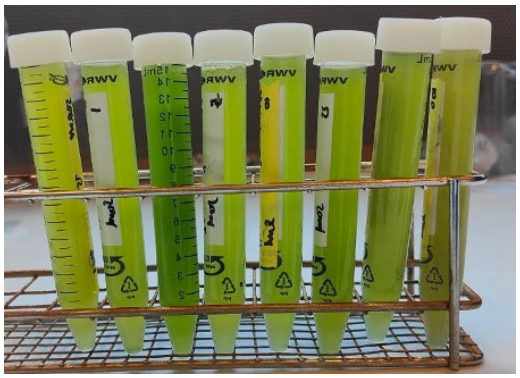

(a) Samples were collected in 20ml centrifuge tubes after 10 days of cultivation. Samples were positioned in increased NP concentration starting with C_{SBRNP} to 100_{SBRNP} from left to right. *Scenedesmus* sp. could be seen growing where the solution was green in colour, and it got darker with increasing concentration.

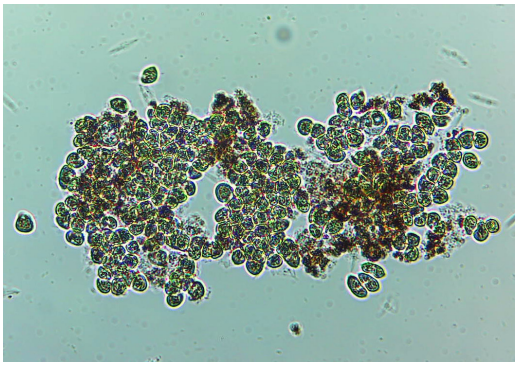

(b) 100_{SBRNP} viewed under the optical microscope of x25 magnification after 10 days of cultivation. Higher *Scenedesmus* sp. concentration could be observed to be clustered with NP compared to initial. The shape of *Scenedesmus* sp. was more irregular compared to 4.25, with black NP particles possibly seen on the surface of microalgae.

Figure 4.27: *Scenedesmus* sp. cultivation with addition of NP after 10 days of cultivation and 100_{SBRNP} viewed under the optical microscope

cultivation could be attributed to the type of limiting nutrients and the depletion of the most readily available nutrient source in the experiment. WW composition can vary, and factors such as season or timing of collection could influence SBR_{WW} characteristics, which may explain the differences observed in the new batch of SBR_{WW} used in this experiment.

Table 4.14: Comparison of initial, final and max of biomass growth, nutrient removal in 10 days cultivation between C_{SBRNP} and 75_{SBR}

Day	C_{SBRNP} mg/l			75_{SBR} mg/l		
	Biomass	TN	TP	Biomass	TN	TP
0	158	68	11.4	168	59	15.9
10	1457	23.2	2.73	1115	14	2.8
Max growth/removal	1663	15.3	2.73	1115	14	2.5

In Figure 4.29, it can be observed that all tested samples were able to grow in the presence of NP, and they all achieved final biomass concentrations higher than C_{SBRNP}. No lag phase was observed in any of the samples, but the presence of NP had an acclimation effect, particularly noticeable at concentrations of 10 mg/l and higher. At these concentrations, a short lag phase or a decrease in biomass was observed after day 4. It took approximately 2 days for the samples to stabilise before resuming exponential growth after day 6. All samples with the addition of NP eventually reached a plateau in the stationary growth phase, with final biomass concentrations

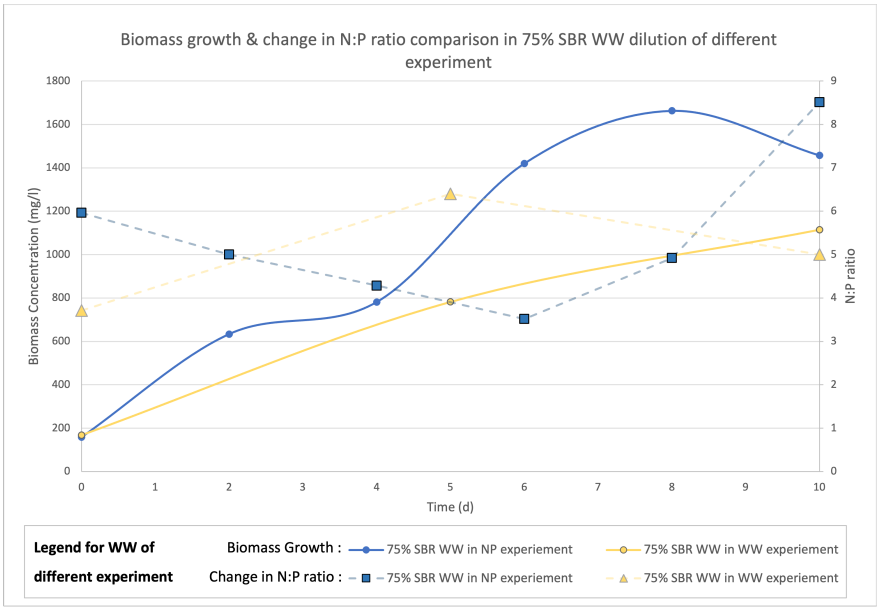

Figure 4.28: Growth rate and N:P comparison of *Scenedesmus* sp. in 2 different SBR 75% dilution. "Control" refers to the C_{SBRNP} used in the NP experiment, while "SBR 75" refers to the 75_{SBR} sample in the previous SBR experiment. The solid line refers to the biomass concentration growth curve with reference from the left y-axis. A dashed line with shaped points refers to the N:P ratio with reference from the right y-axis

ranging from 1695 mg/l for 100_{SBRNP} to 1948 mg/l for 10_{SBRNP}. However, 2.5_{SBRNP} and 25_{SBRNP} exhibited continuous growth beyond the expected stationary phase, reaching final biomass concentrations of 3068 mg/l and 2574 mg/l, respectively. These samples should be expected to transition into their stationary growth phase but continue to increase in biomass. None of the samples with the presence of NP showed signs of growth inhibition, except for a slight reduction in biomass observed in samples with NP concentrations of 10 mg/l or higher. Overall, the addition of NP did not have a detrimental effect on the growth of *Scenedesmus* sp. but stimulated biomass production with respect to increasing concentrations of NP, which led to higher final biomass concentrations.

The increase in biomass concentration observed in 2.5_{SBRNP} and 25_{SBRNP} samples could be attributed to the evaporation of the medium during constant aeration throughout the experiment. The absorbance (ABS) of both samples on day 8 and day 10 was analysed, investigated and compared, as shown in Table 4.15. Significant changes in ABS values could indicate the occurrence of evaporation. Upon comparison, it was found that 2.5_{SBRNP} exhibited a slight increase in ABS, while 25_{SBRNP} showed a decrease in ABS. The ABS values, however, did not show a significant change or difference. The biomass concentrations of 2.5_{SBRNP} and 25_{SBRNP} on day 10 were then remeasured and found to be 3129.6 mg/l and 2824.1 mg/l, respectively. These remeasured values were close to the current biomass concentrations, which indicates that there was no human error in the analysis of the

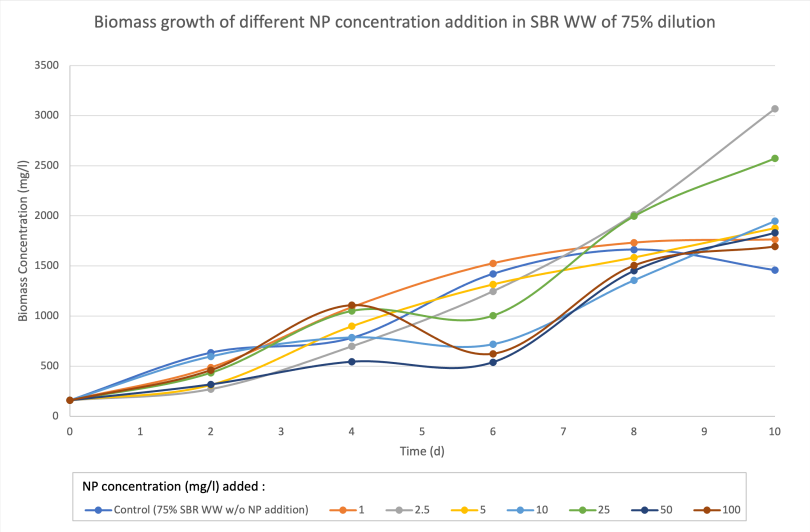

Figure 4.29: *Scenedesmus* sp. biomass growth with different nanoparticles concentration in 75_{SBR}

microalgae TSS measurements. Nevertheless, based on the marking of the conical flask observed from the start to the end of the experiment, there were some indications of evaporation taking place, which could have contributed to the resulting increase in concentration.

Table 4.15: Comparison of Absorbance between day 8 and day 10 for 2.5_{SBRNP} and 25_{SBRNP} with its biomass concentration of current (before ABS test) and remeasured (after ABS test)

Sample	Day 8			Day 10		
	ABS	Biomass (mg/l)		ABS	Biomass (mg/l)	
	(680nm)	current	remeasure	(680nm)	current	remeasure
2.5_{SBRNP}	0.873	2012	-	0.983	3068	3129.6
25_{SBRNP}	0.824	1996	-	0.738	2574	2824.1

The specific growth rate of the samples were analysed, as shown in Figure 4.30. C_{SBRNP} achieved the highest growth rate initially but was observed to decrease over time, reaching a negative and lowest final growth rate. This suggests that C_{SBRNP} was grown with no inhabitant or stress-induced, which resulted in growth at its optimal condition. This allowed C_{SBRNP} to reach each growth phase earlier than the rest. In relation to biomass growth, as depicted in Figure 4.29, samples with NP concentrations of 10mg/l and higher exhibited a decrease in biomass growth, observed from a continuous decrease in growth rate from day 2 onwards, eventually leading to a negative growth rate on day 6. However, by day 8, these samples showed an exponential increase and achieved the highest growth rates before reaching a stationary phase. Among these samples, 50_{SBRNP} achieved the highest growth rate, followed by 100_{SBRNP}, 25_{SBRNP} and 10_{SBRNP}. This pattern suggests that on day 2, *Scenedesmus* sp. started producing and accumulating reactive oxygen species (ROS)

in response to the high NP concentration, leading to abiotic stress. The imbalance of ROS could be the reason for the decrease in growth rate and biomass which induce oxidative stress and damage. After day 6, *Scenedesmus* sp. may have been able to overcome and adapt to the stress after day 6, which promote growth again (Vasistha et al. 2021). 2.5_{SBRNP} was able to achieve the highest biomass at day 8 despite not achieving the highest growth rate due to its constant growth rate throughout the cultivation. Nonetheless, this shows that the addition of NP to *Scenedesmus* sp. improved biomass growth, although higher NP concentrations had a negative impact on growth rate initially before the microalgae adapted and resumed growth.

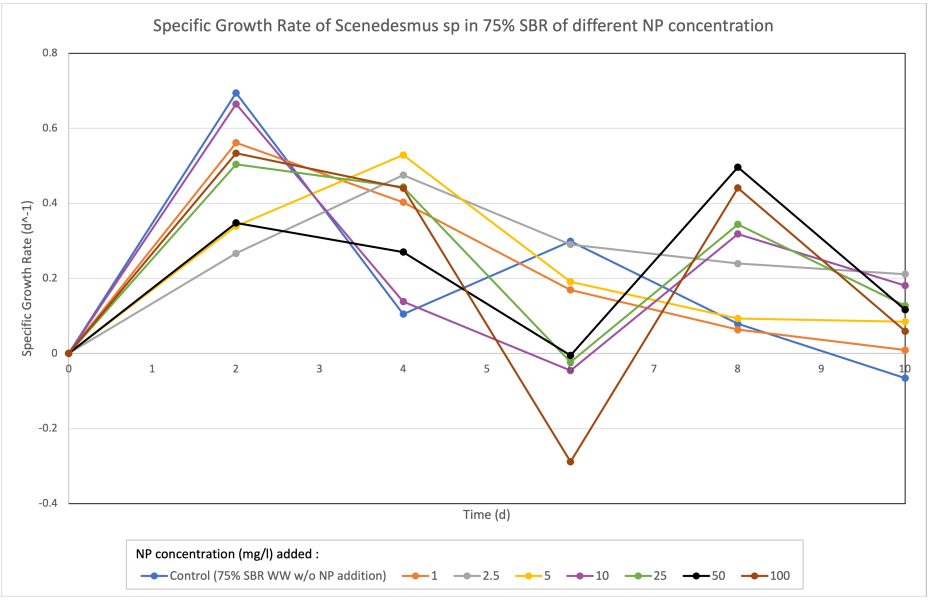

Figure 4.30: Specific growth rate of Scenedemus sp with NP addition in 75_{SBR} in a period of 10-day cultivation. The specific growth rate was calculated from the biomass growth from the selected day to its previous day, which was within 2 days interval.

Fe is considered an essential micronutrient for microalgae, and its dosage can have both positive and negative effects on productivity and biomass. In this experiment, growth was still observed in the presence of Fe_3O_4 NP, suggesting that *Scenedesmus* sp. may be capable of tolerating higher dosages of Fe. A study by He et al. 2017 investigated the effects of different types of NP, including Fe_2O_3, on *Scenedesmus obliquus*. They found that the microalgae exhibited growth in all tested concentrations up to 100mg/l but observed a reduction in biomass and variation in chlorophyll content with increasing NP concentration. Similar to the present experiment, they found that the highest biomass concentration was achieved at 2mg/l of iron NP concentration. The justification of ROS effect on growth inhibition was identified through the analysis of H_2O_2, which was found that increased ROS with increased NP concentration except for growing in the presence of CNTS where it varies (He et al. 2017). Furthermore, the influence of different NP on microalgae has been investigated in other studies as well. For example, Vasistha et al. 2021 studied the impact of ZnO NP by growing *Chlorosarcinopsis* sp. in primary and secondary

treated WW with the addition of ZnO NP at different concentrations. They observed a similar trend where lower NP concentrations of 1 and 10mg/l promoted compatibility and max biomass growth while higher NP concentrations of 50 and 100mg/l showed inhibition. The acclimatisation of *Chlorosarcinopsis* sp. to the presence of NP was also mentioned, with significantly increased biomass in low NP concentrations after a certain period of time (Vasistha et al. 2021).

Iron, in another form, has also been shown to influence microalgae. Wan et al. 2014 demonstrated the positive impact of adding a mixed iron solution to *Chlorella Sorokiniana* cultivation. They found that the addition of Fe^{3+} solution resulted in enhanced growth, lipid production, and other metabolic alterations, surpassing the control values (Wan et al. 2014). These studies collectively suggest that, in general, the addition of NP can significantly influence microalgae growth and productivity. This response may vary depending on the microalgae species, nanoparticle type, and concentration used in the experiments.

4.5.2. Nutrient Removal of *Scenedesmus* sp. with the addition of iron nanoparticles

Scenedesmus sp. was also capable of nutrient removal in the presence of NP in 75_{SBR} as shown in Figure 4.31. Initially, all samples started the experiment with TN concentrations between 64-68 mg/l and phosphorus concentrations of 10-11 mg/l. Throughout the experiment, the nutrient removal fluctuated, with the highest removal observed around day 4, and then the removal rate slowed down or transit into stationary until the end of the experiment. The addition of NP was found to enhance nutrient removal in all samples, resulting in lower nutrient concentrations compared to the C_{SBRNP}. Among the samples, 2.5_{SBRNP} achieved the lowest final nutrient concentrations, with 11.2 mg/l TN and 0.68 mg/l TP. Excluding C_{SBRNP}, 1_{SBRNP} had the highest final TN concentration at 20.4 mg/l, while 5_{SBRNP} had the highest final TP concentration at 2.725 mg/l, similar to C_{SBRNP}. As the values fluctuate, the lowest possible TN removal was achieved by 2.5_{SBRNP}, which is 7.2mg/l.

The enhancement in nutrient removal with the addition of NP can also be observed in Figure 4.32 where an average removal efficiency of 80% or more was achieved. As mentioned earlier, 2.5_{SBRNP} achieved the lowest final nutrient concentrations, resulting in the highest nutrient removal efficiency of 89% for TN and 94% for TP. All samples showed higher nutrient removal efficiency compared to C_{SBRNP} except for 5_{SBRNP}, which had the lowest TP removal efficiency. According to the European Union (EU) regulations for urban wastewater treatment in 2022, tertiary treatment is required to achieve a minimum percentage reduction in 85% TN and 90% TP concentrations. Both parameters are dependent on many factors, and the comparison and evaluation of the minimum nutrient reduction percentage (marked in red) were drawn across the graph with two dashed lines in Figure 4.32 (Commission, 2022). Among the samples, only 2.5_{SBRNP} and 25_{SBRNP} met the EU removal efficiency requirements for both nutrients, while 50_{SBRNP} and 100_{SBRNP} met

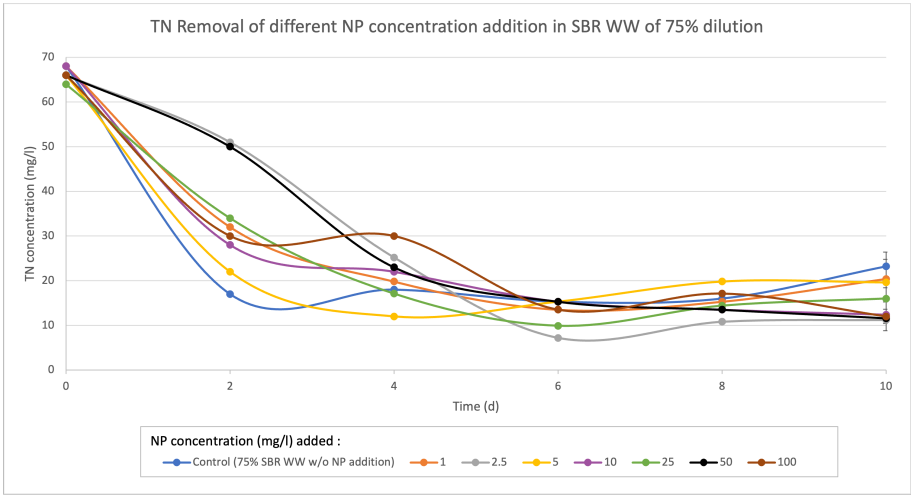

(a) TN removal comparison in 75_{SBR} with addition of different NP concentration

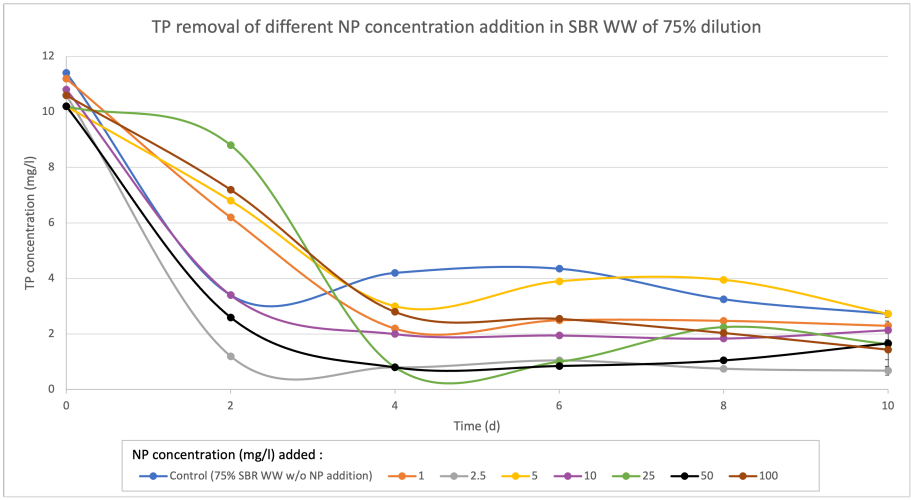

(b) TP removal comparison in 75_{SBR} with addition of different NP concentration

Figure 4.31: Nutrient removal in 75_{SBR} with addition of different NP concentration

the requirement for TP removal only. Comparing these results to the nutrient removal efficiency of *Scenedesmus* sp. in DAF_{WW} and SBR_{WW} in Figure 4.32, none of the samples achieved the required removal efficiency. Based on the result, *Scenedesmus* sp. can be concluded as not beneficial for the bioremediation of wastewater as a secondary treatment, but it shows great potential as a tertiary treatment option with the addition of iron NP.

Iron oxide Fe_3O_4 NP are commonly used in the remediation of wastewater for heavy metal and pollutant removal. They serve as nanosorbents and coagulating agents due to their diffusion capability, high surface area, chemical stability, and aggregation properties. When combined with microalgae cultivation, the presence of iron oxide NPs further enhances nutrient removal through processes such as absorption, electrostatic attraction, oxidation by iron, and increased nutrient assimilation by

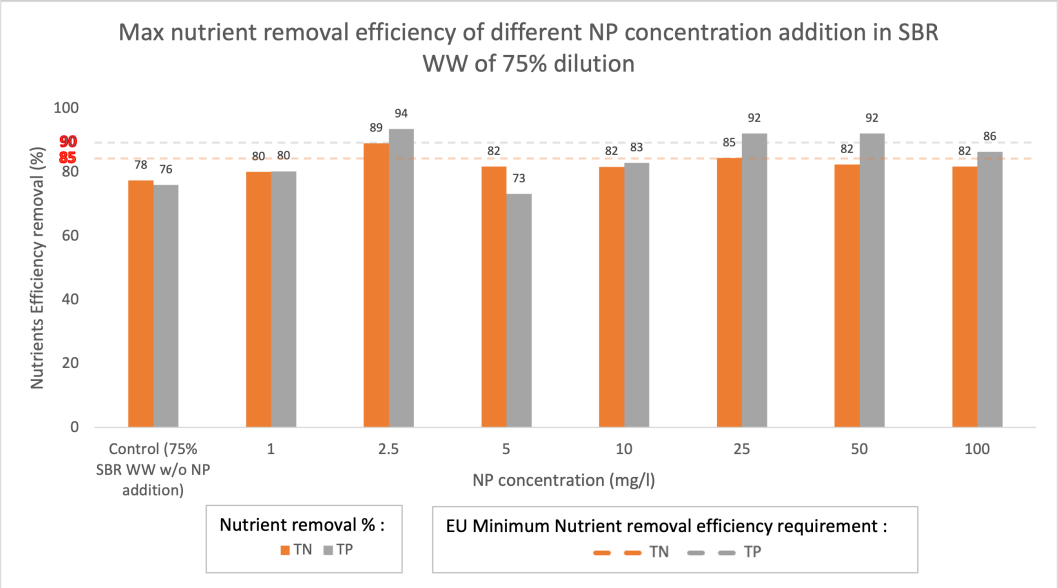

Figure 4.32: The removal efficiency of TN and TP by *Scenedesmus* sp. with different NP concentration in 75_{SBR} were analysed. The requirement of EU minimum Nutrient removal efficiency was added to understand how the addition of NP could benefit from achieving close to the limit set.

microalgae (Eljamal et al. 2022; Xu et al. 2012). Metals, including iron, are essential micronutrients for microalgae, serving as cofactors for enzymes involved in various bioremediation processes, such as phosphorus acquisition, nitrogen assimilation, and nitrate reduction (Miazek et al. 2015). However, most studies on NPs with microalgae have focused on bioremediation of heavy metals, magnetic harvesting, and growth enhancement rather than TN and TP removal (Dubey et al. 2022). Nevertheless, as TN and TP are required for microalgae growth, the growth enhancement facilitated by the addition of NP indirectly increases the uptake rate of these nutrients. Moreover, the presence of NP inhibits bacterial growth and removes contaminants, allowing microalgae to thrive in the cultivated environment.

For example, Vasistha et al. 2021 observed up to 85% TN and 81.5% TP removal efficiency by *Chlorosarcinopsis* sp. in secondary treatment wastewater with the addition of 10mg/l of ZnO NP (Vasistha et al. 2021). Similarly, Xia et al. 2021 conducted an experiment where they added two different NPs, ZnO and Fe_2O_3, where both had a concentration of 10g/l and 20g/l, to artificial wastewater cultivated by *Chlorella Vulgaris*. They found that the addition of NPs resulted in a reduction of ammonia and phosphorus by over 40% and 100%, respectively. Additionally, the presence of Fe_2O_3 NP led to higher removal of ammonia and phosphorus compared to ZnO while also promoting higher lipid content. However, ZnO demonstrated a higher adsorption rate compared to Fe_2O_3 (Xia et al. 2021).

4.5.3. Relationship between *Scenedesmus* sp. kinetic growth and nutrient uptake at different iron nanoparticles concentration

The specific nutrient removal rate was plotted against the average specific growth rate to understand the relationship between these variables at different NP concentrations. The data points were closely clustered around an N:P ratio of 5-6.6 and an average specific growth rate of 0.1 to 0.15 μ as shown in Figure 4.33. All samples with the addition of NP outperformed C_{SBRNP} in both variables, indicating the enhancement of growth and nutrient removal in the presence of NP. Among the samples, 5_{SBRNP}, 10_{SBRNP} and 50_{SBRNP} had N:P ratios higher than 6, with 10_{SBRNP} having the highest ratio of 6.42, while the rest had lower ratios, with 1_{SBRNP} being the lowest. The highest average specific growth rate was observed in 2.5_{SBRNP} at 1.48 μ followed by 25_{SBRNP} at 1.4 μ with the rest clustering between 1.19 to 1.26 μ. This high growth rate of 2.5_{SBRNP} and 25_{SBRNP} corresponded to the high biomass productivity shown in Figure 4.34, at 528 and 496 mg/L/d, respectively. Although 100_{SBRNP} had lower average nutrient removal and growth rates compared to 10_{SBRNP}, 100_{SBRNP} had the highest biomass productivity. This can be attributed to the acclimatisation period, as shown in Figure 4.30 where 100_{SBRNP} initially experienced a significant decrease in average specific growth rate, much lower than 10_{SBRNP} but then exhibited a substantial increase after. This similar trend can be observed when comparing between 50_{SBRNP} and 25_{SBRNP}. The relationship between the average growth rate and average nutrient removal rate throughout the 10-day cultivation varies in opposite directions as the NP concentration changes. Increasing the NP concentration reduces the growth rate while increasing the nutrient removal rate. 1_{SBRNP} was the exception that deviated from this trend. This concludes that the enhancement in the average specific growth rate using NP for *Scenedesmus* sp. in 75_{SBR} wastewater is up til 2.5mg/l, NP concentration and the enhancement in average nutrient removal rate is up til of 10mg/l NP concentration.

However, Figure 4.32 contradicts this conclusion as 2.5_{SBRNP} exhibited the highest nutrient removal efficiency, followed by 25_{SBRNP}. This discrepancy can be attributed to the slight increase in TN after reaching maximum efficiency, which subsequently lowers the N:P ratio. Furthermore, the specific biomass yield resulting from nutrient uptake was also plotted for comparison. The yield was calculated based on each sample's average specific nutrient rate. All samples were able to generate more biomass with 1g of each nutrient compared to C_{SBRNP}, which explains the growth enhancement observed with the addition of NP. The same trend was observed in this plot, where the maximum biomass was produced up to a 2mg/l NP concentration, followed by a decrease in biomass with further increases in NP concentration. However, 10_{SBRNP} and 25_{SBRNP} deviated from this trend with values that did not follow the expected pattern.

Therefore, it can be concluded that the addition of NP promotes biomass growth and nutrient removal in WW, with the optimal condition achieved at an NP concentration of 2.5 mg/l. This concentration resulted in a maximum nutrient removal efficiency of

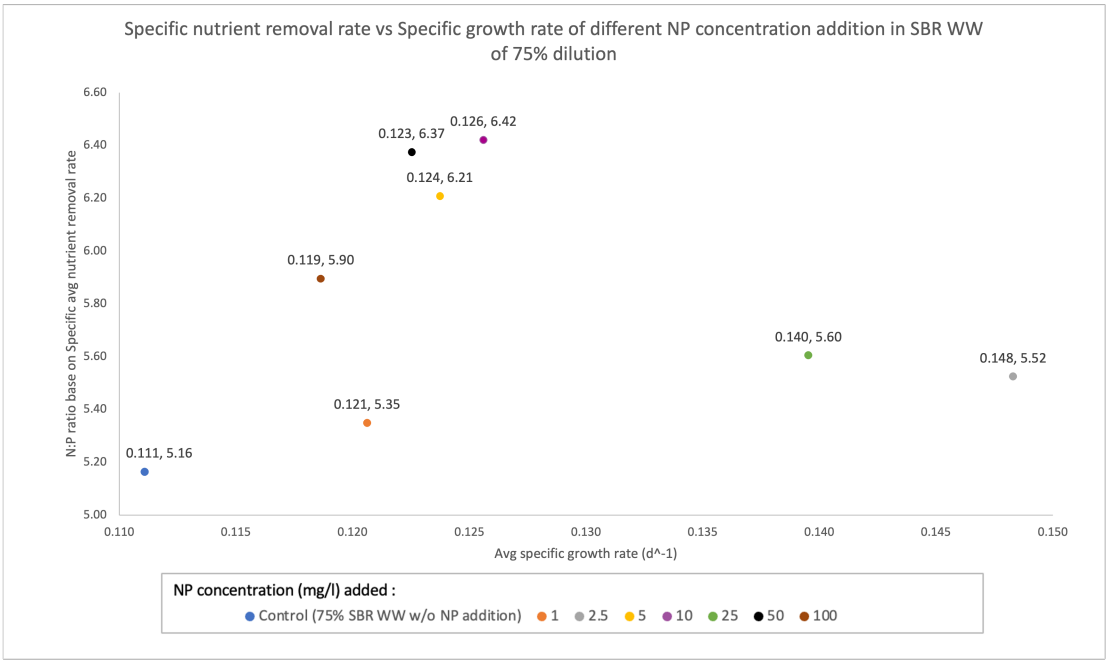

Figure 4.33: N:P ratio based on Specific nutrient removal rate was plotted against the average specific growth rate of *Scenedesmus* sp. on different NP concentrations in 75_{SBR} within 10 days, to understand the relationship in NP addition to microalgae growth rate and nutrient removal rate.

almost 90%, representing a 30% increase in growth rate compared to samples without NP addition. However, as the NP concentration increases, the growth rate and biomass production decrease while the nutrient removal rate increases. The experiment demonstrated that *Scenedesmus* sp. used in this study exhibited extreme tolerance towards Fe_3O_4 NP, as it was able to grow even at a concentration of 100g/l, outperforming the sample without NP addition. This suggests that the *Scenedesmus* sp. could potentially tolerate even higher concentrations of NP. Nonetheless, with the results studied in this experiment, it is recommended to set the tolerance range for *Scenedesmus* sp. towards Fe_3O_4 NP at a concentration of 50mg/l, as it still exhibited a high nutrient removal efficiency of up to 82% TN and 92% TP, with a nutrient removal rate ratio of up to 6.37, and a decent growth rate. NP toxicity was observed starting from the sample containing 10mg/l NP concentration, with toxicity increasing as the concentration increased despite no inhibition of biomass growth observed in this experiment.

For the Biochemical Methane Potential (BMP) test, C_{SBRNP}, 2.5_{SBRNP}, 50_{SBRNP} and 100_{SBRNP} samples were selected to examine the effect of NP addition and different NP concentrations on methane gas production efficiency. These samples were chosen to compare methane production in the absence of NP: (C_{SBRNP}), the optimal condition: (2.5_{SBRNP}), high nutrient removal rate: 25_{SBRNP} and highest NP concentration: 100_{SBRNP}.

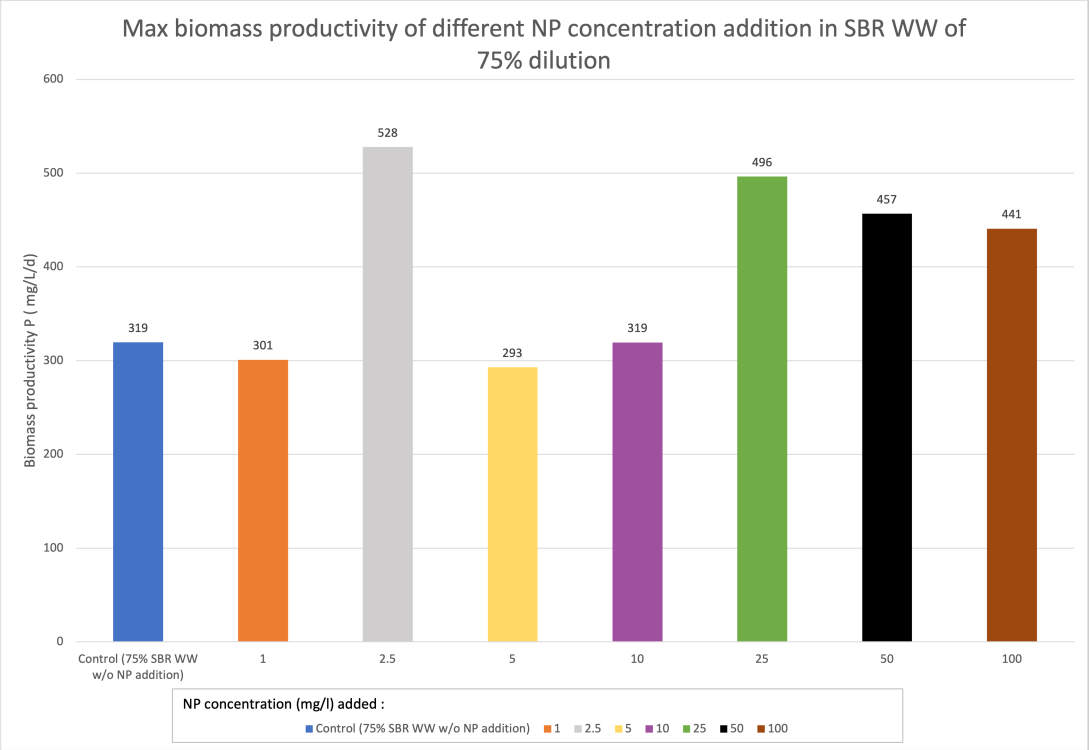

Figure 4.34: The maximum biomass productivity by *Scenedesmus* sp. with different nanoparticles concentration in 75_{SBR} in the 10-day cultivation was compared.

4.6. Biochemical methane potential (BMP) experiment

The selected samples with different NP concentrations were used for biogas production in the Biochemical Methane Potential (BMP) test. In this test, SBR sludge was used as the inoculum, even though most BMP tests typically utilise activated sludge for better biogas efficiency and production. The use of SBR sludge, in this case, was due to time constraints, as it allowed for the possibility of running the experiment for a duration of 30 days. To determine the Substrate to Inoculum (S/I) ratio, the Chemical Oxygen Demand (COD) of the substrate (microalgae) and the Volatile Suspended Solids (VSS) of the inoculum (SBR sludge) were used. For this experiment, a ratio of 1:1 was used. In this section, the acronyms were labelled as follows to identify each sample, where the initials represent the different NP concentration: C_{BMP}; (75_{SBR} without the addition of NP), 2.5_{BMP}, 25_{BMP}, 100_{BMP}. Additionally, the following supporting samples will be referred to as: $Blank_{BMP}$; (Inoculum with no substrate),G_{BMP}; (Inoculum with glucose as substrate)

In a study by Mahdy et al. 2016, it was found that *Scenedesmus* sp. exhibited exponential gas production from the beginning of the experiment until day 10, reaching approximately 100 ml of methane per gram of COD. Afterwards, the gas production continued to increase gradually, reaching a stationary phase around day 25 (Mahdy et al. 2016). Similarly, Mussgnug et al. 2010 conducted experiments using

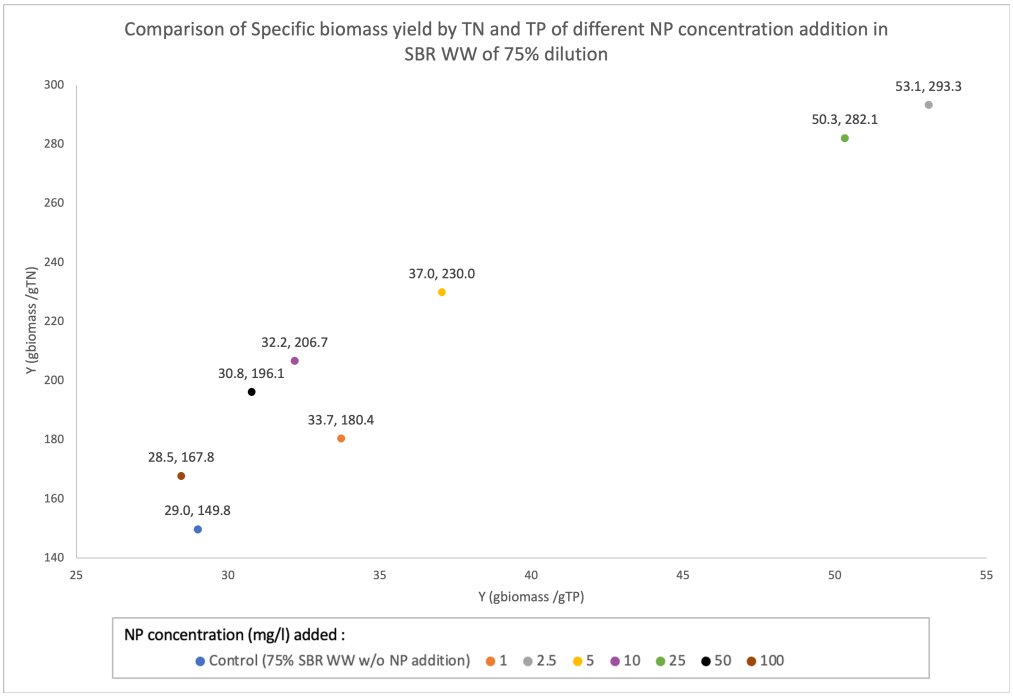

Figure 4.35: Specific biomass yield from TN and TP by *Scenedesmus* sp. with different NP concentrations in 75_{SBR} dilution in 10-day cultivation were analysed.

seven different microalgae species as substrates, including *Scenedesmus obliquus*. They observed a similar trend in biogas production, with a significant increase in gas production until day 10-15, followed by a gradual transition to the stationary phase (Mussgnug et al. 2010). During the initial days of the experiment (day 1 to day 8), low levels of gas were collected, ranging from approximately 6 to 10 ml. However, these amounts were insufficient for reliable and stable results in gas chromatography analysis. Therefore, the gas collection was performed at irregular time intervals to allow for the accumulation of at least 20 ml or more of gas before conducting gas chromatography analysis. All samples showed gas production throughout the experiment but experienced a lag phase before the significant increase in gas production after day 10. In the case of G_{BMP}, a long lag phase was observed, with no gas production observed from day 2 to day 23. Gas production started only after this period, as depicted in Figure 4.36.

The observed lag phase in all samples can be attributed to the presence of facultative aerobes in the SBR sludge, which require time to adapt to anaerobic conditions. It is possible that the obligate aerobes present in the SBR sludge eventually died out, supplementing organic matter for the anaerobic process. This observation is supported by the slight increase in gas production observed in the $Blank_{BMP}$ sample between day 5 and day 8, as shown in Figure 4.36. These findings also suggested that SBR sludge can be used as an inoculum for biogas production. In terms of total gas volume, both 2.5_{BMP} and 25_{BMP} produced approximately 25% more gas compared to C_{BMP}. Among them,2.5_{BMP} had the highest biogas volume of 71.6 ml, followed by

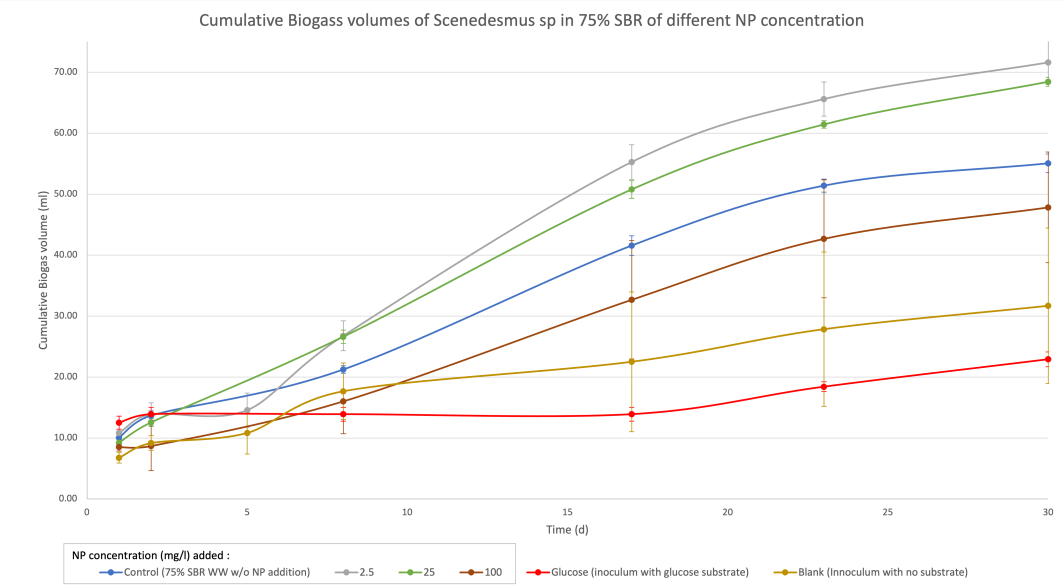

Figure 4.36: Cumulative biogas production volume of *Scenedesmus* sp. with additional of different NP concentration, using SBR sludge as an inoculum for 30 days. Sample of blank (Inoculum with no substrate) and glucose (inoculum with glucose as substrate)

68.4 ml for 25_{BMP}. On the other hand, 100_{BMP} only produced a total gas volume of 47.8 ml, which is 13% lower than C_{BMP}. Excluding $Blank_{BMP}$ and G_{BMP}, all other samples achieved methane content of over 70% with 25_{BMP} exhibiting the highest methane content of 78%. However, G_{BMP} was analysed to only produce 38% methane with a negative of total gas production. The theoretical Yield calculation of CH_4 by a molecule of glucose is 418ml CH_4 /g glucose (Rodriguez-Chiang & Dahl, 2015). Therefore, there might be errors in the gas chromatography analysis due to the low gas volume used as input, which can affect the accuracy of the results. Furthermore, low production of biogas in G_{BMP} attributed to a long lag phase, extended up til the 18-day duration of the experiment. This phenomenon could be, the longer adaptation to glucose, difficulties in breaking down glucose or the unsuitability of glucose as a substrate for the specific SBR sludge used in the experiment

Figure 4.37 presents the cumulative methane volume produced by all samples. The values from $Blank_{BMP}$ were subtracted from all samples to remove any background gas production without a substrate. Due to the inaccurate values G_{BMP}, they are not included in the graph. It can be observed that both 2.5_{BMP} and 25_{BMP} produced more methane gas compared to C_{BMP} with 2.5_{BMP} achieving the highest value of 427.4 ml CH_4/g COD, following by 25_{BMP} at 345.9 ml CH_4/g COD. 100_{BMP} was able to reach methane values close to C_{BMP} with a difference of approximately 18 ml CH_4/g COD. When calculating the methane gas production of $Blank_{BMP}$ by converting VSS to COD using the theoretical value of 1.42, it was found that $Blank_{BMP}$ achieved methane values close to C_{BMP} with a difference of about 8 ml CH_4/g COD. The higher methane production in 2.5_{BMP} could be attributed to the accumulation of lipids

Table 4.16: Summary of biogas production characteristics and results obtained by BMP test of *Scenedesmus* sp. grown with presence of different concentrations of nanoparticles

Sample	COD (mg/l)	Total Biogas production (ml)	Methane CH_4 content (%)	Total methane gas production (ml CH_4/g COD)
C_{BMP}	3400	51.4	76	208.2
2.5_{BMP}	6380	65.6	74	237.1
25_{BMP}	6400	61.4	78	295.6
100_{BMP}	3045	42.7	75	197.7
$Blank_{BMP}$	2650	27.8	86	194.8
G_{BMP}	1067	18.4	38	-369.7

during the cultivation period. A sudden increase in methane production was also observed in 2.5_{BMP} after day 23, which could suggest that the anaerobic bacteria are at their optimal after adaptation to the environment. Lipids are energy-rich compounds that can be converted into biogas with a higher methane content compared to other organic materials. Furthermore, 100_{BMP} exhibited much lower methane values than other NP concentrations. This can be attributed to the toxicity and stress induced on the microalgae, triggering defensive barriers that require significant energy to break down, resulting in low biogas production. Despite that, 100_{BMP} managed to surpassed C_{BMP} after day 23. This slight burst in methane after day 23 could also be due to the unstable temperature in the oven, which fluctuates between 39 to 41°C.

Table 4.17: Summary of literature studies of biogas production, Methane production and content % of raw *Scenedesmus* sp. and other microaglaes

Type of microaglae	S/I	Biogas production $\frac{mlbiogas}{gVSS}$	Methane Production $\frac{mlCH_4}{gCOD}$	CH_4 %	Reference
Scenedesmus sp.	0.5	-	125	62	(Mussgnug et al. 2010)
Scenedesmus sp.	0.5	-	141.6	62	(Mahdy et al. 2016)
Scenedesmus sp.	0.5	-	154	-	(Mendez et al. 2014)
Scenedesmus sp.	1	530.07	263.6	63.4	(Torres et al. 2021)
Chlorella vulgaris		-	150.2	-	(Mendez et al. 2014)
Chlorella sp.	1	473.87	227.4	68.16	(Torres et al. 2021)
Nannochloropsis sp.	1	518.42	250.4		(Torres et al. 2021)

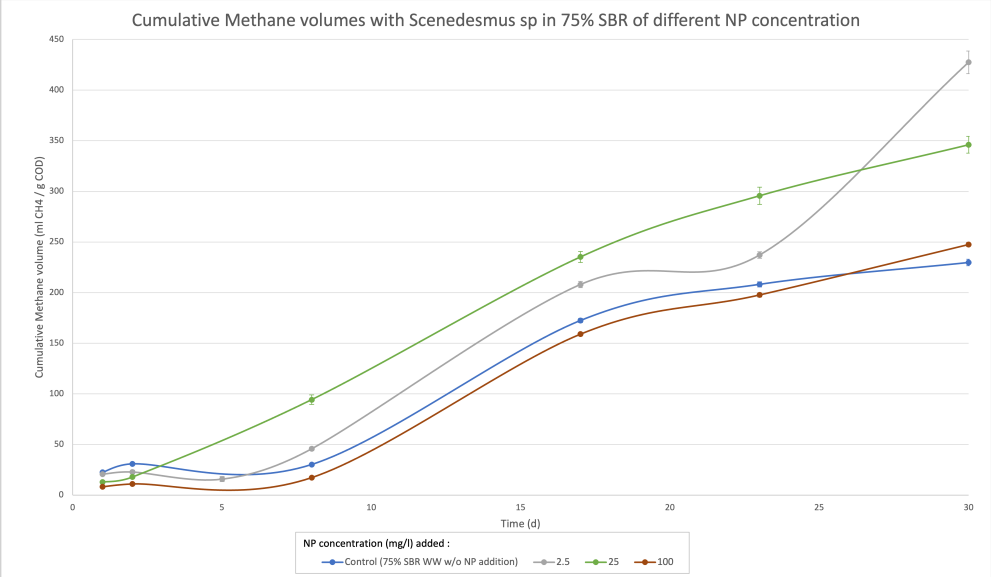

Figure 4.37: Methane production volume of *Scenesdesmus* sp. with additional of different NP concentration in SBR sludge as an inoculum. All the samples were subtracted with blank to remove any background gas production that may occur in the absence of an actual substrate. Inoculum with glucose as substrate was not able to produce enough gas and therefore removed from the graph.

Comparing the results obtained in this experiment with literature values for raw *Scenedesmus* species, Mussgnug et al. 2010 reported a methane production of 125 ml CH_4/g COD with 62% of methane content, Mahdy et al. 2016 found similar values of approximately 141.6 ml CH_4/g COD with 62% of methane content and Mendez et al. 2014 reported a value 154 ml CH_4/g COD. These studies used an inoculum-to-substrate ratio of 0.5, while in this experiment, the ratio was 1. Therefore, it is justifiable that the methane gas production and content in this experiment were higher, reaching 229.7 ml CH_4/g COD and 76%, respectively.

Table 4.18: Summary of literature studies of biogas production, Methane production and content % of microalgae grown with different types of NP

Type of microaglae	Type of NP used	Biogas production ml biogas /g VSS	Reference
Chlorella Pyrenoidosa	Fe_2O_3	605	(Rana et al. 2020)
Enteromorpha	Fe_3O_4	>620	(Zaidi et al. 2018)
Enteromorpha	Ni	>620	(Zaidi et al. 2018)
Enteromorpha	Co	545	(Zaidi et al. 2018)
Enteromorpha	MgO	535	(Zaidi et al. 2018)

Furthermore, the addition of NP to the growth of *Scenedesmus* sp. was found to enhance methane production by about 60% when comparing C_{BMP} and 25_{BMP}. In a study by Rana et al. 2020, the addition of 30mg/l of Fe_2O_3 NP to *Chlorella Pyrenoidosa* cultivation resulted in a 25.14% increase in biogas production, reaching 605 ml biogas /g VSS. Similarly, Zaidi et al. 2018 conducted an experiment using green microalgae (*Enteromorpha*) and observed a positive effect on biogas production with the presence of NP. In particular, the addition of 10ml/g of Fe_3O_4 NP led to a 20% increase in biogas yield. Comparing these findings to the present experiment, which showed a 15% increase in biogas production, it can be concluded that the addition of Fe_3O_4NP enhances biogas and methane production.

Compared to other microalgae species, *Scenedesmus* sp. had been found to exhibit lower biogas and methane production. This can be attributed to its hemicellulose cell wall, which provides rigidity and serves as a protective barrier against degradation factors, making it less easily degradable (Mahdy et al. 2016). Additionally, other hindering properties, such as proteins with lower hydrolysis rates, can contribute to the low anaerobic biodegradability of some species (Mahdy et al. 2016).

Among the samples tested in the BMP test, 2.5_{BMP} demonstrated the highest biogas and methane production, showing competitive results compared to 25_{BMP}, also in terms of kinetic growth and nutrient removal. However, 25_{BMP} and 100_{BMP} exhibited NP toxicity and stress on the microalgae with decreasing biogas produced. With its ability to meet EU nutrient removal requirements, highest biomass productivity and methane production, 2.5_{BMP}shows strong potential for scaling up and application trials. 100_{BMP} had the lowest biogas and methane production and would not be a favourable choice for upscaling.

4.7. Technical Difficulties and Issues

Conducting and executing a successful experiment relies on various factors, including the availability of appropriate equipment, sufficient time for learning and familiarising oneself with different testing methods. This section discusses the technical difficulties and issues faced during the experiment, which hindered the comprehensive analysis of the conducted research.

4.7.1. Insufficient Data Points Affecting Graphical Representation Quality

One of the primary challenges encountered during the experiment was the limited number of data points collected. In general, a greater number of data points, such as conducting triplicate tests, enables the generation of robust graphs and facilitates statistical analysis, ensuring good reliability, stability, and higher accuracy. However, due to limited resources, the frequency of data collection was compromised and restricted. Resources were allocated and divided to accommodate a series of experiments. Examples of limited resources include nutrient test kits and filter paper.

4.7.2. Limited time for experimentation

Time constraints also posed significant limitations to the experiment process, which were further amplified by the limited resources. Conducting a rigorous experiment requires adequate time for proper planning and execution, especially when aiming for high-quality sample analysis. However, the thesis was bound to a short time frame.

The scheduling and planning of this thesis heavily relied on the preparation and cultivation of microalgae, which required more than 10 days each. This restriction affected the ability to conduct experiment replications and potential troubleshooting, resulting in significant time constraints. Moreover, the limited available resources resulted in less data collection.

4.7.3. Unfamiliarity with testing methods

The experiment demanded time and effort to master the methods used. For instance, the inoculation of microalgae into a nutrient medium for cultivation in sterile conditions could be challenging for new researchers. Equipment and machine requirements may also vary across different laboratories, necessitating method calibration to achieve comparable results. A lack of familiarity with the testing methods can lead to errors and inconsistencies, impacting the precision and reliability of the data. Therefore, time is necessary to study and gain a good understanding of the testing methods before their implementation. However, the limited time frame provided prevented extensive practice and refinement to improve the accuracy and consistency of data collection.

Although the experiment faced the aforementioned challenges, resulting in limitations to the amount of collected data, it also provided opportunities for troubleshooting and learning to achieve the objectives set for this study. These limitations should be considered when exploring new methods or continuing this study for future research.

Concluding remarks

Although *Scenedesmus* sp. showed nutrient removal capability and growth potential in all wastewater samples of different dilutions, optimal results were achieved when growing the microalgae in SBR_{WW}. Both SBR_{WW} and (DAF_{WW}) demonstrated competitive results, but (SBR_{WW}) was chosen due to its superior TP removal efficiency of 82.4%. Furthermore, (SBR_{WW}) underwent a secondary treatment process, which removed possible inhibition factors for microalgae cultivation. (75_{SBR}) was selected for upscaling due to its stability in nutrient removal. (100_{SBR}) and (25_{SBR}) were also competitive choices. Despite their high TN removal efficiency, (100_{SBR}) was nitrogen limiting, and (25_{SBR}) would not be cost-effective in terms of wastewater volume usage. Moreover, both options resulted in low phosphorus removal.

The addition of NP resulted in the enhancement of growth and nutrient removal capabilities of *Scenedesmus* sp. No growth inhibition of microalgae was observed. Instead, the values exceeded those obtained by (C_{SBRNP}) in both growth kinetics and nutrient removal. The optimal NP concentration addition was (2.5_{SBRNP}), which achieved the highest biomass production with a nutrient removal efficiency above 85%, meeting EU standards, whereas (25_{SBRNP}) came in second place. Despite the high NP concentrations of (50_{SBRNP}) and (100_{SBRNP}), they were able to produce higher biomass, growth rate, and TP removal efficiency than expected. C_{SBRNP}, (2.5_{SBRNP}), (2.5_{SBRNP}), and (100_{SBRNP}) were chosen for the BMP test to identify the effect of biogas production with NP addition and how it changes with concentration.

Using *Scenedesmus* sp. grown in the presence of NP, they have shown improvement in biogas production and methane content, with the high values observed in 25_{BMP} at % and 78%, respectively. This suggests an increase in lipid accumulation during growth with the presence of high NP concentrations induced by metal toxicity. (100_{BMP}) resulted in lower gas production, indicating the effect of toxicity and stress during growth, which triggered the production of a defensive barrier that can be very energy costly to break down.

5.1. Conclusion

In conclusion, adding 2.5 mg/l of Fe_3O_4 NP to *Scenedesmus* sp. cultivation in SBR wastewater resulted in optimal biomass production, nutrient removal, and highest in biogas production.

Further studies could explore such as :

1. Changing other parameters, such as pH and temperature, while growing *Scenedesmus* sp. with different types of NP.
2. Continual studies could focus on the enhancement of lipids and other compositions induced by metal toxicity toward biogas production by Fe_3O_4 NP and other types of NP.
3. As growth was observed in *Scenedesmus* sp. in PW, further studies can be on PW: change in pigmentation and composition accumulation induced by salinity stress toward desalination of produced water by *Scenedesmus* sp
4. *Scenedesmus* sp. had shown magnetic capability after cultivating with Fe_3O_4 NP, continual studies could look into the efficiency of microalgae magnetic harvesting and recovery of Fe_3O_4 NP.
5. The study of Fe_3O_4 NP recovery can be combined with the study on the biosynthesis of Fe_3O_4 NP by *Scenedesmus* sp

References

Abdel-Raouf, N., Al-Homaidan, A., & Ibraheem, I. (2012). Microalgae and wastewater treatment. *Saudi journal of biological sciences*, *19*(3), 257–275.

Al-Ghouti, M. A., Al-Kaabi, M. A., Ashfaq, M. Y., & Da'na, D. A. (2019). Produced water characteristics, treatment and reuse: A review. *Journal of Water Process Engineering*, *28*, 222–239.

Amini Fard, F., Jalilzadeh Yengejeh, R., & Ghaeni, M. (2019). Efficiency of microalgae scenedesmus in the removal of nitrogen from municipal wastewaters. *Iranian Journal of Toxicology*, *13*(2), 1–6.

Arora, N., Laurens, L. M., Sweeney, N., Pruthi, V., Poluri, K. M., & Pienkos, P. T. (2019). Elucidating the unique physiological responses of halotolerant scenedesmus sp. cultivated in sea water for biofuel production. *Algal Research*, *37*, 260–268.

Bauer, D. E., Conforti, V., Ruiz, L., & Gomez, N. (2012). An in situ test to explore the responses of scenedesmus acutus and lepocinclis acus as indicators of the changes in water quality in lowland streams. *Ecotoxicology and Environmental Safety*, *77*, 71–78.

Bold, H. C. (1949). The morphology of chlamydomonas chlamydogama, sp. nov. *Bulletin of the Torrey Botanical Club*, 101–108.

Calicioglu, O., & Demirer, G. N. (2022). Role of microalgae in circular economy. In *Integrated wastewater management and valorization using algal cultures* (pp. 1–12). Elsevier.

Chandrasekhar, K., Raj, T., Ramanaiah, S., Kumar, G., Banu, J. R., Varjani, S., Sharma, P., Pandey, A., Kumar, S., & Kim, S.-H. (2022). Algae biorefinery: A promising approach to promote microalgae industry and waste utilization. *Journal of Biotechnology*, *345*, 1–16.

Che, R., Huang, L., & Yu, X. (2015). Enhanced biomass production, lipid yield and sedimentation efficiency by iron ion. *Bioresource Technology*, *192*, 795–798.

Chen, X., Zhang, C., Tan, L., & Wang, J. (2018). Toxicity of co nanoparticles on three species of marine microalgae. *Environmental Pollution*, *236*, 454–461.

Cheregi, O., Ekendahl, S., Engelbrektsson, J., Strömberg, N., Godhe, A., & Spetea, C. (2019). Microalgae biotechnology in nordic countries–the potential of local strains. *Physiologia plantarum*, *166*(1), 438–450.

Choudhury, F. K., Rivero, R. M., Blumwald, E., & Mittler, R. (2017). Reactive oxygen species, abiotic stress and stress combination. *The Plant Journal*, *90*(5), 856–867.

Chowdury, K. H., Nahar, N., & Deb, U. K. (2020). The growth factors involved in microalgae cultivation for biofuel production: A review. *Computational Water, Energy, and Environmental Engineering*, *9*(4), 185–215.

Commission, E. (2022). Proposal for a directive of the european parliament and of the council concerning urban wastewater treatment (recast).

Darvehei, P., Bahri, P. A., & Moheimani, N. R. (2018). Model development for the growth of microalgae: A review. *Renewable and Sustainable Energy Reviews*, *97*, 233–258.

Das, P., AbdulQuadir, M., Thaher, M., Khan, S., Chaudhary, A. K., Alghasal, G., & Al-Jabri, H. M. S. (2019). Microalgal bioremediation of petroleum-derived low salinity and low ph produced water. *Journal of Applied Phycology*, *31*, 435–444.

Difusa, A., Talukdar, J., Kalita, M. C., Mohanty, K., & Goud, V. V. (2015). Effect of light intensity and ph condition on the growth, biomass and lipid content of microalgae scenedesmus species. *Biofuels*, *6*(1-2), 37–44.

Dubey, S., Chen, C.-W., Haldar, D., Tambat, V. S., Kumar, P., Tiwari, A., Singhania, R. R., Dong, C.-D., & Patel, A. K. (2022). Advancement in algal bioremediation for organic, inorganic, and emerging pollutants. *Environmental Pollution*, 120840.

Eida, M. F., Darwesh, O. M., & Matter, I. A. (2018). Cultivation of oleaginous microalgae scenedesmus obliquus on secondary treated municipal wastewater as growth medium for biodiesel production. *Journal of Ecological Engineering*, *19*(5).

Eljamal, O., Eljamal, R., Maamoun, I., Khalil, A. M., Shubair, T., Falyouna, O., & Sugihara, Y. (2022). Efficient treatment of ammonia-nitrogen contaminated waters by nano zero-valent iron/zeolite composite. *Chemosphere*, *287*, 131990.

Encarnação, T., Burrows, H. D., Pais, A. C., Campos, M. G., & Kremer, A. (2012). Effect of n and p on the uptake of magnesium and iron and on the production of carotenoids and chlorophyll by the microalgae nannochloropsis sp. *Journal of Agricultural Science and Technology. A*, *2*(6A), 824.

Esteves, A. F., Soares, S. M., Salgado, E. M., Boaventura, R. A., & Pires, J. C. (2022). Microalgal growth in aquaculture effluent: Coupling biomass valorisation with nutrients removal. *Applied Sciences, 12*(24), 12608.

Fazal, T., Rehman, M. S. U., Javed, F., Akhtar, M., Mushtaq, A., Hafeez, A., Din, A. A., Iqbal, J., Rashid, N., & Rehman, F. (2021). Integrating bioremediation of textile wastewater with biodiesel production using microalgae (chlorella vulgaris). *Chemosphere*, *281*, 130758.

Gomes, J., Cocke, D., Das, K., Guttula, M., Tran, D., & Beckman, J. (2009). Treatment of produced water by electrocoagulation. *EPD Congress 2009: Proceedings of sessions and symposia held during TMS 2009 Annual Meeting & Exhibition, San Francisco, California*, 15–19.

González-Fernández, C., Sialve, B., Bernet, N., & Steyer, J.-P. (2012). Thermal pretreatment to improve methane production of scenedesmus biomass. *Biomass and bioenergy*, *40*, 105–111.

Gour, R. S., Garlapati, V. K., & Kant, A. (2020). Effect of salinity stress on lipid accumulation in scenedesmus sp. and chlorella sp.: Feasibility of stepwise culturing. *Current Microbiology*, *77*, 779–785.

Graham, E. J. S., Dean, C. A., Yoshida, T. M., Twary, S. N., Teshima, M., Alvarez, M. A., Zidenga, T., Heikoop, J. M., Perkins, G. B., Rahn, T. A., et al. (2017). Oil and gas produced water as a growth medium for microalgae cultivation: A review and feasibility analysis. *Algal Research*, *24*, 492–504.

Hakim, M. A. A., Al-Ghouti, M. A., Probir, D., Abu-Dieyeh, M., Ahmed, T. A., Aljabri, H. M. S., et al. (2018). Potential application of microalgae in produced water treatment. *Desalination and Water Treatment*, *135*, 47–58.

He, M., Yan, Y., Pei, F., Wu, M., Gebreluel, T., Zou, S., & Wang, C. (2017). Improvement on lipid production by scenedesmus obliquus triggered by low dose exposure to nanoparticles. *Scientific reports*, *7*(1), 15526.

Jena, J., Pradhan, N., Nayak, R. R., Dash, B. P., Sukla, L. B., Panda, P. K., & Mishra, B. K. (2014). Microalga scenedesmus sp.: A potential low-cost green machine for silver nanoparticle synthesis. *Journal of Microbiology and Biotechnology*, *24*(4), 522–533.

Ji, J., Long, Z., & Lin, D. (2011). Toxicity of oxide nanoparticles to the green algae chlorella sp. *Chemical Engineering Journal*, *170*(2-3), 525–530.

Johnson, B. M., Kanagy, L. E., Rodgers, J. H., & Castle, J. W. (2008). Chemical, physical, and risk characterization of natural gas storage produced waters. *Water, air, and soil pollution*, *191*, 33–54.

Khan, M. I., Shin, J. H., & Kim, J. D. (2018). The promising future of microalgae: Current status, challenges, and optimization of a sustainable and renewable industry for biofuels, feed, and other products. *Microbial cell factories*, *17*(1), 1–21.

Lürling, M. (2003). Phenotypic plasticity in the green algae desmodesmus and scenedesmus with special reference to the induction of defensive morphology. *Annales de Limnologie-International Journal of Limnology*, *39*(2), 85–101.

Mahdy, A., Mendez, L., Tomás-Pejó, E., del Mar Morales, M., Ballesteros, M., & González-Fernández, C. (2016). Influence of enzymatic hydrolysis on the biochemical methane potential of chlorella vulgaris and scenedesmus sp. *Journal of Chemical Technology & Biotechnology*, *91*(5), 1299–1305.

Mendez, L., Mahdy, A., Ballesteros, M., & González-Fernández, C. (2014). Methane production of thermally pretreated chlorella vulgaris and scenedesmus sp. biomass at increasing biomass loads. *Applied energy*, *129*, 238–242.

Miazek, K., Iwanek, W., Remacle, C., Richel, A., & Goffin, D. (2015). Effect of metals, metalloids and metallic nanoparticles on microalgae growth and industrial product biosynthesis: A review. *International Journal of Molecular Sciences*, *16*(10), 23929–23969.

Moondra, N., Jariwala, N. D., & Christian, R. A. (2021). Microalgae based wastewater treatment: A shifting paradigm for the developing nations. *International Journal of Phytoremediation*, *23*(7), 765–771.

Msanne, J., Polle, J., & Starkenburg, S. (2020). An assessment of heterotrophy and mixotrophy in scenedesmus and its utilization in wastewater treatment. *Algal research*, *48*, 101911.

Mussgnug, J. H., Klassen, V., Schlüter, A., & Kruse, O. (2010). Microalgae as substrates for fermentative biogas production in a combined biorefinery concept. *Journal of biotechnology*, *150*(1), 51–56.

Nadersha, S., & Hassan, A. A. (2022). Biodesalination and treatment of raw hypersaline produced water samples using indigenous wastewater algal consortia. *Desalination*, *528*, 115638.

Nayak, M., Rath, S. S., Thirunavoukkarasu, M., Panda, P. K., Mishra, B. K., & Mohanty, R. C. (2013). Maximizing biomass productivity and CO_2 biofixation

of microalga, scenedesmus sp. by using sodium hydroxide. *Journal of microbiology and biotechnology*, *23*(9), 1260–1268.

Nicholas, E. R., & Cath, T. Y. (2021). Evaluation of sequencing batch bioreactor followed by media filtration for organic carbon and nitrogen removal in produced water. *Journal of Water Process Engineering*, *40*, 101863.

Nie, H., Nie, M., Diwu, Z., Wang, L., Yan, H., Lin, Y., Zhang, B., & Wang, Y. (2020). Biological treatment of high salinity and low ph produced water in oilfield with immobilized cells of p. aeruginosa ny3 in a pilot-scale. *Journal of hazardous materials*, *381*, 121232.

Oliveira, G. A., Carissimi, E., Monje-Ramírez, I., Velasquez-Orta, S. B., Rodrigues, R. T., & Ledesma, M. T. O. (2018). Comparison between coagulation-flocculation and ozone-flotation for scenedesmus microalgal biomolecule recovery and nutrient removal from wastewater in a high-rate algal pond. *Bioresource technology*, *259*, 334–342.

Oncel, S. S. (2013). Microalgae for a macroenergy world. *Renewable and Sustainable Energy Reviews*, *26*, 241–264.

Pancha, I., Chokshi, K., Maurya, R., Trivedi, K., Patidar, S. K., Ghosh, A., & Mishra, S. (2015). Salinity induced oxidative stress enhanced biofuel production potential of microalgae scenedesmus sp. ccnm 1077. *Bioresource Technology*, *189*, 341–348.

Pessôa, L., Cruz, E., Deamici, K., Bomfim, B., Santana, N., Vieira, S., Silva, J., Pontes, L., Oliveira, C., Druzian, J., et al. (2022). A review of microalgae-based biorefineries approach for produced water treatment: Barriers, pretreatments, supplementation, and perspectives. *Journal of Environmental Chemical Engineering*, 108096.

Plöhn, M., Spain, O., Sirin, S., Silva, M., Escudero-Oñate, C., Ferrando-Climent, L., Allahverdiyeva, Y., & Funk, C. (2021). Wastewater treatment by microalgae. *Physiologia Plantarum*, *173*(2), 568–578.

Posten, C., & Walter, C. (2012). *Microalgal biotechnology: Potential and production*. Walter de Gruyter.

Rana, M. S., Bhushan, S., & Prajapati, S. K. (2020). New insights on improved growth and biogas production potential of chlorella pyrenoidosa through intermittent iron oxide nanoparticle supplementation. *Scientific Reports*, *10*(1), 14119.

Ren, H.-Y., Dai, Y.-Q., Kong, F., Xing, D., Zhao, L., Ren, N.-Q., Ma, J., & Liu, B.-F. (2020). Enhanced microalgal growth and lipid accumulation by addition of different

nanoparticles under xenon lamp illumination. *Bioresource Technology*, *297*, 122409.

Rhee, G.-Y., & Gotham, I. J. (1981). The effect of environmental factors on phytoplankton growth: Temperature and the interactions of temperature with nutrient limitation 1. *Limnology and Oceanography*, *26*(4), 635–648.

Rodriguez-Chiang, L. M., & Dahl, O. P. (2015). Effect of inoculum to substrate ratio on the methane potential of microcrystalline cellulose production wastewater. *BioResources*, *10*(1), 898–911.

Shen, Q.-H., Jiang, J.-W., Chen, L.-P., Cheng, L.-H., Xu, X.-H., & Chen, H.-L. (2015). Effect of carbon source on biomass growth and nutrients removal of scenedesmus obliquus for wastewater advanced treatment and lipid production. *Bioresource Technology*, *190*, 257–263.

Silambarasan, S., Logeswari, P., Sivaramakrishnan, R., Incharoensakdi, A., Cornejo, P., Kamaraj, B., & Chi, N. T. L. (2021). Removal of nutrients from domestic wastewater by microalgae coupled to lipid augmentation for biodiesel production and influence of deoiled algal biomass as biofertilizer for solanum lycopersicum cultivation. *Chemosphere*, *268*, 129323.

Silambarasan, S., Logeswari, P., Sivaramakrishnan, R., Incharoensakdi, A., Kamaraj, B., & Cornejo, P. (2023). Scenedesmus sp. strain sd07 cultivation in municipal wastewater for pollutant removal and production of lipid and exopolysaccharides. *Environmental Research*, *218*, 115051.

Singh, B., Guldhe, A., Rawat, I., & Bux, F. (2014). Towards a sustainable approach for development of biodiesel from plant and microalgae. *Renewable and sustainable Energy reviews*, *29*, 216–245.

Singh, J., & Gu, S. (2010). Commercialization potential of microalgae for biofuels production. *Renewable and sustainable energy reviews*, *14*(9), 2596–2610.

Soares, J., Kriiger Loterio, R., Rosa, R. M., Santos, M. O., Nascimento, A. G., Santos, N. T., Williams, T. C. R., Nunes-Nesi, A., & Arêdes Martins, M. (2018). Scenedesmus sp. cultivation using commercial-grade ammonium sources. *Annals of Microbiology*, *68*(1), 35–45.

Spolaore, P., Joannis-Cassan, C., Duran, E., & Isambert, A. (2006). Commercial applications of microalgae. *Journal of bioscience and bioengineering*, *101*(2), 87–96.

Sulochana, S. B., & Arumugam, M. (2020). Targeted metabolomic and biochemical changes during nitrogen stress mediated lipid accumulation in scenedesmus

quadricauda casa cc202. *Frontiers in Bioengineering and Biotechnology*, *8*, 585632.

Tam, N., & Wong, Y. (1989). Wastewater nutrient removal by chlorella pyrenoidosa and scenedesmus sp. *Environmental Pollution*, *58*(1), 19–34.

Torres, A., Padrino, S., Brito, A., & Dıaz, L. (2021). Biogas production from anaerobic digestion of solid microalgae residues generated on different processes of microalgae-to-biofuel production. *Biomass Conversion and Biorefinery*, 1–14.

Tripathi, R., Singh, J., & Thakur, I. S. (2015). Characterization of microalga scenedesmus sp. istga1 for potential co2 sequestration and biodiesel production. *Renewable Energy*, *74*, 774–781.

Udaiyappan, A. F. M., Hasan, H. A., Takriff, M. S., & Abdullah, S. R. S. (2017). A review of the potentials, challenges and current status of microalgae biomass applications in industrial wastewater treatment. *Journal of Water Process Engineering*, *20*, 8–21.

Vargas-Estrada, L., Torres-Arellano, S., Longoria, A., Arias, D. M., Okoye, P. U., & Sebastian, P. (2020). Role of nanoparticles on microalgal cultivation: A review. *Fuel*, *280*, 118598.

Vasistha, S., Khanra, A., & Rai, M. P. (2021). Influence of microalgae-zno nanoparticle association on sewage wastewater towards efficient nutrient removal and improved biodiesel application: An integrated approach. *Journal of Water Process Engineering*, *39*, 101711.

Wan, M., Jin, X., Xia, J., Rosenberg, J. N., Yu, G., Nie, Z., Oyler, G. A., & Betenbaugh, M. J. (2014). The effect of iron on growth, lipid accumulation, and gene expression profile of the freshwater microalga chlorella sorokiniana. *Applied microbiology and biotechnology*, *98*, 9473–9481.

Wang, C., Yu, X., Lv, H., & Yang, J. (2013). Nitrogen and phosphorus removal from municipal wastewater by the green alga chlorella sp. *Journal of environmental biology*, *34*(2 suppl), 421.

Wang, L., Min, M., Li, Y., Chen, P., Chen, Y., Liu, Y., Wang, Y., & Ruan, R. (2010). Cultivation of green algae chlorella sp. in different wastewaters from municipal wastewater treatment plant. *Applied biochemistry and biotechnology*, *162*, 1174–1186.

Xia, C., Van Le, Q., Chinnathambi, A., Salmen, S. H., Alharbi, S. A., & Tola, S. (2021). Role of zno and fe2o3 nanoparticle on synthetic saline wastewater on growth,

nutrient removal and lipid content of chlorella vulgaris for sustainable production of biofuel. *Fuel*, *300*, 120924.

Xin, L., Hong-Ying, H., & Jia, Y. (2010). Lipid accumulation and nutrient removal properties of a newly isolated freshwater microalga, scenedesmus sp. lx1, growing in secondary effluent. *New biotechnology*, *27*(1), 59–63.

Xin, L., Hong-ying, H., Ke, G., & Jia, Y. (2010). Growth and nutrient removal properties of a freshwater microalga scenedesmus sp. lx1 under different kinds of nitrogen sources. *Ecological Engineering*, *36*(4), 379–381.

Xin, L., Hong-Ying, H., Ke, G., & Ying-Xue, S. (2010). Effects of different nitrogen and phosphorus concentrations on the growth, nutrient uptake, and lipid accumulation of a freshwater microalga scenedesmus sp. *Bioresource technology*, *101*(14), 5494–5500.

Xin, L., Hong-Ying, H., & Yu-Ping, Z. (2011). Growth and lipid accumulation properties of a freshwater microalga scenedesmus sp. under different cultivation temperature. *Bioresource technology*, *102*(3), 3098–3102.

Xu, P., Zeng, G. M., Huang, D. L., Feng, C. L., Hu, S., Zhao, M. H., Lai, C., Wei, Z., Huang, C., Xie, G. X., et al. (2012). Use of iron oxide nanomaterials in wastewater treatment: A review. *Science of the total environment*, *424*, 1–10.

Zaidi, A. A., RuiZhe, F., Shi, Y., Khan, S. Z., & Mushtaq, K. (2018). Nanoparticles augmentation on biogas yield from microalgal biomass anaerobic digestion. *International Journal of Hydrogen Energy*, *43*(31), 14202–14213.

Zhou, W., Li, Y., Min, M., Hu, B., Zhang, H., Ma, X., Li, L., Cheng, Y., Chen, P., & Ruan, R. (2012). Growing wastewater-born microalga auxenochlorella protothecoides umn280 on concentrated municipal wastewater for simultaneous nutrient removal and energy feedstock production. *Applied Energy*, *98*, 433–440.